Antioxidant System Contributes to Cellular Protection and Long-Life

（抗酸化システムは細胞保護と長寿命に貢献する）

Eisuke Tasaki

2017

Table of contents

List of abbreviations

2HG	2-hydroxyglutarate
2HIB	2-hydroxyisobutyrate
2OG	2-oxoglutarate
8-OHdG	8-hydroxy-2’-deoxyguanosine
ALT2	Mitochondrial alanine aminotransferase
CAT	Catalase
CO_2	Carbon dioxygen
CS	Citrate synthase
Cu/Zn-SOD	Copper-zinc superoxide dismutase
DHR123	Dihydrorhodamine 123
DMEM	Dulbecco's modified Eagle medium
DPPH	2,2-diphenyl-1-picrylhydrazyl
DW	Distilled water
EGFP	Enhanced green fluorescent protein
EPI	Enhanced product ion
ER	Endoplasmic reticulum
ESI	Electrospray ionization
ETC	Electron transport chain
EtOH	Ethanol
FBS	Fetal bovine serum
FM	Female–male mating pairs
FRD	Fumarate dehydrogenase
GAPDH	Glyceraldehyde phosphate dehydrogenase

GC-MS	Gas-chromatography-mass spectrometry
GPx	Glutathione peroxidase
H_2O_2	Hydrogen peroxide
HIF	Hypoxia inducible factor
HK	Hexokinase
HPLC	High performance liquid chromatography
HRP	Horseradish peroxidase
IDH1	Cytoplasmic isocitrate dehydrogenase [NADP]
IDH2	Mitochondrial isocitrate dehydrogenase [NADP]
IDH3A	Mitochondrial isocitrate dehydrogenase [NAD] alpha subunit
IDH3B	Mitochondrial isocitrate dehydrogenase [NAD] beta subunit
L2HGDH	L-2-hydroxyglutarate dehydrogenase
LDH	Lactate dehydrogenase
MDA	Malondialdehyde
MDH1	Cytoplasmic malate dehydrogenase
MDH2	Mitochondrial malate dehydrogenase
MRM	Multiple reaction monitoring
ND	Not detected
NS	No significance
O_2	Oxygen
OGDH	Mitochondrial 2-oxoglutarate dehydrogenase
PBS	Phosphate buffered saline
PC	Protein carbonyl
PDH	Pyruvate dehydrogenase
PEPCK	Phosphoenolpyruvate carboxykinase

PFK	Phosphofructokinase
PHGPx	Phospholipid hydroperoxide glutathione peroxidase
PK	Pyruvate kinase
PPP	Pentose phosphate pathway
PVDF	Polyvinylidene fluoride
Prx	Peroxiredoxin
ROS	Reactive oxygen species
RQ	Rhodoquinone
SDS	Sodium dodecyl sulfate
SEM	Standard error of the mean
SOD	Superoxide dismutase
TAD	Transaldolase
TBARS	Thiobarbituric acid reactive substances
TCA	Trichloroacetic acid /or Tricarboxylic acid
TKT	Transketolase
TLC	Thin-layer chromatography
Trx	Thioredoxin
TrxR	Thioredoxin reductase
UFA	Unsaturated fatty acids quantification assay
UV	Ultraviolet
qRT-PCR	Quantitative real-time polymerase chain reaction
β-AIB	β-aminoisobutyrate

GENERAL INTRODUCTION

Understanding mechanisms of the ageing process is a fascinating and fundamental problem in biology. The oxidative stress theory of aging states that the accumulation of oxidative damage causes aging [1]. Reactive oxygen species (ROS), typically caused by environment stress, aerobic metabolism, and reproduction, play a positive role in processes such as cell growth signaling at permissible levels, but over-generation cause injurious oxidative stress to biomolecules and the accumulation of damage is associated with aging and negative effects on longevity [2–5]. Antioxidant activities of several antioxidant enzymes and antioxidants are thought to contribute to stress resistance associated with an organism's lifespan [5]. However, the role of antioxidant system in organisms is not totally understood. Therefore, this thesis attempts to answer some of these questions by the study consisting of two parts.

In Part I (Chapter I), we demonstrated that testis specific antioxidant enzyme peroxiredoxin 4 (Prx4t) has protective role against ROS-induced damage in mammalian cell line. The major functions of Prx include thioredoxin (Trx)-dependent peroxidase activity [6], modulation of intracellular signaling through hydrogen peroxide (H_2O_2) as a second messenger, and regulation of cell proliferation [7–9]. Although these divergent biological functions have been reported for individual Prx members, the detailed antioxidant function of Prx family members remains unknown. Our findings indicate that Prx4t actually plays a protective role against oxidative stress in mammalian cells.

In Part II (Chapter II–IV), we attempted to investigate the mechanism by which eusocial termite reproductives (queens) achieve long lifespan. Previously, the evolution of eusociality is associated with a 100-fold increase in intrinsic lifespan of reproductives (mostly females) [10]. While the current knowledge of the molecular bases of ageing is

generally that most of the work has been done using short-lived model organisms such as yeast, flies, worms (nematode), and mice, their lifespan are too short to argue all organisms' longevity and aging (*e.g.* average lifespan of nematode *Caenorhabditis elegans* is 12–18 days [11] in contrast with human average lifespan of 71.4 years (2015, WHO's global health observatory data)). Thus, because of their abnormal characteristics implying the presence of an extraordinary anti-aging mechanism, eusocial insect queens have attracted much attention, and they are promising subjects for aging research [12]. However, the molecular mechanisms that allow eusocial insects queens to have great longevity are not yet understood. In this part, I focused eusocial subterranean termite *Reticulitermes speratus* to investigate these issue. I assessed the level of oxidative stress between *R. speratus* queens and non-reproductive workers in Chapter II. In addition, I compared two major antioxidant enzyme activities among several insect species and these gene expression levels between *R. speratus* castes. Moreover, in Chapter III, I investigated whether uric acid, which is known as an antioxidant for organisms, contributes to the termite survival.

Although eusocial reproductives and non-reproductive workers have same genome information, they exhibit phenotypic dimorphisms such as longevity and fertility by some epigenetic regulation. Although understanding the regulatory mechanism is an important challenge for future aging research, findings of the mechanism have been studied little in termites. In Chapter IV, I approached the problem by focusing on an environmental factor hypoxia in termite nest.

In summary, the findings of this thesis not only indicate that an antioxidant enzyme actually plays a protective role against oxidative stress in mammalian cells and that antioxidant system contributes to longevity of *R. speratus* queens, but also can be applied to understanding the molecular basis of the physiology and behavior of eusocial termites, which underlie aging and longevity.

PART I: Testis-specific Peroxiredoxin 4 contributes to cellular protection.

CHAPTER I: Protective role of testis-specific peroxiredoxin 4 against cellular oxidative stress.

1.1 ABSTRACT

Peroxiredoxin (Prx), a newly discovered antioxidant enzyme, has an important role in hydrogen peroxide reduction. Among six Prx genes (Prx1–6) in mammals, Prx4 gene is alternatively spliced to produce the somatic cell form (Prx4) and the testis specific form (Prx4t). In our previous study, Prx4 knockout mice displayed testicular atrophy with an increase in cell death due to oxidative stress. However, the antioxidant function of Prx4t is unknown. In this study, we demonstrate that Prx4t plays a protective role against oxidative stress in the mammalian cell line HEK293T. The Prx4t-EGFP plasmid was transferred into HEK293T cells; protein expression was confirmed in the cytoplasm. To determine the protective role of Prx4t in cells, we performed image-based analysis of Prx4t-EGFP expressed cells exposed to UV irradiation and hydrogen peroxide using fluorescent probe CellROX. Our results suggested that Prx4t-EGFP expressed cells had reduced levels of oxidative stress compared with cells that express only EGFP. This study highlights that Prx4t plays an important role in cellular antioxidant defense.

1.2 INTRODUCTION

Antioxidant enzymes such as superoxide dismutase (SOD), glutathione peroxidase (GPx), and catalase play protective roles against oxidative stress caused by elevated reactive oxygen species (ROS), as well as antioxidants [4]. Peroxiredoxins (Prxs) have attracted attention in recent years as a new family of thiol-specific antioxidant proteins [6]. Six distinct genes comprise the mammalian Prx family and have been divided into three Prx subtypes; four typical 2-Cys Prx, one atypical 2-Cys Prx, and one 1-Cys Prx [13]. The major functions of these Prxs include thioredoxin (Trx)-dependent peroxidase activity [6], modulation of intracellular signaling through hydrogen peroxide (H_2O_2) as a second messenger, and regulation of cell proliferation [7–9]. Although other divergent biological functions have been reported for individual Prx members, the detailed antioxidant function of Prx family members remains unknown.

Among mammalian Prx family members, Prx4 demonstrates unique properties. Two types of Prx4 are alternatively transcribed from the single Prx4 gene, somatic cell type Prx4 and testis specific Prx4t [14]. It has been reported that Prx4 is primarily located in the endoplasmic reticulum (ER)/ Golgi apparatus, in spite of the presence of a secretory signal sequence [15]. Prx4 plays an important role in regulating disulfide bond formation in proteins and protecting cells from ER stress by metabolizing hydrogen peroxide [14,16]. On the other hand, Prx4t is entirely restricted to testicular cells, with induction that is sexual maturation-dependent. Surprisingly, Prx4 gene knockout mice have indicated that expression of Prx4t decreases compared to wild type mice, and that testicular atrophy and increased cell death is due to oxidative stress [17]. Therefore, we hypothesized that Prx4t protects cells from ROS-induced damage; however, the cellular antioxidant function is poorly understood.

In this study, we show that Prx4t contributes to the suppression and scavenging of ROS in mammalian HEK293T cells by using fluorescent microscopy and image-based cytometry. Our findings indicate that Prx4t actually plays a protective role against oxidative stress in mammalian cells.

1.3 MATERIALS AND METHODS

Cell culture and transfection

HEK293T cells were cultured in Dulbecco's Modified Eagle Medium (DMEM; Thermo Fisher Scientific, MA, USA) with 10% fetal bovine serum (v/v; FBS). Cells were incubated at 37°C in a carbon dioxide (CO_2) gas incubator (Waken B Tech Co. Ltd., Japan) with 5% CO_2. Mouse Prx4t cDNA (Ensembl Transcript ID: ENSMUST00000130349.2) was subcloned into the pEGFP-N1 vector (Clontech, Takara Bio Inc., Japan) and was named Prx4t-EGFP. HEK293T cells were transfected with the Prx4t-EGFP plasmid or the EGFP (pEGFP-N1) plasmid using the Lipofectamine® reagent (Invitrogen, Thermo Fisher Scientific, MA, USA) according to the manufacturer's manual. Briefly, 1.5 mL tubes containing 100 μL OPTI (Gibco, Thermo Fisher Scientific, MA, USA), 1 μL plus reagent (Invitrogen, Thermo Fisher Scientific, MA, USA), and 2 μg Prx4t-EGFP plasmid or EGFP plasmid, respectively, were prepared and incubated for 5 min at 25°C. After that, 100 μL OPTI and 2.5 μL lipofectamin agent (Invitrogen, Thermo Fisher Scientific, MA, USA) were added to each tube, and tubes were incubated for 30 min at 37°C. After 24 h incubation, HEK293T cells were washed by OPTI-MEM (Gibco, Thermo Fisher Scientific, MA, USA), and incubated with reagent mixed by 800 μL OPTI-MEM added to the cell dishes. After 5 h incubation at 37°C, dishes were treated with 1 mL DMEM containing 20% FBS (final FBS concentration 10%; v/v) and incubated overnight at 37°C.

Immunoblot analysis

HEK293T cells transfected with the Prx4t-EGFP or EGFP plasmid were washed three times with PBS and lysed in buffer (20 mM Tris-HCl, 2% protease inhibitor cocktail; v/v), followed by centrifugation at 17000 *g* for 10 min. Protein concentrations of the supernatant

were determined using a BCA protein assay kit (Thermo Fisher Scientific, MA, USA). Cell fractionation was performed using the ProteoExtract® subcellular proteome extraction kit (Calbiochem, Merck, Darmstadt, Germany) followed by concentration using a common methanol/ chloroform protein precipitation method. SDS-PAGE was perform with 10% polyacrylamide gels (w/v); separated proteins were transferred to polyvinylidene fluoride (PVDF) membranes (AmershamHybond™ P; GE healthcare, Little Chalfont, UK), blocked for 2 h in 1% skim milk in TBST (w/v; 0.1% TBS and 0.05% Tween-20), and probed overnight at 4°C with rabbit polyclonal antibodies. After binding of the appropriate HRP conjugate anti-rabbit IgG antibody (Santa Cruz Biotechnology Inc., Santa Cruz, CA, USA), the ECL plus western blotting detection system (GE healthcare, Little Chalfont, UK) was used. Results are shown as one representative experiment.

Prx activity assay

Harvested cells were washed twice with PBS and homogenized by sonication in tubes with buffer (20 mM Tris-HCl, 2% protease inhibitor cocktail; v/v), followed by centrifugation at 17000 *g* for 30 min at 4°C. Supernatants containing proteins were transferred to new tubes and used for experiments as samples. Each sample was measured for protein concentration using the BCA protein assay kit before the extractions. Prx activity was determined using an indirect assay that links Prx-mediated oxidation of thioredoxin (Trx) with the recycled reduction of Trx_{ox} (-S-S-) to Trx_{red} (-SH) by TrxR (thioredoxin reductase) using NADPH as the reductant. Quantification of the Prx activity was assayed by measuring the decomposition of NADPH by monitoring absorbance at 340 nm at 37°C for 5 min. The reaction was started by the addition of the reaction buffer containing 200 μM NADPH, 1.5 μM yTrx, 0.8 μM yTrxR, 50 mM Hepes-NaOH buffer (pH 7.0), and 1mM EDTA to 100 μg total protein following addition of 100 μM H_2O_2. The

Prx activity was defined as the rate of disappearance of NADPH, and we calculated arbitrary units relative to the value from the control.

Detection of reactive oxygen species (ROS)

ROS were detected using the cell-permeable, peroxide-sensitive probes, CellROX Orange Reagent and CellROX Deep Red Reagent (Invitrogen, Thermo Fisher Scientific, MA, USA) according to the manufacturer's instructions. The dye exhibits bright orange fluorescence upon oxidation by ROS. We prepared HEK293T cells transduced with blank, Prx4t-EGFP plasmid, or EGFP plasmid for 24 h. For Hydrogen peroxide (H_2O_2) stress assays, cells were incubated with 5 μM CellROX Orange reagent in PBS for 30 min; 250 μM H_2O_2 was added after 15 min of treatment. For UV irradiation stress assays, cells were incubated with 5 μM CellROX Orange reagent in PBS for a 5 min period of irradiation with UV-B (312 nm, 5 mJ/ cm^2; TF-20M; Vilber Lourmat, Marne la Vallée, France) followed by incubation at 37°C for 30 min. The cells were observed using a Leica AF 6000 LX fluorescence microscope system (Leica Microsystems, Leica, Wetzlar, Germany). Fluorescence signal intensity was calculated by ImageJ software (Wayne Rasband, NIH) as previously described [18,19]. Cells were also harvested by trypsin treatment for cell cytometry analysis; harvested cells were examined by a Tali® image-based cytometer (Life technologies, Thermo Fisher Scientific, MA, USA), which is a 3-channel (bright field, green fluorescence, and red fluorescence) benchtop cytometer. $CellROX^+$ ratios in $EGFP^+$ cells were calculated as oxidative damaged cell ratios.

Statistical analysis

Statistical differences were determined by the two-sided Mann-Whitney's *U*- test. Differences with $p < 0.05$ were considered significant. All data in graphs are presented as

means ± standard errors of the mean (SEM).

1.4 RESULTS

Expression and localization of Prx4t-EGFP in HEK293T cells.

To determine the localization of Prx4t in mammalian cells, we first tried to express Prx4t in the mammalian cell line HEK293T. We prepared a Prx4t–EGFP fusion construct (pEGFP-N1-Prx4t) and an EGFP control plasmid (pEGFP-N1) for transfection assays (Fig 1.1A). Typically, endogenous mouse Prx4t has been shown to localize only to the cytosol of testicular cells [20]. Consistent with this previous report, we observed the expression of Prx4t-EGFP in the cytosol of HEK293T cells using a fluorescence microscope system (Fig 1.1B). Prx4t-EGFP protein localization was also determined by western blot after cell fractionation and Prx4t-EGFP was present only in the cytosolic fraction (Fig 1.1C). In addition, we found that the Prx activity of Prx4t-EGFP expressed cells was significantly high compared with that of the control cells (Fig 1.1D). These results indicate that the Prx4t-EGFP expressed cells may serve as a model for facilitating the understanding of the antioxidant function of Prx4t in mammalian cells.

Prx4t-expressing cells showed lower ROS levels compared to control cells.

Since it has been reported that the overexpression of antioxidant enzymes protects cells against oxidative stress [21–23], we examined whether Prx4t-transfection increases the antioxidant ability of the cells. In this investigation, we performed fluorescence microscopy after the Prx4t-EGFP-CellROX combination method. As a result, we observed that cells expressing Prx4t-EGFP demonstrated decreased CellROX fluorescence compared to cells just expressing EGFP (Fig 1.2A). Quantification of CellROX fluorescence revealed that Prx4t expression contributes to the cellular antioxidant ability after oxidative stress, even in untreated control cells (Fig 1.2B). Therefore, we were able to demonstrate that

Prx4t can actually play a protective role against oxidative stress in mammalian cells.

Cytometrical analysis indicated that Prx4t plays a protective role against oxidative stress caused by H_2O_2 treatment or UV-irradiation.

We quantified the antioxidant effect of Prx4t in HEK293T cells using an image-based cytometer after treatment with 250 μM H_2O_2 or UV (312 nm)-irradiation for 5 min. Cells, which were mainly transfected with Prx4t-EGFP or the EGFP control plasmid, were located in the right field on the panels ($EGFP^+$ cells; Fig 1.3). The histograms indicate oxidatively damaged cell ratios, calculated as average $CellROX^+$ ratios in the $EGFP^+$ cells. Interestingly, the percentage of oxidatively damaged fractions of Prx4t-EGFP-expressing cells were lower than the percentage of EGFP-expressing cells, even in the untreated condition (Fig 1.3A). Consistent with microscopic observations, Prx4t-EGFP-expressing cells showed high resistance against oxidative stress after H_2O_2 treatment or UV-irradiation compared to EGFP-expressing cells (Fig 1.3B, C).

1.5 DISCUSSION

Prx4t, a newly described member of the Prx family, is specifically expressed in testicular cells [20]. Prx4 gene knockout mice, in which Prx4t expression is decreased compared to wild type mice, show increased spermatogenic cell death due to oxidative stress [14,17]. However, the antioxidant function of Prx4t against oxidative stress has not yet been evaluated. In the present study, the overexpression of Prx4t protected HEK293T cells from H_2O_2- or UV- induced oxidative stress as determined by image-based cytometer analysis (Fig 1.3). These results are compatible with the typical enzymatic function of Prx in antioxidant defense. This study further evaluated the antioxidant function of Prx4t by fluorescence microscopy. Consistent with image-based cytometer results, we determined that Prx4t-expressing cells achieve a higher resistance against oxidative stress than control cells (Fig 1.2). In the two image-based analysis, especially in Fig 1.3A, we detected that overexpression of Prx4t suppresses oxidative stress in cultured cells even in control condition. We considered that this was caused by stress accumulation during experiment operation and in vitro culture stress because of ambient 21% oxygen. Moreover, we observed higher Prx activity in Prx4t overexpressed cells than in control cells (Fig 1.1D). These results indicate that Prx4t plays a protective role against oxidative stress in mammalian cells.

Generally, mammalian Prxs are classified as six isoforms [3]. These Prxs are thought to have Trx-dependent peroxidase activity, in which H_2O_2, as well as a wide range of organic hydroperoxides (ROOH), are reduced and detoxified [2]. Interestingly, previous studies have demonstrated that typical 2-Cys Prxs, which include mammal Prx1–4, play as regulators of H_2O_2-sensing cellular signaling [8,9,24,25]. Prx4t may play another role, such as in the signal regulation of mammalian cells; therefore, further studies are needed to

evaluate the function of Prx4t, which is distinct from the antioxidant behavior in mammalian cells.

Intrinsically, Prx4t is specifically expressed in sexually matured testes. In the testes, spermatogenic cells experience dramatic changes in the gene expression, morphogenesis, and redox environment during spermatogenesis. Although the chromatin of somatic cells is constituted by histones in ordinary somatic cells, sperm nuclear histones are replaced by protamines during the spermatogenic process [26]. The protamines of primates and rodents contain multiple cysteine residues that are oxidized to form disulfide bridges (sulfoxidation) that contribute to resistance against oxidative stress in the chromatin of spermatogenic cells; Prx4t is thought to play an important function as a sulfoxidase during spermatogenesis [14,27]. This sulfoxidase function of Prx4t is similar to the protein folding function of Prx4 localized to the ER/ Golgi apparatus [28]. In summary, we showed possibility that Prx4t may not only function as a sulfoxidase but also may have an antioxidant function in spermatogenic cells during spermiogenesis.

1.6 FIGURES

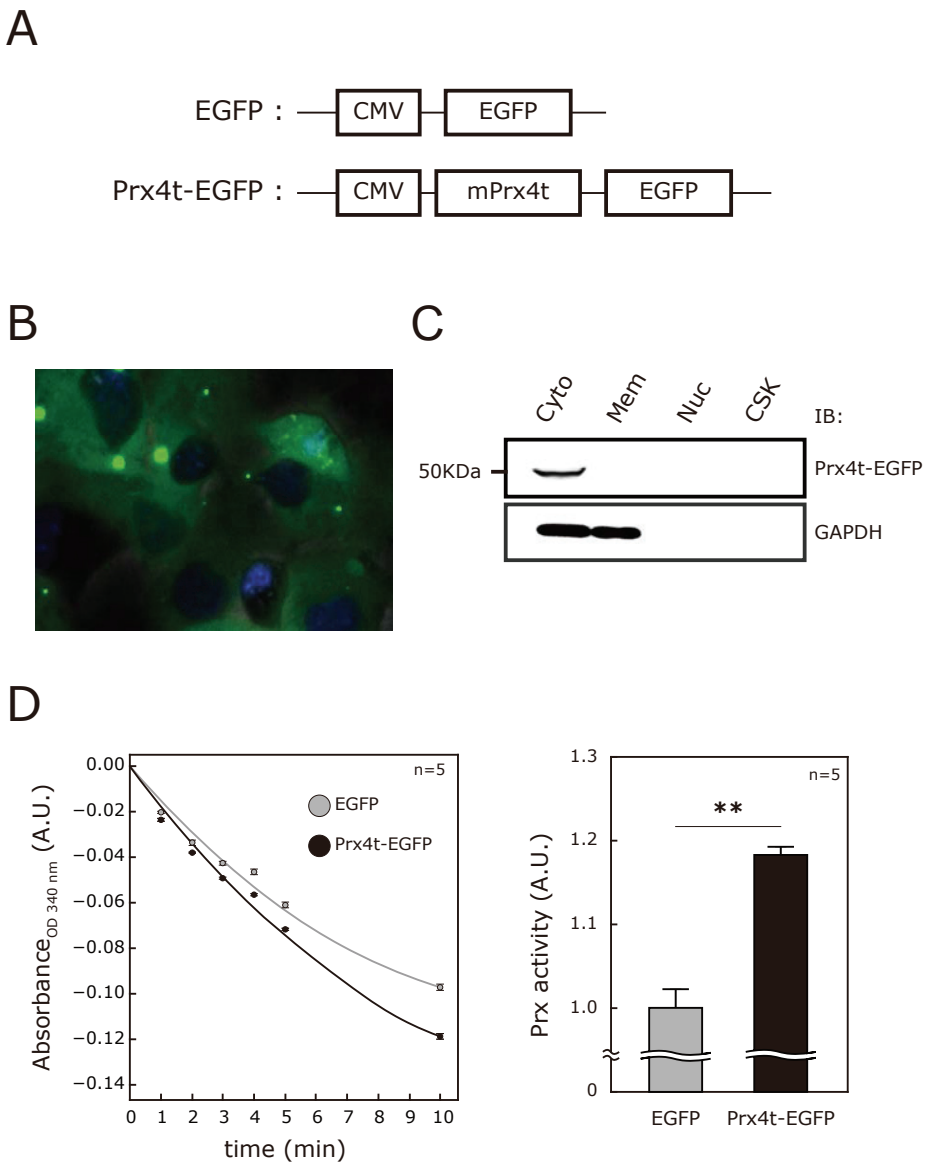

Fig 1.1 | Prx4t-EGFP expression and localization in HEK293T cells. (A) Prx4t-EGFP and EGFP constructs. (B) A representative image of HEK293T cells ectopically expressing Prx4t-EGFP is shown. The representative fluorescence image was taken using a

fluorescence microscope system (Leica). Prx4t-EGFP, green. (C) Cytosol (Cyto), membrane and membranous organelles (Mem), nucleus (Nuc), and cytoskeleton (CSK) extracts were prepared from Prx4t-EGFP- transfected HEK293T cells separated by SDS-PAGE. Prx4t-EGFP protein was monitored by western blot. (D) Time course for degradation of absorbance of NADPH (*left*) and the mean of quantitative Prx activity from the slope (*right*) in EGFP or Prx4t-EGFP expressed cells is shown. *P*-values were derived from two-sided Mann-Whitney's *U*- test (**$P < 0.01$). A.U., arbitrary unit. Data are means ± SEM; n = 5.

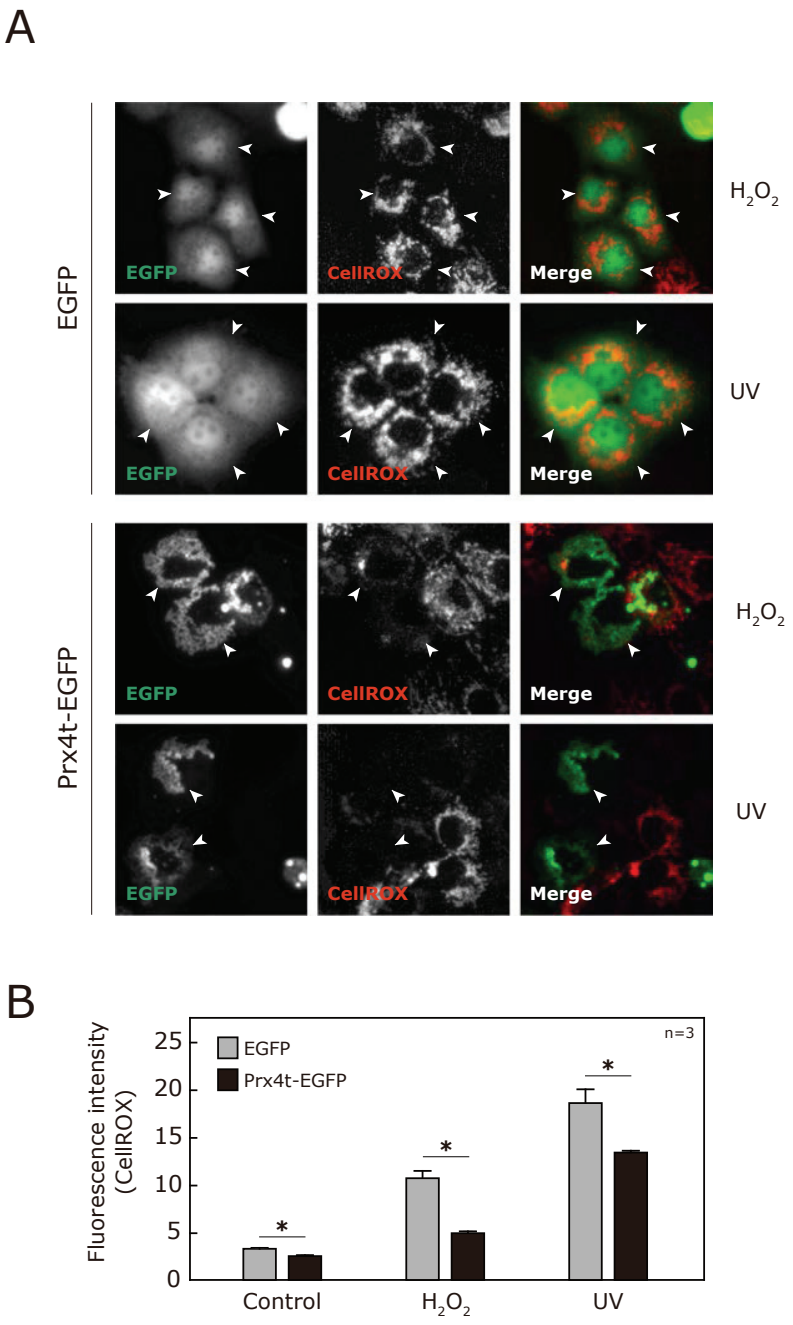

Fig 1.2 | Intracellular ROS detection in HEK293T cells expressing Prx4t-EGFP.

Intracellular ROS detection in HEK293T cells expressing Prx4t-EGFP. (A) HEK293T cells

expressing Prx4t-EGFP or EGFP were stimulated with 250 μM H_2O_2 treatment or 5 min UV-irradiation. These fluorescence images were taken using a fluorescence microscope system (Leica). Prx4t-EGFP or EGFP normally expressing cells were pointed by white arrow. (B) Quantitative analyses of fluorescence intensity are shown. The CellROX fluorescence intensities were measured as ROS levels in the cells expressing Prx4t-EGFP or EGFP. Gray and black bars indicate the cells expressing EGFP and Prx4t-EGFP, respectively. P values were derived from two-sided Mann-Whitney's *U*- test (*$P < 0.05$). Data are means ± SEM; n = 3.

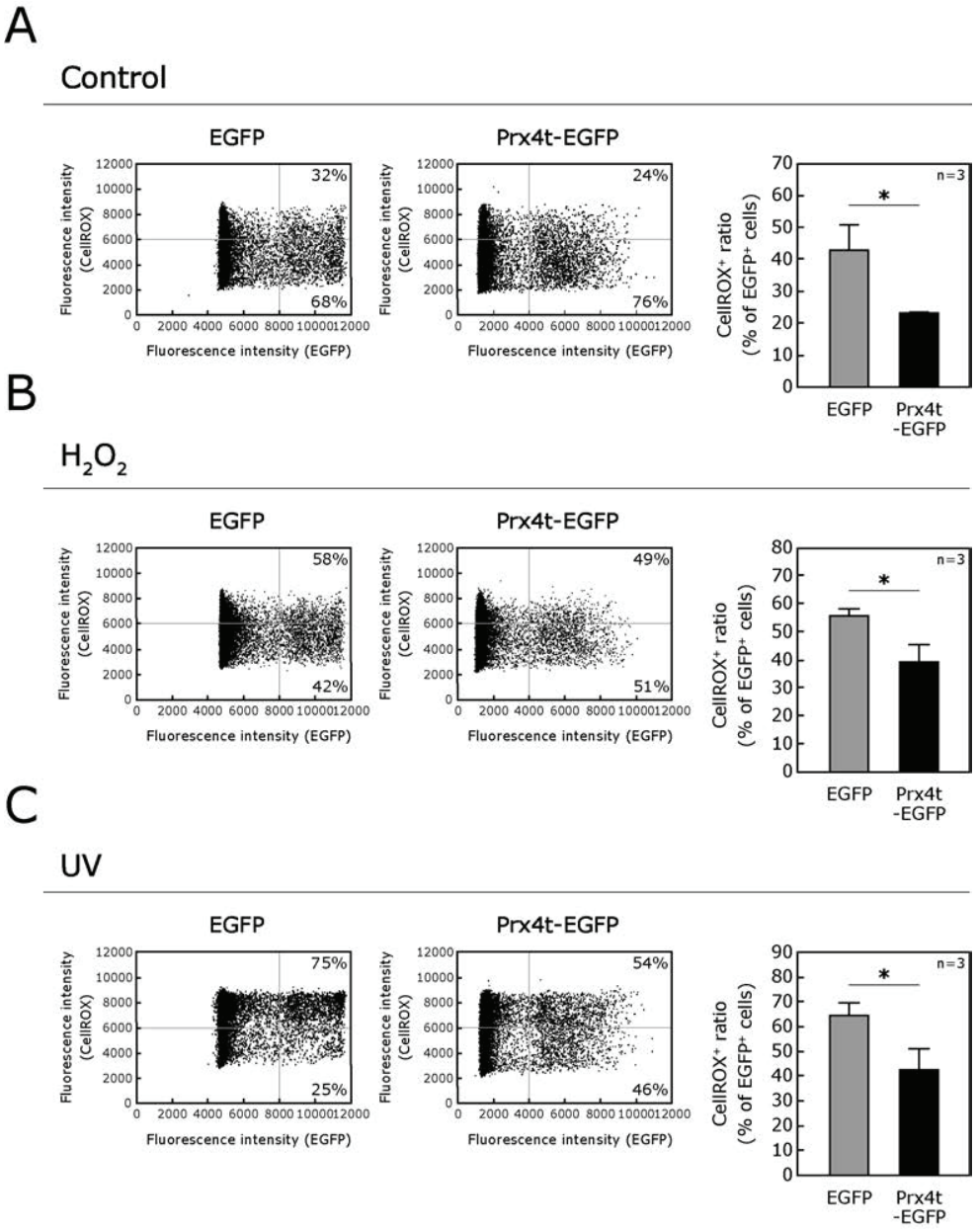

Fig 1.3 | Image-based cytometry analysis of HEK293T cells transfected with the Prx4t-EGFP. (A-C) The representative plots of the analyzed data in HEK293T cells transfected with EGFP plasmid (left panel) or Prx4t-EGFP plasmid (right panel). The $EGFP^+$ and $CellROX^+$ areas were gated by the dotted line at appropriate fluorescence

densities. Histograms show the quantification of CellROX$^+$ ratios (% of EGFP$^+$ cells). Cells were untreated controls (A) or treated with H_2O_2 (B) or UV (C) before analysis. Gray and black bars indicate the cells expressing EGFP and Prx4t-EGFP, respectively. *P*-values were derived from two-sided Mann-Whitney's *U*- test (*$p < 0.05$). Data are means ± SEM; n = 3.

PART II: Antioxidant System of Long-Lived Termite, *Reticulitermes speratus*.

CHAPTER II: Antioxidant enzymes: An efficient antioxidant system in long-lived queen.

2.1 ABSTRACT

The trade-off between reproduction and longevity is known in wide variety of animals. Social insect queens are rare organisms that can achieve a long lifespan without sacrificing fecundity. The extended longevity of social insect queens, which contradicts the trade-off, has attracted much attention because it implies the existence of an extraordinary anti-aging mechanism. Here, we show that queens of the termite *Reticulitermes speratus* incur significantly lower oxidative damage to DNA, protein and lipid and have higher activity of antioxidant enzymes than non-reproductive individuals (workers and soldiers). The levels of 8-hydroxy-2'-deoxyguanosine (oxidative damage marker of DNA) were lower in queens than in workers after UV irradiation. Queens also showed lower levels of protein carbonyls and malondialdehyde (oxidative damage markers of protein and lipid, respectively). The antioxidant enzymes of insects are generally composed of catalase (CAT) and peroxiredoxin (Prx). Queens showed more than two times higher CAT activity and more than seven times higher expression levels of the CAT gene *RsCAT1* than workers. The CAT activity of termite queens was also markedly higher in comparison with other solitary insects and the queens of eusocial Hymenoptera. In addition, queens showed higher expression levels of the Prx gene *RsPRX6*. These results suggested that this efficient antioxidant system can partly explain why termite queens achieve long life. This study provides important insights into the evolutionary linkage of reproductive division of labor and the development of queens' oxidative stress resistance in social insects.

2.2 INTRODUCTION

The key character of eusociality is reproductive division of labor within collaborative groups. Social species such as ants, honeybees, and termites have one or a limited number of individuals that produce most or all of the offspring (queens), and a large number of individuals that forego reproduction for group beneficial activities (workers). In these insects, queens live up to 10 times longer than non-reproductive workers [10,29–31]. Longevity is typically negatively correlated with fecundity and the extent of this trade-off varies within and among species [32]. Previous studies have shown that germline-ablated worms had an extended lifespan [33], and sterile females also showed greater longevity compared with fertile flies [34]. Although most animal species show a gradual decline in reproduction with age [35], social insect queens are thought to be the only animals known that can live for long periods while also producing many offspring per day [36]. Because of their abnormal characteristics implying the presence of an extraordinary anti-aging mechanism, social insect queens have attracted much attention, and they are promising subjects for aging research [12]. However, the molecular mechanisms that allow social insects queens to have great longevity are not yet understood.

The oxidative stress theory of aging states that the accumulation of oxidative damage causes aging [1]. Reactive oxygen species (ROS), typically caused by environment stress, aerobic metabolism, and reproduction, play a positive role in processes such as cell growth signaling at permissible levels, but over-generation cause injurious oxidative stress to biomolecules and the accumulation of damage is associated with aging and negative effects on longevity [2–5]. Several enzymes such as catalase (CAT) and peroxiredoxin (Prx) are involved in ROS detoxification. Hydrogen peroxide (H_2O_2) can transform into a highly reactive hydroxyl radical in the presence of reduced metal atoms. CAT efficiently converts

H_2O_2 to water and oxygen without the production of other ROS. Prx also reduces H_2O_2 and functions only when coupled to a sulfhydryl-reducing system such as thioredoxin or glutathione. These antioxidant enzyme activities contribute to stress resistance associated with an organism's lifespan. Treatment with CAT and superoxide dismutase (SOD) mimetics extended longevity because of the protective effect against oxidative stress in *Caenorhabditis elegans* [37,38]. In the model insect *Drosophila melanogaster*, overexpression of CAT and SOD resulted in reduced levels of oxidative stress and an extended lifespan [39,40]. Therefore, long-lived social insect queens should have efficient antioxidant systems that eliminate ROS more effectively in order to prevent the accumulation of oxidative damage, in part due to high fecundity [41,42]. In relation to the hypothesis that antioxidant activity mediates longevity of social insect queens, several reports have been published. Parker *et al.* showed that copper-zinc SOD (Cu/Zn-SOD) activity and SOD gene expression do not associate with long lifespan of queens in the black garden ant *Lasius niger* [43]. Corona *et al.*, who also obtained similar results, demonstrated that the honeybee *Apis mellifera* queens have lower or equal levels of antioxidant gene expression in comparison with workers [44]. Importantly, these studies indicated that a robust antioxidant activity is not prerequisite for longevity in social insect queens and is confined to only eusocial Hymenoptera (ants and honeybees). Eusocial Isoptera (termite) queens may also have as longer lifespan and higher fecundity as the queens of Hymenoptera [10]; however, termite queens have never been studied. Therefore, we focused on a subterranean termite *Reticulitermes speratus* and paid attention to their antioxidant system against oxidative stress.

In this study, we investigated whether long-lived and fertile termite queens have higher antioxidant activities than non-reproductive individuals. First, we found that the oxidation levels of DNA, protein, and lipid were significantly lower in queens of *R.*

speratus in comparison with workers. To our knowledge, this is first report about the differences in oxidative stress resistance observed between termite queens and workers. Next, to demonstrate the cause of the high oxidative stress resistance of termite queens, we compared several antioxidant activities and antioxidant gene expression levels between queens and non-reproductive workers, soldiers, and nymphs. In contrast to previous reports, we were able to show that termite queens have higher antioxidant activities than non-reproductive individuals. The CAT activity of termite queens was markedly higher than in other solitary insects and the queens of eusocial Hymenoptera. We hypothesize that high activity and expression of antioxidant enzymes, especially CAT, are primed to respond rapidly and scavenge ROS that cause oxidative stress, and consequently termite queens attain both greater longevity and sustained high fecundity.

2.3 MATERIALS AND METHODS

Sample

Bombyx mori (larvae, pupae and adults) and *Drosophila melanogaster* (adults; Oregon R) were provided by Prof. J Kobayashi and Prof. R Murakami, respectively. Solitary mantises *Tenodera aridifolia* (adults) were collected from grounds of Yamaguchi University. Three colonies of wasp *Vespa simillima xanthoptera* (larvae, workers, adult males, and queens) were received from an exterminator. Three colonies of ant *Camponotus obscuripes* (workers and queens) and 11 colonies of termite *Reticulitermes speratus* (workers, soldiers, nymphs, and queens [mature neotenic queens]) were collected from the experimental forest of Yamaguchi University, which is part of Mt. Himeyama in Yamaguchi, western Japan. Except as where specified in the figure legends, all insect samples were classified by sex, and one individual was used per sample, although we pooled 10 individuals of *D. melanogaster* adults, 5 individuals of *C. obscuripes* workers. In *R. speratus*, we used different pooled termite samples from different colonies for each experiment as described (Table 1.1). For oxidative damage analysis, we prepared termite samples after 20 min irradiation with UV-B (312 nm, 10.4 kJ/ m2; Vilber Lourmat TF-20M) on a Petri dish. Then, to irradiate all samples equally, stimulations were performed for each group of 5 individuals of workers or a queen and we observed that individuals were alive (Fig 2.1). These insect samples were preserved at –80°C until use.

8-Hydroxy-2'-deoxyguanosine assay

The concentration of 8-hydroxy-2'-deoxyguanosine (8-OHdG) was determined in extracted insect DNA using a EpiQuik™ 8-OHdG DNA damage quantification direct kit (colorimetric) (Epigentek) in accordance with the manufacturer's instructions. Briefly, total

DNA was extracted using a DNA extractor® TIS kit (Wako Pure Chemical Industries) from termite whole bodies. DNA was bound to wells that have high DNA binding affinity. Then the 8-OHdG present in the DNA was detected by using capture and detection antibodies. An enhancer solution was used to enhance the signal followed by reading the absorbance using a spectrophotometer at 450 nm within 2–15 min. The results are expressed as relative quantification (%) to the positive control provided by the kit and normalized to the input DNA (ng). Six biological replicates were performed, each with five workers and a queen (Table 1.1).

Protein carbonyl assay

Oxidative protein was quantified as PC using a protein carbonyl colorimetric assay kit (Cayman Chemical) in accordance with the manufacturer's instructions. Briefly, termite whole bodies were homogenized in 200 µL ice-cold buffer (20 mM Tris-HCl, 1 mM EDTA, 2% protease inhibitor cocktail (v/v)). After centrifugation at 16200 *g* for 10 min at 4°C, the supernatants were placed into a new tube with 2,4-dinitrophenylhydrazine reagent followed by incubation in the dark at room temperature for 60 min. Then, 1 mL of 20% trichloroacetic acid (TCA) solution (w/v) was added to the samples before centrifugation at 16200 *g* for 10 min. The pellets were washed three times with 1 mL of (1:1) ethanol/ethyl acetate mixture. The obtained pellets were resuspended in guanidine hydrochloride solution. After vortexing and centrifugation, we measure the absorbance of the supernatant at 370 nm. The levels of PC were calculated as the amount relative to the total protein amount. Three biological replicates were performed, each with five workers and two queens (Table 1.1).

Unsaturated fatty acids quantification assay

For quantification of unsaturated fatty acids (UFAs), we used a lipid quantification Kit (Colorimetric; Cell Biolabs) in accordance with manufacturer's instructions. Briefly, lipid standards and lipid samples were extracted from the whole bodies of termites using 300 µL (1:1) chloroform/methanol mixture at –20°C followed by resuspension in dimethyl sulfoxide (Wako), which was incubated with 18 M sulfuric acid at 90°C for 10 min. After mixing with vanillin reagent, these samples were incubated at 37°C for 15 min. The levels of UFAs were detected at a wavelength of 540 nm and calculated from the standard curve of lipid standard. The corrected value of lipid was calculated as follows: UFA (µg)/sample weight (mg). Three biological replicates were performed, each with five workers, three nymphs, and two queens (Table 1.1).

Thiobarbituric acid reactive substances assay

As assessment of oxidative damage by lipid peroxidation was determined by using a Thiobarbituric acid reactive substances (TBARS) assay kit (Cayman chemical). Briefly, termite whole bodies were homogenized in 200 µL ice-cold buffer (20 mM Tris-HCl, 2% protease inhibitor cocktail (v/v)). Malondialdehyde (MDA) standard or samples were mixed with 50 µL 10% SDS solution (w/v) and 1 mL color reagent (0.53% thiobarbituric acid (w/v) in 10% acetic acid solution (v/v) and 1.5% sodium hydroxide solution (v/v)), and incubated for 30 min at 100°C. Samples were incubated on ice for 10 min to stop the reaction and then centrifuged at 17000 *g* for 10 min at 25°C. The absorbance of the obtained supernatant was determined at 532 nm and levels calculated from a standard curve of the MDA standard. The corrected value of MDA was calculated as follows: MDA (nmol)/ sample weight (mg). We made three biological replications, each with five workers, three nymphs, and two queens (Table 1.1).

Protein extraction

Whole bodies of insect samples stored at –80°C were first ground to powder in liquid nitrogen and then homogenized by sonication in the tubes with buffer (20 mM Tris-HCl, 2% protease inhibitor cocktail (v/v)), followed by centrifugation at 17000 *g* for 30 min at 4°C. The supernatant containing proteins was transferred to a new tube and used as a sample. Each sample had its protein concentration measured using a BCA protein assay kit before extraction. These protein samples were preserved at –80°C until use for antioxidant activity assays.

Antioxidant enzyme activity assays

The activities of antioxidant enzymes were determined as in a previous report [45]. Briefly, quantification of CAT activity was assayed by measuring the decomposition of hydrogen peroxide (H_2O_2) by monitoring absorbance at 240 nm. The reaction was started by the addition of 15 μg total protein to a reaction buffer containing 50 mM Tris-HCl (pH 7.5), 2.5 mM EDTA and 10 mM H_2O_2. CAT activity was defined as the rate of disappearance of H_2O_2 and we calculated arbitrary units relative to the value from *R. speratus* workers. Prx activity was determined using an indirect assay that links Prx-mediated oxidation of thioredoxin (Trx) with the recycled reduction of Trx_{ox} (-S-S-) to Trx_{red} (-SH) by TrxR (thioredoxin reductase) using NADPH as a reductant. The absorbance at 340 nm was monitored at 30°C for 5 min. Similar to the CAT activity assay, we also calculated arbitrary units relative to the value from *R. speratus* workers in the Prx activity assay. Three biological replicates were performed for all insect samples classified by sex. In only queens of *R. speratus*, 12 and 9 replications were made for CAT and Prx activity, respectively. Except as specified in the text and figure legend, the obtained data from solitary insects and non-reproductive individuals of *R. speratus* classified by sex were

mixed, by which the ratio of males and females was 1:1. This means that the mixed sample size becomes n = 6.

Quantitative real-time PCR

The whole transcriptome of *R. speratus* was examined using Next-generation RNA-sequencing technology in the previous study [46]. We obtained mRNA sequences of antioxidant genes from the transcriptome data through a Blast search with the amino acid sequences of translated antioxidant genes in the termite *Zootermopsis nevadensis*, and designed primer pairs for each the gene using Primer3 (version 1.1.4; [47]; Table 1.2). Using ISOGEN reagent (Nippon gene), total RNA was extracted individually from whole bodies of termite workers, soldiers, nymphs, or queens which were frozen with liquid nitrogen and stored at –80°C until extraction. Immediately, cDNA was synthesized from the RNA using a PrimeScriptTM RT reagent kit (Takara), and preserved at –20°C. Quantitative real-time PCR (qRT-PCR) was performed using a LightCycler (Roche) with QuantiTect® SYBR® Green PCR (Qiagen). All procedures were performed in accordance with each manufacturer's protocol. GAPDH was selected as the reference gene. Relative expression levels were calculated using a typical ΔΔCt method. Twelve biological replicates were performed, each with three workers, three soldiers, and two nymphs of *R. speratus*. Nine replications were made for one queen of *R. speratus*. Except as specified in the text and figure legends, the obtained data from non-reproductive individuals of *R. speratus* classified by sex were mixed, by which the ratio of males and females was 1:1.

Statistical analysis

R software package (version 3.2.2) was used for most statistical analyses. Unpaired t test followed by *P*-value correction using Holm's method [48] for multiple comparisons

was performed on the different sets of data. All data in graphs are presented as the mean ± standard error of the mean (SEM), and all calculated *P*-values are provided in figure legends. Differences were considered significance when the *P*-value was * $p < 0.05$, ** $p < 0.01$.

2.4 RESULTS

Oxidative DNA, protein, and lipid damage in termite queens was markedly lower than non-reproductive workers.

To investigate whether high resistance to oxidative stress allows termite queens to achieve long lifespan, we performed a comparison of oxidative damage to biomolecules in *R. speratus* queens and workers (Fig 2.2A). The major biomolecules susceptible to oxidative damage are DNA [49], protein [50], and lipids [51] in most organisms. First, we assessed the levels of oxidative DNA damage using a detection assay for 8-hydroxy-2'-deoxyguanosine (8-OHdG), which is widely accepted as a sensitive marker of oxidative DNA damage. Although the 8-OHdG values in queens did not differ from the value in workers in control conditions, increased oxidative DNA damage due to UV irradiation, which produces singlet molecular oxygen and increases 8-OHdG levels [52], was suppressed only in queens but not in workers (Fig 2.2B). Next, we assessed the levels of oxidative protein damage by detection of protein carbonyls (PCs), which are major biomarkers of oxidative damage of protein. To measuring PCs, we performed a colorimetric assay using the reaction of 2,4-dinitrophenylhydrazine with PCs to produce hydrazone, which can be analyzed spectrophotometrically [53]. Queens showed lower levels of PCs than workers in normal conditions and post UV irradiation (Fig 2.2C). Lastly, we assessed the levels of oxidative lipid damage in queens and workers using a thiobarbituric acid reactive substances (TBARS) assay, which is a well-established method for screening for malondialdehyde (MDA), the end product of lipid peroxidation [54,55]. Then, because workers showed markedly low levels of unsaturated fatty acids (UFAs) susceptible to ROS, in comparison with queens (Fig 2.3), the values of MDA were revised by the UFA amounts in queens and workers. The corrected values of MDA were

significantly lower in queens compared with workers (Fig 2.2D). Additionally, augmented MDA due to UV irradiation was suppressed in queens, whereas queens had higher and equal UFA levels in comparison with workers and nymphs, respectively (Fig 2.4). Together, these results suggested that the ability to maintain lower oxidative stress in biomolecules is responsible for termite queens showing dramatically greater longevity.

High catalase activity and *RsCAT1* gene expression levels provide an efficient antioxidant system in termite queens.

The major antioxidant enzymes in insects are CAT and Prx, which play a role in the management of oxidative damage [56]. Because *R. speratus* queens showed markedly lower levels of oxidative damage in comparison with workers (Fig 2.2), we next investigated whether termite queens had higher antioxidant activities than non-reproductive individuals and other insect species. Furthermore, we confirmed whether antioxidant activities were supported by gene transcription levels or not. To measure levels of antioxidant gene expression, we identified two CAT genes (*RsCAT1* and *RsCAT2*) and four Prx genes (*RsPRX1*, *RsPRX4*, *RsPRX5* and *RsPRX6*) by the method described below (Table 1.3). Queens showed significantly higher CAT activity than not only termite non-reproductive individuals (workers, soldiers, and nymphs), but also other solitary insects (*Drosophila melanogaster*, *Bombyx mori*, and *Tenodera aridifolia*) and eusocial queens of Hymenoptera (*Vespa simillima xanthoptera* and *Camponotus obscuripes*) (Fig 2.5A). Then, the values of CAT activity in solitary insects were pooled for male-female data (1:1). Separate male and female data for CAT activity are shown in Fig 2.6. These results indicated that a different antioxidant system to protect biomolecules from oxidative stress has evolved between Isoptera and eusocial Hymenoptera. Next, we investigated CAT gene expression levels between individuals of *R. speratus*. As a result, we found that

queens had a significantly higher level of *RsCAT1* expression but not *RsCAT2* expression, which was not consistent with their CAT activity (Fig 2.5B, C). A previous report demonstrated that CAT activity is essential for longevity and fertility in sand fly [57,58], suggest the possibility that the high CAT activity and *RsCAT1* expression are important for termite queens for both an extraordinary long lifespan and high fertility.

Termite queens have high Prx gene *RsPRX6* expression in comparison with non-reproductive individuals.

As a result of a continuous study of antioxidant enzymes, we investigated Prx activity in *R. speratus*. Here, we found that Prx activity of *R. speratus* queens was slightly higher, but not significantly different, than in non-reproductive individuals (Fig 2.7A). There was also no difference in the comparative analysis between insect species (Fig 2.8). Of note, *R. speratus* queens showed markedly higher expression levels of the Prx gene *RsPRX6*, which belongs to the 1-Cys Prx subgroup and has been reported as a factor that rescues declining brain function with advancing age in honeybees [59] (Fig 2.7B). *R. speratus* queens showed higher expression levels of *RsPRX1* and *RsPRX4*, which belong to the typical 2-Cys Prx subgroups, than in nymphs but not workers and soldiers (Fig 2.7C, D). There was no difference of the expression level of *RsPRX5* belonging to the atypical 2-Cys Prx subgroup between queens and non-reproductive individuals (Fig 2.7E).

A previous report described GPx activity as almost absent in insects [60]. However, we investigated the expression level of two GPx genes, *RsGPX* and *RsPHGPX*, to confirm if this is also the case in termite individuals. Non-reproductive individuals had higher levels of *RsGPX* and *RsPHGPX* gene expression than queens (Fig 2.9). GPx activity is too low to be measured in invertebrates [60]; therefore, we considered that the difference in the expression levels among *R. speratus* castes was not important for their antioxidant system.

Taken together, these findings suggested that higher *RsPRX6* gene expression plays an important role in the efficient antioxidant system of termite queens in order to attain great longevity despite their fertile phenotype, as well as CAT activity and *RsCAT1* expression.

2.5 DISCUSSION

Although the question of how social insect queens achieve long lifespan in comparison with non-reproductive individuals has attracted much attention, the molecular mechanisms involved are not yet understood. Recently, several studies about this mechanism have been reported using ants [10,43,61] and honeybees [44,62–64]. Nevertheless, to our knowledge, no research has been published on termite queens, which exhibit extraordinary longevity and fertility as well as ants and honeybees. In the present study, we demonstrated for the first time that an efficient antioxidant system may partly explain this phenomenon in the eusocial subterranean termite *R. speratus*. The oxidative stress theory is a major aging hypothesis and suggests that an efficient antioxidant system contributes to lifespan extension in many organisms including insects [56]. Generally, oxidative stress is caused by over-generation of ROS, and the accumulation of oxidative damage to biomolecules is associated with aging and longevity [2–5]. Here, we revealed that the termite queens maintain lower levels of 8-OHdG than workers after UV irradiation and also constantly maintain lower levels of PC and MDA (Fig 2.2).

From this result, we hypothesized that the queens have a highly efficient antioxidant system. Therefore, we paid attention to the antioxidant enzymes CAT and Prx, which are thought to be major components of the antioxidant system in insects [56], and we investigated whether queens have high antioxidant enzyme activity. We demonstrated that queens had higher CAT activity and *RsCAT1* gene expression levels than non-reproductive individuals in *R. speratus* (Fig 2.5A, B). Surprisingly, CAT activity of queens was also markedly higher in comparison with other solitary insects and eusocial Hymenoptera (Fig 2.5A). These results indicated that CAT plays a role in the efficient antioxidant system in *R. speratus*. A previous study reported that CAT plays a central role in protecting the oocyte

and early embryo from ROS damage in the mosquito *Anopheles gambiae* [58]. Furthermore, another study proposed that CAT is important for female fecundity and mortality in the phlebotomine sand fly *Lutzomyia longipalpis* [57]. These studies also supported our hypothesis that termite queens have an efficient antioxidant system to attain greater longevity.

Although Prx activity in queens was non-significantly higher than the activities in non-reproductive individuals, queens had higher expression levels of *RsPRX6* encoding 1Cys-Prx (Fig 2.7A, B). Abundant 1Cys-Prx expression during embryogenesis was reported in *D. melanogaster* [65], suggesting that *RsPRX6* may be associated with a high rate of cell proliferation during embryogenesis, consistent with the fertile phenotype of termite queens. The levels of 1Cys-Prx expression rescue declining brain function at advanced age in honeybees [59], which also supports the anti-aging phenotype of termite queens. Consequently, these results propose that, because termite queens have an efficient antioxidant system composed of antioxidant enzymes, especially CAT, queens achieve striking longevity.

Previously, Parker *et al.* showed that long-lived queens do not have higher Cu/Zn-SOD activity and SOD gene expression than short-lived adult workers and males in the black garden ant *Lasius niger* [43]. Corona *et al.* also obtained similar results in the honeybee *Apis mellifera* [44]. These two reports indicated that the antioxidant enzymes are not relevant to the unusual characteristics of social insect queens. These findings, which are in contradiction with our results, suggested the possibility that the antioxidant systems of termites are partially different from the antioxidant system of ants and honeybees (or wasps). On the other hand, because we investigated only CAT and Prx in *R. speratus* in this present study, further studies are needed to evaluate other antioxidants such as SOD and vitellogenin, which is a precursor of yolk protein that is thought to be important for social

evolution in all social insects [66].

We observed similar antioxidant activity in termite queens compared with other insects (Fig 2.8). Aerobic respiration is one of the major sources of ROS resulting in oxidative stress [67] and it also has an important role in an organism's lifespan [3]. It is unclear why termite queens do not have higher antioxidant activities than other insect species, but one possibility is that termites, which generally live in hypoxic subterranean habitats (e.g., in wood), might repress their aerobic respiration causing ROS production. Interestingly, several termite species indicated ubiquitously higher respiratory quotients (the rate between oxygen consumption and carbon dioxide emission) above 1.00 [68], suggesting that termites may be capable of repressing aerobic respiration. For this reason, we expected slightly lower levels of ROS generation in the termite body. Therefore, further studies are needed to evaluate the level of ROS production between short-lived and long-lived insects. Moreover, because lower termites such as *R. speratus* have a lot of gut symbionts [69], it remains to be determined whether the antioxidant ability of termites depends on their gut symbiont. Furthermore, we used termite samples that were age-indeterminate in this present study. Thus, long-term studies are also needed to determine the true longevity of termite reproductives in the future.

This comparative study exploits the untapped resource of natural variation in longevity in the eusocial termite *R. speratus*. To the best of our knowledge, we have revealed for the first time that termite queens suffer lower levels of oxidative damage than non-reproductive workers, and that an efficient antioxidant system consisting of several antioxidant enzymes, especially high CAT activity from *RsCAT1* gene expression, may play an important role in their oxidative stress resistance. These findings highlight not only the question of how termite queens achieve long lifespan, but also the evolutionary linkage of reproductive division of labor in social insects.

2.6 FIGURES AND TABLES

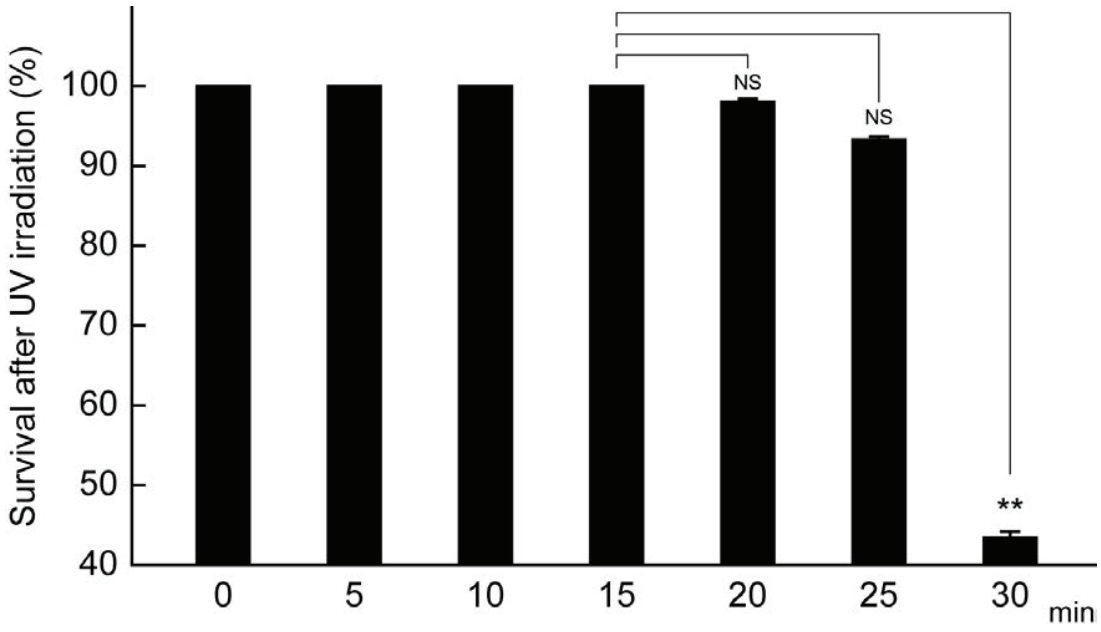

Fig 2.1 | Survival rate after UV irradiation in *R. speratus* workers. Average survival was calculated immediately after 0, 5, 10, 15, 20, 15, and 30 min UV-B irradiation (312 nm, 10.4 kJ/ m^2; Vilber Lourmat TF-20M). Although we observed 100%, 98%, and 93% survival of workers after 0–15, 20, and 25 min irradiation, respectively, workers irradiated for 30 min showed only 43% survival ($p < 0.001$). Six biological replicates were performed for each group of 10 individuals of workers on a Petri dish. Error bars represent standard error of the mean (SEM). Significance was measured by unpaired t test (NS, no significance; **$p < 0.01$).

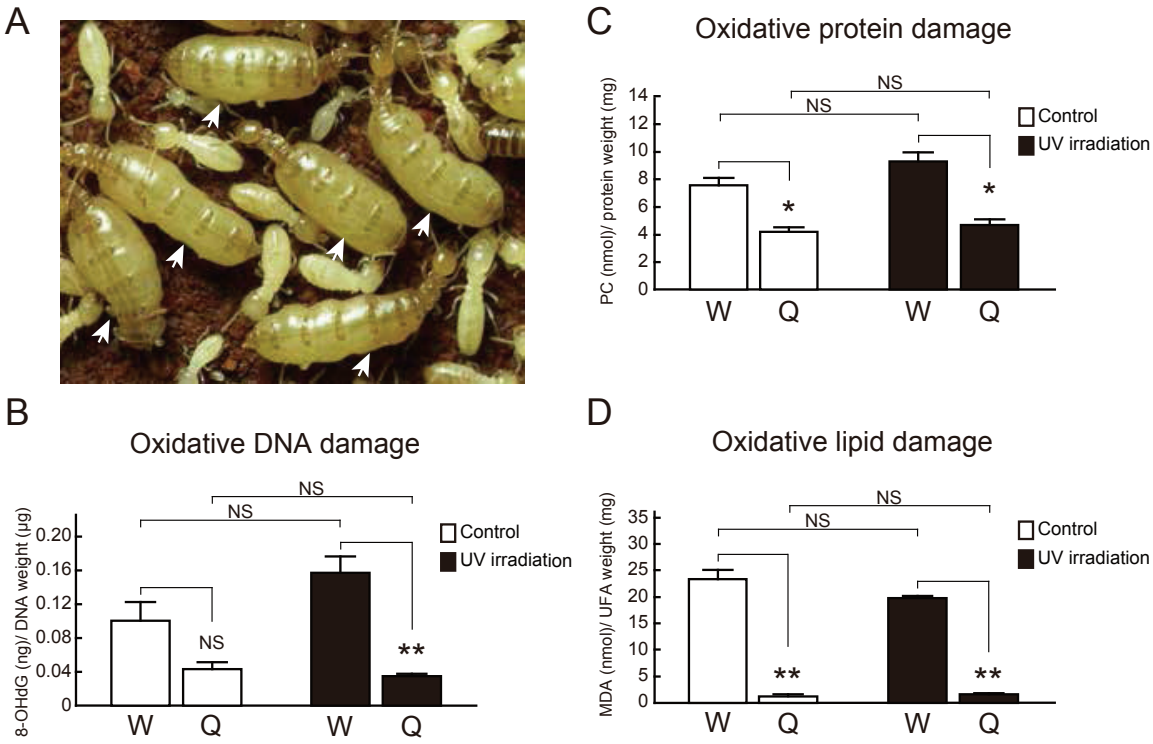

Fig 2.2 | The levels of oxidative damage are different between queens and non-reproductive workers in *R. speratus*. Q, queens; W, workers. (A) The high caste polymorphism between queens and workers in eusocial termite *R. speratus*. Arrowheads indicate queens. (B) No difference in oxidative DNA damage was observed between queens and workers in control conditions (n = 6; for queen/worker: p = 0.106). However, after UV irradiation, queens showed lower levels of 8-OHdG than workers (n = 6; p < 0.001). (C) The levels of protein carboxyl were lower in the body of queens in comparison with workers in control conditions (n = 3; p = 0.019), as well as after UV irradiation (n = 3; p = 0.016). (D) Queens also had lower levels of oxidative lipid damage than workers in both control conditions (n = 3; p < 0.001) and UV irradiated conditions (n = 3; p < 0.001). We used pooled samples, shown as below (Table 1.1), for each replication. White and black

bars indicate control and post UV irradiation, respectively. Error bars represent standard error of the mean (SEM). Significance was measured using unpaired t test followed by Holm's adjustment (NS, no significance; *$p < 0.05$, **$p < 0.01$).

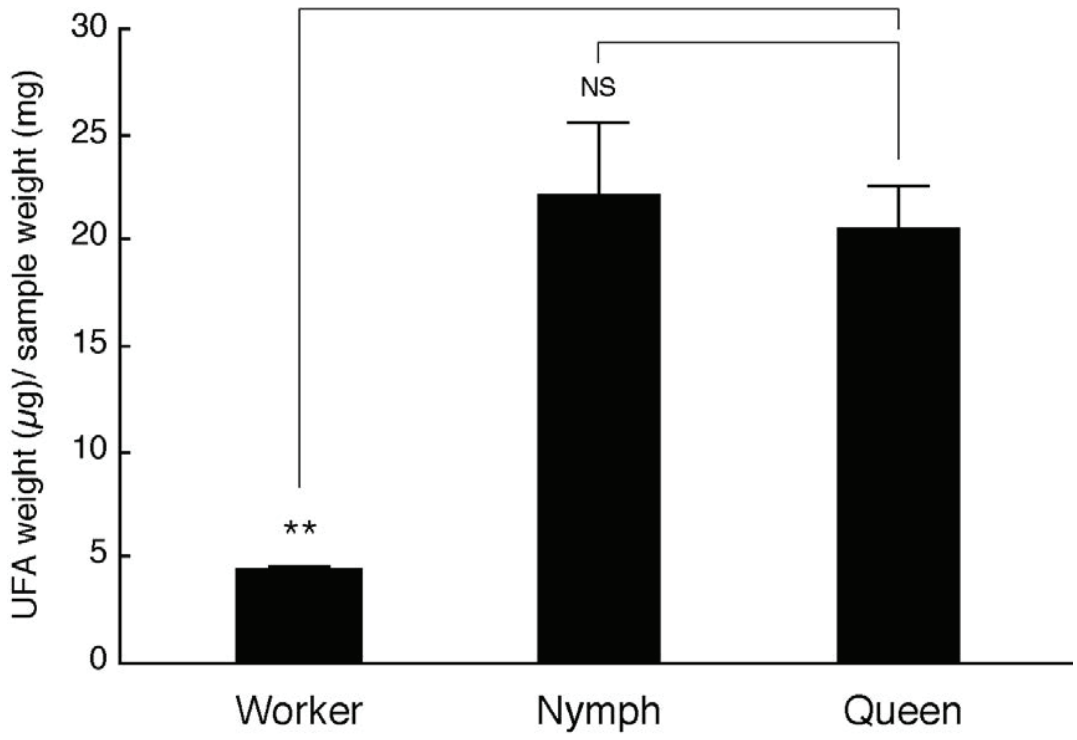

Fig 2.3 | Results of unsaturated fatty acids quantification assay. Queens had higher levels of UFAs susceptible to oxidation than non-reproductive workers ($p = 0.003$) but not nymphs ($p = 0.719$). These data suggested why irradiation cannot increase the malondialdehyde (MDA) levels in workers (Fig 2.3). We used pooled samples, shown as below (Table 1.1), for 3 replications. Error bars represent standard error of the mean (SEM). Significance was measured by unpaired t test followed by Holm's adjustment (NS, no significance; $^{**}p < 0.01$).

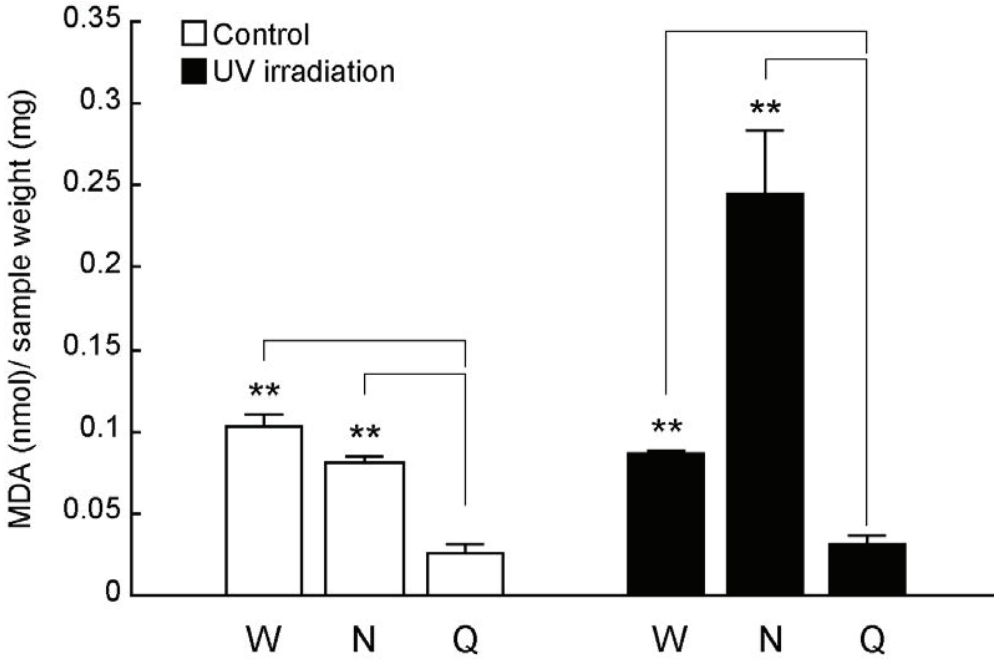

Fig 2.4 | Results of Thiobarbituric acid reactive substances (TBARS) assay. TBARS assays demonstrated that queens had lower levels of malondialdehyde (MDA) than workers ($p = 0.002$) and nymphs ($p = 0.002$) in control conditions. Moreover, after UV irradiation, we found that queens also had a potential to maintain lower MDA levels than workers ($p < 0.001$) and nymphs ($p = 0.005$). We used pooled samples, shown as below (Table 1.1), for 3 replications. W, workers; N, nymphs; Q, queens. White and black bars indicate control and post UV irradiation, respectively. Error bars represent standard error of the mean (SEM). Significance was measured by unpaired t test followed by Holm's adjustment (**$p < 0.01$).

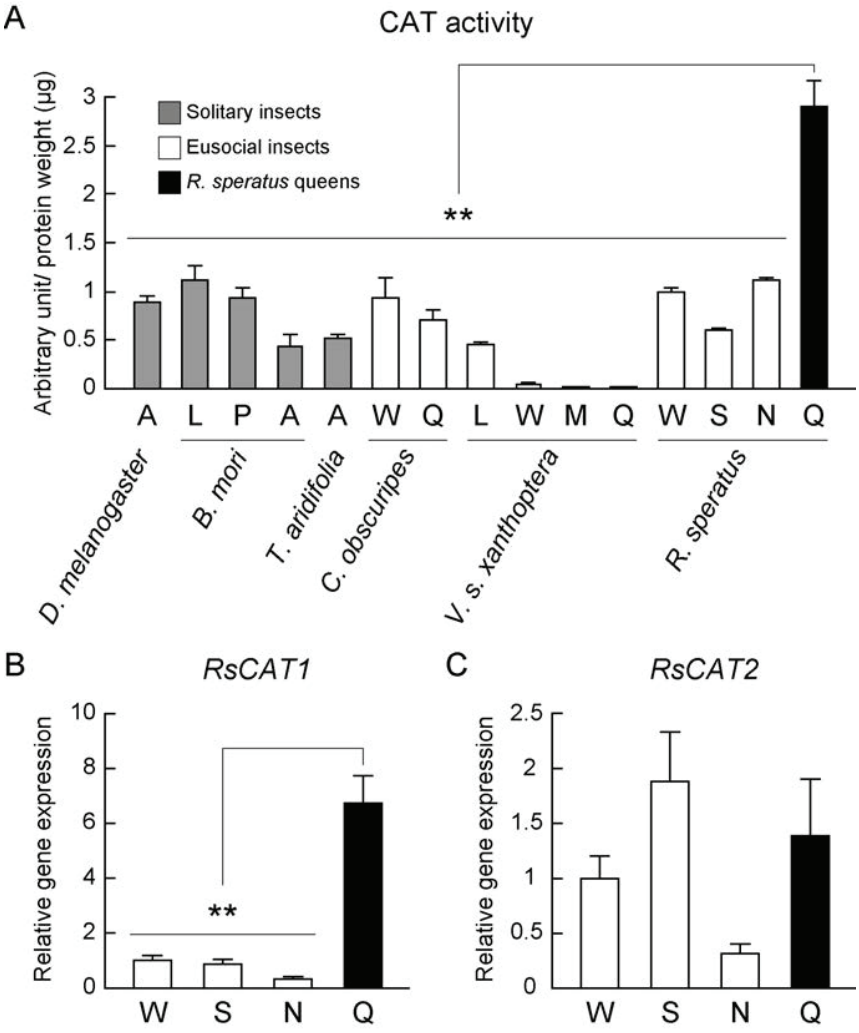

Fig 2.5 | Termite queens have high CAT activity and gene *RsCAT1* expression. A, adults; L, larvae; P, pupae; W, workers; M, male adults; Q, queens; S, soldiers; N, nymphs. (A) Queens of *R. speratus* (n = 12) had markedly higher CAT activity than *D. melanogaster* adults (n = 6; 10 individuals per replicate; $p < 0.001$), *B. mori* larvae (n = 6; $p = 0.001$), *B. mori* pupae (n = 6; $p = 0.001$), *B. mori* adults (n = 6; $p < 0.001$), *T. aridifolia* adults (n = 6; $p < 0.001$), *C. obscuripes* workers (n = 6; 5 individuals per replicate; $p = 0.001$), *C. obscuripes* queens (n = 3; $p = 0.001$), *V. s. xanthoptera* larvae (n = 3; $p = 0.001$),

V. s. xanthoptera workers (n = 3; p = 0.001), *V. s. xanthoptera* adult males (n = 3; p = 0.001), *V. s. xanthoptera* queens (n = 3; p = 0.001), *R. speratus* workers (n = 6; p = 0.001), *R. speratus* soldiers (n = 6; p < 0.001), and *R. speratus* nymphs (n = 6; p = 0.001). The values of CAT activity in solitary insects were pooled male-female data (1:1). (B) Queens of *R. speratus* (n = 9) also showed higher CAT gene *RsCAT1* expression than non-reproductive workers (n = 12; p < 0.001), soldiers (n = 12; p < 0.001), and nymphs (n = 12; p < 0.001). (C) There was no difference in CAT gene *RsCAT2* expression between queens (n = 9) and non-reproductive individuals (n = 12; for queen/worker: p = 0.915; for queen/soldier: p = 0.915; for queen/nymph: p = 0.092). Except as specified in the text, we used one individual of solitary insects or eusocial Hymenoptera for several replications, whereas termite samples were pooled as described below (Table 1.1). All data obtained between male and female of solitary insects and non-reproductive individuals of *R. speratus* were mixed by which the ratio of males and females was 1:1. Gray, white, and black bars indicate solitary insects, eusocial insects, and *R. speratus* queens, respectively. Error bars represent standard error of the mean (SEM). Significance was measured using unpaired t test followed by Holm's adjustment (**p < 0.01).

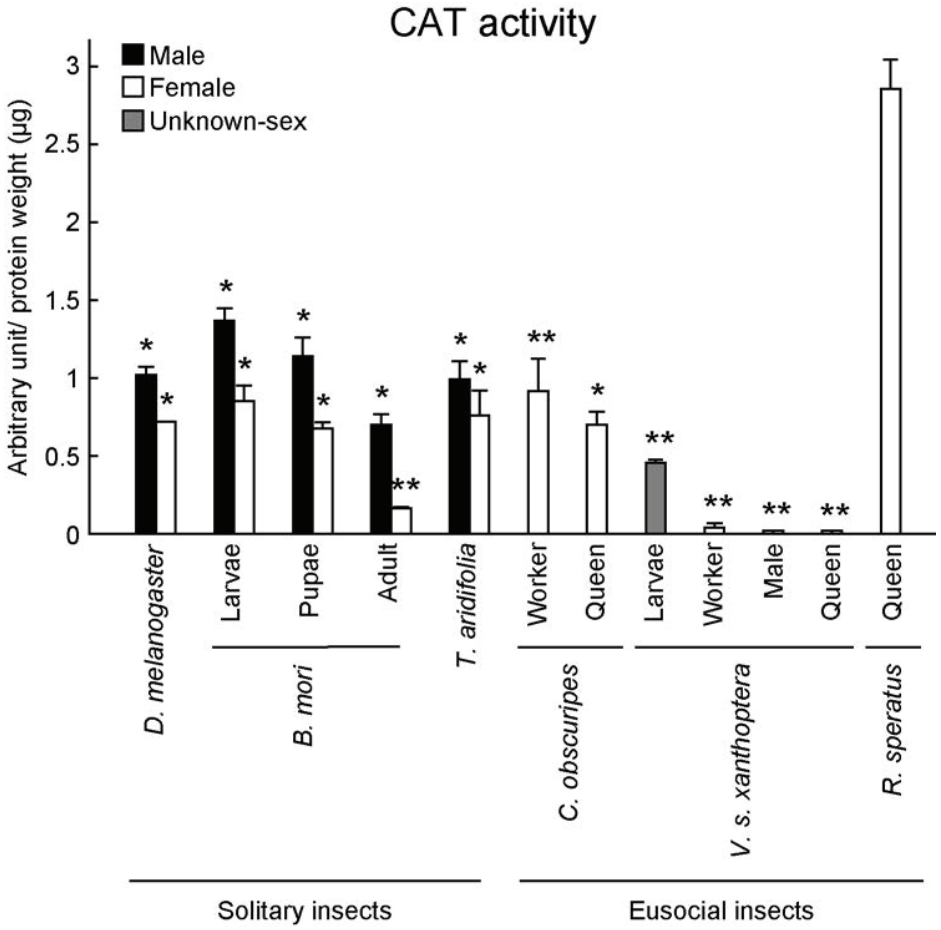

Fig 2.6 | Measurement of CAT activity in several insects. Termite queens (n = 12) had higher CAT activity than *D. melanogaster* adult males (n = 3; p = 0.013), *D. melanogaster* adult females (n = 3; p = 0.011), *B. mori* larvae males (n = 3; p = 0.016), *B. mori* larvae females (n = 3; p = 0.011), *B. mori* pupae males (n = 3; p = 0.014), *B. mori* pupae females (n = 3; p = 0.011), *B. mori* adult males (n = 3; p = 0.011), *B. mori* adult females (n = 3; p = 0.003), *T. aridifolia* adult males (n = 3; p = 0.008), *T. aridifolia* adult females (n = 3; p = 0.006), *C. obscuripes* workers (n = 6; p = 0.002), *C. obscuripes* queens (n = 3; p = 0.0011), *V. s. xanthoptera* larvae (n = 3; p = 0.006), *V. s. xanthoptera* workers (n = 3; p = 0.002), *V. s. xanthoptera* adult males (n = 3; p = 0.002), and *V. s. xanthoptera* queens (n = 3; p =

0.002). Black, white, and gray bars indicate male, female, and unknown-sex, respectively. Error bars represent standard error of the mean (SEM). Significance was measured by unpaired t test followed by Holm's adjustment (*$p < 0.05$, **$p < 0.01$).

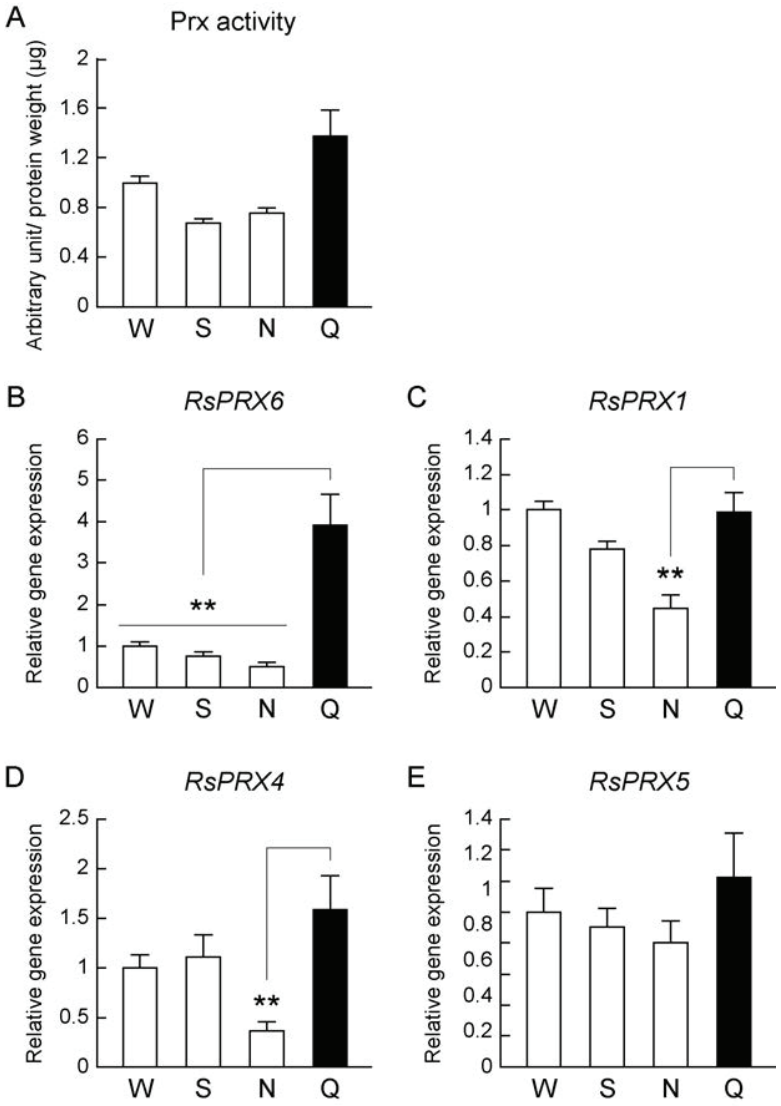

Fig 2.7 | Termite queens have high level of 1-Cys Prx gene *RsPRX6* expression. W, workers; S, soldiers; N, nymphs; Q, queens. (A) There was no difference in Prx activity between queens (n = 9) and non-reproductive individuals (n = 3; for queen/worker: p = 0.342; for queen/soldier: p = 0.279; for queen/nymph: p = 0.279). (B) Queens (n = 9) had higher levels of *RsPRX6* gene expression than workers (n = 12; p < 0.001), soldiers (n = 12;

$p < 0.001$), and nymphs ($n = 12$; $p < 0.001$). (C) Queens ($n = 9$) also had higher *RsPRX1* gene expression than nymphs ($n = 12$; $p = 0.002$) but not workers ($n = 12$; $p = 0.885$) or soldiers ($n = 12$; $p = 0.149$). (D) The level of *RsPRX4* gene expression in queens ($n = 9$) was also higher than nymphs ($n = 12$; $p = 0.003$) but not workers ($n = 12$; $p = 0.184$) or soldiers ($n = 12$; $p = 0.236$). (E) There was no difference in *RsPRX5* gene expression between queens ($n = 9$) and non-reproductive individuals ($n = 12$; for queen/worker: $p = 0.555$; for queen/soldier: $p = 0.555$; for queen/nymph: $p = 0.524$). We used pooled samples for each replication, shown as below (Table 1.1), for several replications. All data obtained between male and female of non-reproductive individuals were mixed by which the ratio of males and females was 1:1. White and black bars indicate non-reproductive individuals and queens, respectively. Error bars represent standard error of the mean (SEM). Significance was measured by unpaired t test followed by Holm's adjustment (**$p < 0.01$)

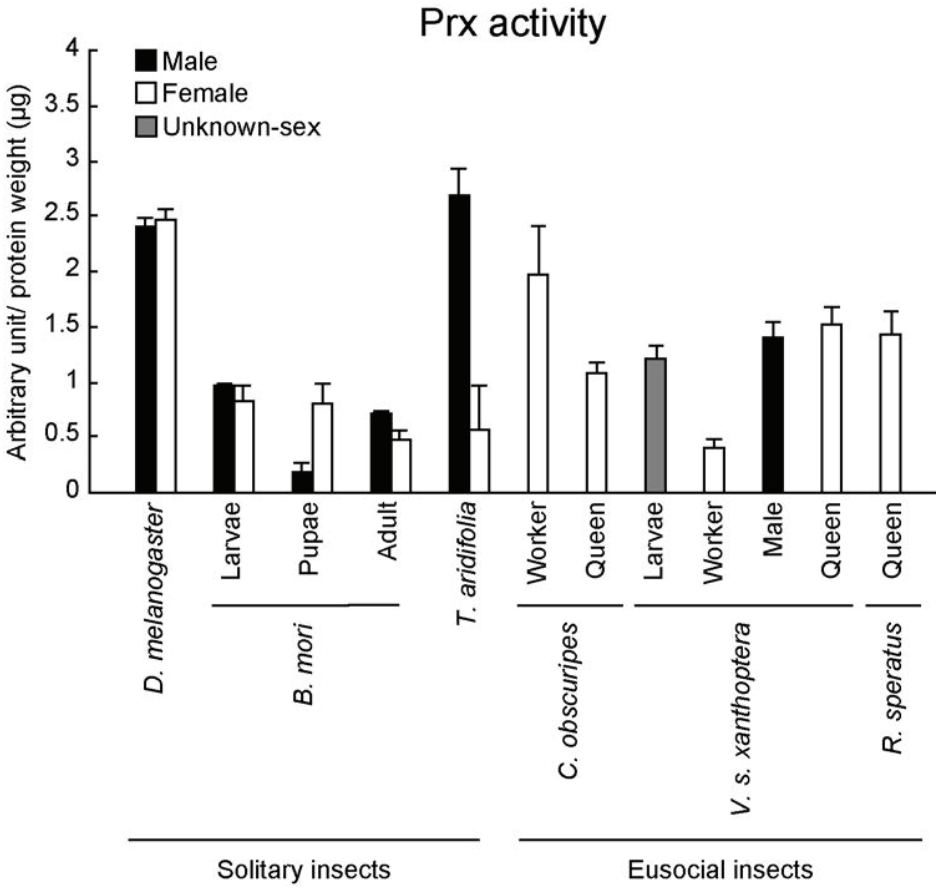

Fig 2.8 | Measurement of Prx activity in several insects. There is no difference in Prx activity between termite queens and other insects. Termite queens had almost the same activity as *D. melanogaster* adult males (n = 3; p = 0.396), *D. melanogaster* adult females (n = 3; p = 0.359), *B. mori* larvae males (n = 3; p = 0.267), *B. mori* larvae females (n = 3; p = 1.000), *B. mori* pupae males (n = 3; p = 0.169), *B. mori* pupae females (n = 3; p = 1.000), *B. mori* adult males (n = 3; p = 0.879), *B. mori* adult females (n = 3; p = 0.403), *T. aridifolia* adult males (n = 3; p = 0.179), *T. aridifolia* adult females (n = 3; p = 0.793), *C. obscuripes* workers (n = 3; p = 1.000), *C. obscuripes* queens (n = 3; p = 1.000), *V. s. xanthoptera* larvae (n = 3; p = 1.000), *V. s. xanthoptera* workers (n = 3; p = 0.359), *V. s.*

xanthoptera adult males (n = 3; p = 1.000), and *V. s. xanthoptera* queens (n = 3; p = 1.000). Black, white, and gray bars indicate male, female, and unknown-sex, respectively. Error bars represent standard error of the mean (SEM). Significance was measured by unpaired t test followed by Holm's adjustment (*p < 0.05, **p < 0.01).

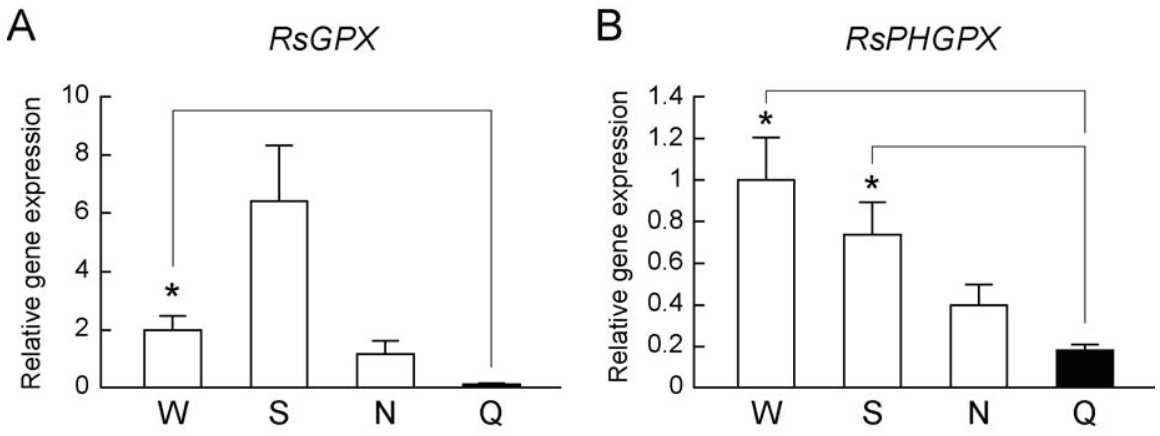

Fig 2.9 | The level of GPX genes *RsGPX* and *RsPHGPX* expression in *R. speratus*. The levels of GPx gene expression were equal or lower in queens compared with non-reproductive individuals. W, workers; S, soldiers; N, nymphs; Q, queens (A) Queens (n = 6) had no significant difference in the levels of *RsGPX* expression in comparison with soldiers (n = 12; p = 0.068) and nymphs (n = 12; p = 0.103). Nevertheless, queens showed lower levels than workers (n = 12; p = 0.039). (B) Queens (n = 6) had almost the same levels of *RsPHGPX* expression than nymphs (n = 12; p = 0.138). However, queens had slightly lower levels of *RsPHGPX* expression than workers (n = 12; p = 0.040) and soldiers (n = 12; p = 0.049). We used pooled samples, shown as below (Table 1.1), for several replications. All data obtained between male and female of non-reproductive individuals were mixed by which the ratio of males and females was 1:1. White and black bars indicate non-reproductive individuals and queens, respectively. Error bars represent standard error of the mean (SEM). Significance was measured by unpaired t test followed by Holm's adjustment (*$p < 0.05$).

Table 1.1 | Termite sample list

Analysis	Colony ID	Termite samples (pooled number of individuals per replications)
TBARS assay and lipid quantification	YY141021A	Worker (5), nymph (3), and queen (2)
Protein carbonyl assay	YY150910A	Worker (5) and queen (2)
8-OHdG assay	YY151022A	Worker (5) and queen (1)
8-OHdG assay	YY160729A	Worker (5) and queen (1)
CAT and Prx activities	YY140731A	Worker (10), soldier (8), nymph (5), and queen (4)
CAT and Prx activities	YY140914A	Queen (4)
CAT and Prx activities	YY141014A	Queen (4)
CAT activity	YY140930A	Queen (4)
CAT and Prx genes expression	YY130807A	Worker (3), soldier (3), nymph (2), and queen (1)
CAT and Prx genes expression	YY151118A	Worker (3), soldier (3), nymph (2), and queen (1)
CAT and Prx genes expression	YY140919A	Queen (1)

Numbers in Colony IDs indicate the dates when the colonies were collected (e.g., colony YY141021A was collected on October 21, 2014).

Table 1.2 | Sequences of primers used in this study

Target gene	Sequence (5'–3')	Amplicon (bp)
RsCAT1	Forward; TGGCTATGGCTCTCACACATTC	91
	Reverse; TTTGATGCCTTGGTCTGTCTTG	
RsCAT2	Forward; CGGGGCTTTGCTGTGAA	84
	Reverse; GTCCCTGATAAAGAAGATTGGTGTG	
RsPRX1	Forward; TCTGACCGTGTAGCCGAGTTT	106
	Reverse; CCTTCTTGCGTGGAGTGTTG	
RsPRX4	Forward; TGTATGCCCTACAGAAATTCTTGC	131
	Reverse; CCTTCCTTGGTGTGTTTGTCC	
RsPRX5	Forward; GCTGTAAGGCGTGTAGTGTTGTCT	85
	Reverse; GCTTGTCACCAACCTGAATAACC	
RsPRX6	Forward; GAATTCCCGAATTTCAAAGCAG	97
	Reverse; CCGAAGGATGCGAAAACAA	
RsGPX	Forward; ATGTTCGGCCAGGGAATG	117
	Reverse; TTGTGGAAGGGCAATGTTTCT	
RsPHGPX	Forward; GAAATAGTGTGCTTTGCCAGGTC	120
	Reverse; AGTTCCTCCTTGCTTGTGCTTC	
RsGAPDH	Forward; CCATAGAAAAGGCTTCTGCACATT	89
	Reverse; AACAACAAACATTGGGGCATC	

Table 1.3 | Target gene information for this study

Target gene	Target gene ID	Accession no.	Query genes (GeneBank no.)	Query species
RsCAT1	comp783914_c0_seq4	FX983162	Catalase (KDR07976.1)	*Z. nevadensis*
RsCAT2	comp808329_c0_seq1	FX983163	Catalase (KDR21530.1)	*Z. nevadensis*
RsPRX1	comp811232_c3_seq2	FX983166	Typical 2Cys-Peroxiredoxin (KDR08683.1)	*Z. nevadensis*
RsPRX4	comp795973_c0_seq1	FX983167	Typical 2Cys-Peroxiredoxin (KDR20462.1)	*Z. nevadensis*
RsPRX5	comp804180_c8_seq4	FX983168	Atypical 2Cys-Peroxiredoxin (KDR23852.1)	*Z. nevadensis*
RsPRX6	comp804234_c2_seq1	FX983169	1Cys-Peroxiredoxin (KDR15106.1)	*Z. nevadensis*
RsGPX	comp807654_c0_seq1	FX983170	Glutathione peroxidase 6-like (KDR10349.1)	*Z. nevadensis*
RsPHGPX	comp780877_c0_seq2	FX983171	Phospholipid hydroperoxide glutathione peroxidase (KDR22003.1)	*Z. nevadensis*
RsGAPDH	comp666388_c0_seq2	FX983172	Glyceraldehyde 3-phosphate dehydrogenase (KDR24072.1)	*Z. nevadensis*

CHAPTER III: Uric acid: An Important Antioxidant Contributing to Survival in Termites.

3.1 ABSTRACT

Reactive oxygen species (ROS) are generated spontaneously in all organisms and cause oxidative damage to biomolecules when present in excess. Accumulated oxidative damage accelerates aging; enhanced antioxidant capacity may be a positive factor for longevity. Recently, numerous studies of aging and longevity have been performed using short-lived animals, however, longevity mechanisms remain unknown. Here we show that a termite *Reticulitermes speratus* that is though to be long-lived eusocial insect than other solitary insects uses large quantities of uric acid as an antioxidant against ROS. We demonstrated that the accumulation of uric acid considerably increases the free radical-scavenging activity and resistance against ultraviolet-induced oxidative stress in laboratory-maintained termites. In addition, we found that externally administered uric acid aided termite survival under highly oxidative conditions. The present data demonstrates that in addition to nutritional and metabolic roles, uric acid is an essential antioxidant for survival and contributes significantly to longevity. Uric acid also plays important roles in primates but causes gout when present in excess in humans. Further longevity studies of long-lived organisms may provide important breakthroughs with human health applications.

3.2 INTRODUCTION

Numerous studies of longevity and lifespan extension have been performed using various organisms, including yeast, fruit fly, nematodes, and mice, and various metabolic pathways and molecules have been implicated in life span extension [2]. In particular, growth hormone, insulin, insulin like growth factor-1, and target of rapamycin pathways have been actively investigated, and sirtuin genes have been identified as 'longevity genes' that are upregulated in animals whose lives have been prolonged by caloric restriction [70]. Sirtuins are NAD^+-dependent protein deacetylases that regulate various downstream molecules and are highly conserved from yeast to human [71]. In addition to life span-extension using caloric restriction, long-lived organisms have been generated by genetic engineering [72].

Yeast, fruit fly, nematodes, and mice are ideal models for studying the mechanisms of longevity, with relatively short lifespan and short gestation times. However, novel animal models have recently been made applicable for longevity studies following the development of techniques, such as new generation sequencing analysis. Among these, the naked mole rat *Heterocephalus glaber* and the blind mole rats *Spalax sp*. and *Nannospalax sp*. are subterranean eusocial rodents with extraordinarily long lifespans and resistance to tumorigenesis [73]. Although several studies of these animals are underway, the core mechanisms of longevity remain unidentified. Various eusocial insects are long-lived and reproductive and non-reproductive individuals contribute distinct services to colonies of ants, bees, wasps, and termites. In particular, the lifespans of reproductive and non-reproductive termites differ by 10–100 fold, although the longevity of non-reproductive termites is much longer than that of common solitary insects [10,12,30]. Although extensions of life span have been of interest for a long time, the mechanisms that contribute to longevity remain unknown.

In this study, we investigated the contribution of oxidative defences to the longevity of termites. Specifically, reactive oxygen species (ROS) are generated spontaneously during normal metabolic activities, and excessive ROS generation causes damage to biomolecules, such as DNA, proteins, and lipids. Accordingly, accumulated oxidative damage has been shown to reduce lifespan in mice, insects, yeast, and nematodes, whereas enhanced antioxidant capacity contributes to longevity [39,74]. In addition, immotile plants have various antioxidants such as ascorbic acid and flavonoids that protect against strong oxidative stress in harsh environments. In the present study, we hypothesised that long-lived termites have strong oxidative defence mechanisms and showed that the common Japanese termite *R. speratus* produces large quantities of the strong antioxidant uric acid, which contributes to longevity.

3.3 MATERIALS AND METHODS

Samples and treatments

Termites *(Reticulitermes speratus*), mantises (*Tenodera aridifolia*) and ants (*Camponotus obscuripes*) were collected in the campus of Yamaguchi University. Fruit flies (*Drosophila melanogaster*) and silkworms (*Bombyx mori*) were a kind gift from Prof. R. Murakami and Prof. J. Kobayashi at Yamaguchi University, respectively. Hornets (*Vespa simillima*) were obtained from a pest exterminator. Insect samples were divided into categories of sex, developmental stage, and caste, and were stored at −80°C until use.

Frozen samples were powdered in liquid nitrogen using a mortar and pestle. After dissolving in sample buffer containing 20 mM Tris-HCl (pH 7.5) and 2% protease inhibition cocktail (Nacalai Tesque, Kyoto, Japan), samples in tubes were homogenized further using a sonicator (TOMY UD-201, Tokyo, Japan) on ice. Samples were then centrifuged at 17,000 × *g* for 10 min at 4°C, and protein concentrations in supernatants were determined using BCA Protein Assay Kits (ThermoFischer scientific, Massachusetts, USA).

Heat- and proteinase- resistance tests were performed by boiling the extracts from *R. speratus* soldiers for 10 min or by treating them with 2% proteinase K (Takara, Kusatsu, Japan) and 0.3% sodium dodecyl sulphate (Wako, Tokyo, Japan) followed by warming to 55°C.

Oxidative damage analyses were performed using UV-B irradiation (312 nm, 10.4 kJ/ m2) with a UV irradiator (Vilber Lourmat TF-20M, Eberhardzell, Germany). In these experiments, five individual termites per group were prepared on petri dishes and were irradiated equally. Termites remained alive after irradiation.

For termite survival assays, 30 workers or soldiers were maintained on cellulose

paper in 35 mm dishes. In allopurinol-feeding experiments, 1 mL of 100 mM allopurinol (Wako, Tokyo, Japan) was dropped on the cellulose paper and was consumed with the paper. Uric acid feeding was administered by dropping 1 mL of 0.6 mM uric acid suspension onto cellulose papers, and 1 mL of 100 mM allopurinol in 0.6 mM uric acid suspension was dropped onto cellulose papers of the cotreatment group. DW was used as a control group. In experiments with paraquat feeding, 0.05 M paraquat, and/or 0.05 M uric acid were dropped onto cellulose paper in the same manner.

Free radical scavenging activity assay

Antioxidant activities of soluble insect extracts were evaluated using 1, 1-diphenyl-2-picryl hydrazyl (DPPH) radical scavenging assays according to established protocols with modifications [75]. Briefly, frozen insects were powdered in liquid nitrogen and samples were extracted using 500 μL of deionized water. Subsequently, 50 μL samples containing 7.5 μg of protein and 0.02–0.2 mM trolox standards were prepared in 96-well plates, and 100 μL aliquots of 0.15 mM DPPH (Merck Millipore, Massachusetts, USA) solution in EtOH was added to the wells. After incubating for 30 min at 25°C, absorbance of plate wells was measured at 517 nm using a spectrophotometer. Free radical scavenging activities were calculated as trolox equivalents (μM)/protein weight (mg).

***In vivo* imaging of reactive oxygen species (ROS)**

In vivo detection of ROS in termite bodies was achieved by injecting the ROS-sensitive reagent dihydrorhodamine 123 (DHR123; ThermoFischer scientific, Massachusetts, USA). Briefly, 25 μM (or 0–40 μM only in supplement figure) DHR123 was prepared and loaded into a glass capillary (Drummond, Pennsylvania, USA). DHR123 solution was then injected into the thorax of CO_2-anesthetised termites using a FemtoJet

microinjector (Eppendorf, Hamburg, Germany). Injected termites were then subjected to UV irradiation for 0, 5, and 10 min (312 nm; 0, 2.6, and 5.2 kJ/m^2, respectively; Vilber Lourmat TF-20M) through trial- and- error, and fluorescence was observed using a fluorescence microscope (Leica AF 6000 macro modular system, Wetzlar, Germany). Fluorescent intensities of saved images were analysed and quantified using Image J. In this injection method, the injection volume was controlled throughout the series of experiments by using the same glass capillary.

Thiobarbituric acid reactive substances (TBARS) assay

Oxidative damage was assessed according to lipid peroxidation using the methods reported by Iuchi *et al*. [45] with TBARS assay kits (Cayman chemical, Michigan, USA). Briefly, whole termite worker bodies were UV irradiated for 20 min (312 nm; 10.4 kJ/m^2) according to a previous method (in Chapter II) and subsequently homogenised in 200 µL of ice-cold buffer containing 20 mM Tris-HCl (pH 7.5) and 2% protease inhibitor cocktail. Malondialdehyde (MDA) standards and samples were mixed with 50 µL of 10% SDS solution and 1 mL of colour reagent containing 0.53% thiobarbituric acid, 10% acetic acid, and 1.5% sodium hydroxide, and were incubated for 30 min at 100°C. Samples were then incubated on ice for 10 min to stop the reaction and were finally centrifuged at 17,000 × *g* for 10 min at 25°C. Absorbance of the obtained supernatants was determined at 532 nm and TBARS levels were calculated from a MDA standard curve.

HPLC and LC/MS/MS analysis

358.1 mg of *R. speratus* termite soldiers were homogenised by sonication (TOMY UD-201) in 5.0 mL of ice-cold LC/MS grade water (Kanto chemical, Tokyo, Japan). After centrifugation, supernatants were collected and cleared through 0.22 µm filters (Millex®GP,

Merck Millipore, Massachusetts, USA) for HPLC analyses. Sample extracts were then applied to a Superiorex ODS 5 m (4.6 × 150 mm) column (Shiseido, Tokyo, Japan) and were analysed using a LC-20A system (Shimadzu Scientific Instrument, Tokyo, Japan) under the following conditions: Column temperature, 40°C; injection volume, 10 mL; flow rate, 0.6 mL/min, detection wavelength, 190–320 nm; mode, gradient mode using 0.05% acetic acid (A) and 100% methanol (B) as the mobile phase. In these gradient analyses, the starting solvent was 95% (A) and the concentration of (B) was then increased to 25% over 4.5 min. The concentration of (B) was then maintained at 25% for 1.5 min and was then decreased to 5% over 10 min. Elutes were fractionated and collected every 10 s and antioxidant activities of fractions were measured using DPPH assays.

To identify the termite antioxidant, samples were analysed using a 3200 Q TRAP LC/MS/MS system (AB Sciex Pte. Ltd., Massachusetts, USA) equipped with an ESI interface operated in negative-ion mode. Termite antioxidants were analysed in accordance with the method of Kim *et al.* [76] Analytical conditions were configured as for HPLC analyses, and uric acid (Wako) in 5 mM ammonia solution was used as a standard. LC samples were obtained from *R. speratus* soldiers and were further purified using thin-layer chromatography (TLC Silica gel 60 RP-18 F254s, EMD Millipore). Uric acid standard and LC samples were analysed in negative electrospray ionization (ESI) mode and the chemical structure was identified using a multiple reaction monitoring-enhanced product ion (MRM-EPI) scan. The parent ion of uric acid was m/z 167.0 and the major EPI was m/z 124.0.

Quantification of uric acid contents

Termite uric acid contents were quantified using Uric acid-C kits (Wako, Tokyo, Japan) according to the manufacturer's instructions. Briefly, 3–5 individuals were

desiccated by sonication in 0.5 mL of DW and were then centrifuged at 17,000 × *g* for 10 min at 4°C. Subsequently, 300 μL supernatants were retrieved as sample extracts, and 50 μL aliquots were mixed with working reagent and incubated for 10 min at 37°C. Uric acid contents were determined colorimetrically and were compared with serially diluted standard uric acid solutions.

Statistical analysis

Statistical tests and significances are specified in every figure legend. Most statistical analyses were performed using R software package (version 3.2.2). Multiple comparisons were performed using unpaired two-tailed *t*-tests followed by *P* value correction using Holm's method [48]. Data are presented as means ± standard errors of the mean (SEM), and all calculated *P* values are presented in the figure legends. Survival tests were performed using Peto-Peto and Cochran-Mantel-Haenszel log -rank methods in Excel (Microsoft, Washington, USA).

3.4 RESULTS

Termites have high free radical scavenging activity.

Initially, we determined total antioxidant capacities in soluble extracts from whole bodies of various insect species, including eusocial species. DPPH free radical scavenging assays revealed that the Japanese termite *R. speratus* has high antioxidant activity compared with other insects (Fig 3.1A). This high activity was detected in bodies of all termite castes apart from workers. Moreover, the heat- and proteinase-resistant antioxidant in these termites was not ascorbic acid (Figs 3.1B, C and 3.2). The antioxidant accumulated in the abdomen but was present at low levels in the guts of soldier bodies, indicating endogenous generation in individuals (Fig 3.3).

Strong antioxidant protects bodies from oxidative stress in termites.

In subsequent studies, we investigated antioxidant function inside termite bodies using the ROS-sensitive agent dihydrorhodamine123 (DHR123) after microinjection into lateral thoraxes of *R. speratus* workers and soldiers (Figs 3.4A and 3.5). After ultraviolet (UV) irradiation producing ROS [52] for 0, 5, and 10 min, fluorescence intensity was measured using a fluorescent microscope. These analyses showed low quantities of the antioxidant in workers and concomitant sensitivity to UV irradiation. In contrast, soldiers containing high amounts of the antioxidant were more resistant to UV irradiation than workers (Fig 3.4B). These data suggest the possibility that this antioxidant protects termites from oxidative stress generated by UV irradiation. To investigate the importance of this termite antioxidant in oxidative stress defence system, we subjected termites to varying oxidative conditions and measured changes in antioxidant quantities in termite bodies after maintenance under aerobic (opened) and anaerobic (closed) conditions. Free radical

scavenging activity of the termite antioxidant was gradually increased in workers that were maintained under aerobic conditions (Fig 3.4C). In further experiments, we investigated whether the termite antioxidant is protective against oxidative damage to biomolecules, and measured lipid peroxidation products using assays of thiobarbituric acid reactive substances TBARS assays. After the induction of oxidative stress by UV irradiation, the lipid peroxidation marker malondialdehyde (MDA) was present at lower concentrations in workers that had been maintained under laboratory conditions for 5 weeks than in freshly collected individuals (Fig 3.4D), suggesting that biomolecules in termite bodies are protected by this antioxidant.

Uric acid is an antioxidant in termites.

In a previous report, uric acid gradually accumulated inside termite bodies after maintenance in a laboratory for a long time [77]. Uric acid is also known to exhibit strong free radical-scavenging activity in humans and several insects [78–80].Therefore, we hypothesized that the increased antioxidant might be uric acid in laboratory-maintained workers. To determine the role of uric acid in the observed antioxidant activities of termites, soluble extracts from termite soldiers were fractionated using HPLC (Fig 3.6A) and free radical scavenging activities of the collected samples were measured. In these experiments, peak free radical scavenging activities (Fig 3.6B) corresponded with the highest peak for uric acid in HPLC fractions. Subsequently, this peak fraction was applied to LC-MS/MS analyses and the implied antioxidant was compared with a uric acid standard. These analyses indicated that peaks of the fragmented ion from termite samples matched those of the uric acid standard (Fig 3.6C), indicating that the major antioxidant in termites is uric acid (product ion-monitoring data are shown in Fig 3.7). In further experiments, we determined the proportion of total antioxidant activity that can be ascribed to uric acid by

treating extracts with the uric acid conversion enzyme uricase (Fig 3.8A). These experiments showed that antioxidant activities in extracts diminished with decrease in uric acid concentrations (Fig 3.8B), suggesting that uric acid is a pivotal antioxidant in termite bodies.

Uric acid enhances termite worker survival in laboratory assays.

Although termite workers have comparatively low levels of uric acid immediately after collection from the field, laboratory-maintained workers accumulated uric acid [77]. Consistent with these previous reports, the body colour of *R. speratus* workers gradually changed to white under laboratory conditions (Fig 3.9A). Consequentially, we compared UV resistance of three groups of workers after maintenance under laboratory conditions at various times. In these experiments, uric acid levels and antioxidant activities increased with time in laboratory-maintained workers (Figs 3.9B and C), and ROS levels decreased inside the body (Fig 3.9D). Because laboratory conditions (open air) may be more aerobic than the insides of termite colonies (confined spaces), the present increases in antioxidant activity due to uric acid accumulation are likely an adaptation to oxidative stress.

Finally, we investigated whether termite uric acid is essential for survival by monitoring survival of termite workers in the presence of the uric acid synthesis inhibitor allopurinol. Allopurinol dose-dependently decreased survival, suggesting that uric acid depletion from worker bodies leads to death (Fig 3.10A). Externally administered antioxidants, including vitamin C, E, and some flavonoids reportedly improved longevity in various animal models [81]. Thus, in further experiments, we examined the effect of added uric acid and observed positive effects on termite longevity. Specifically, orally ingested uric acid rescued survival rates following allopurinol intake (Fig 3.10B). Moreover, decreased uric acid contents and free radical scavenging activities of allopurinol-treated

termite bodies were recovered by uric acid intake (Fig 3.10C).

Given that uric acid has been considered an important nitrogen source for many insects, including termites [82], uric acid depletion by allopurinol may lead to death irrespective of its antioxidant activities. Thus, to investigate whether uric acid improves termite longevity under highly oxidative conditions, and to distinguish between antioxidant and nutritional roles, termite workers were fed uric acid concurrently with the pro-oxidant paraquat. The survival curves in Fig 3.10D indicate that uric acid intake rescues termite survival rates in the presence of paraquat, suggesting that uric acid contributes to termite longevity essentially as an antioxidant.

3.5 DISCUSSION

Herein, we have presented evidence that in addition to roles as a nutritional source of nitrogen, large quantities of uric acid in some termite castes play antioxidant roles. Furthermore, we demonstrate that uric acid positively participates in termite longevity and stress responses. Uric acid is the main end product of nitrogen metabolism in insects, reptiles and birds, whereas the main end product in mammals is urea. Uric acid functions as a major plasma antioxidant, and is the end product of purine metabolism in most primates including humans. Several insect species use uric acid as a protective compound. Accordingly, body colour of the silkworm *Bombyx mori* is reportedly influenced by epithelial uric acid, which protects against UV radiation from the sun. Several uric acid-deficient silkworm mutants have been generated in previous studies and these mutants have translucent skin owing to a deficiency in xanthine dehydrogenase, which synthesises uric acid [83]. Uric acid contents in silkworms were also reduced after feeding with the specific xanthine dehydrogenase inhibitor allopurinol, and uric acid-depleted silkworms were hypersusceptible to UV irradiation [79]. Moreover, in experiments with the fruit fly *Drosophila melanogaster*, the uric acid-deficient mutant *rosy* was susceptible to high temperatures and oxidative stress [80]. These data suggest that uric acid plays important antioxidant roles in addition to those as a metabolic product. Thus, to investigate the function of uric acid as a defence mechanism, we assessed the internal redox status of termite bodies using a ROS-sensitive fluorescent reagent, and visualised *in vivo* oxidative stress in whole insect bodies.

UV irradiation is an artificial source of oxidative stress for termite species, because termite workers and soldiers are rarely exposed to sunlight. Thus, to model physiologically relevant oxidative stress, we reduced uric acid in termites using allopurinol and examined

survival. Allopurinol intake markedly reduced termite survival rates in a dose-dependent manner (Fig 3.10A), reflecting the importance of uric acid. Because allopurinol has a purine skeleton, it also acts on enzymes of nucleic acid metabolism, likely leading to toxicity and decreased longevity irrespective of uric acid depletion. Thus, to distinguish between these effects we supplemented allopurinol-treated termite workers with uric acid. Under these conditions, uric acid administration rescued survival, indicating that even exogenous uric acid can compensate for deficiencies in uric acid production, and that endogenous uric acid is positively associated with survival. To determine whether uric acid functions as an antioxidant inside termite bodies, we performed experiments with the toxic pro-oxidant paraquat and observed decreased termite survival that again could be arrested by intake of uric acid. These observations indicate that uric acid protects against paraquat toxicity, possibly reducing oxidative stress by scavenging paraquat-mediated ROS. Furthermore, absolute uric acid intake was associated with increased survival rates, indicating survival advantages of increased uric acid contents. Previous studies suggest that termite uric acid is degraded by intestinal anaerobic bacteria and is reused as a source of carbon, nitrogen, and energy [82,84]. As a potential mechanism for uric acid accumulation, termites that are maintained outside of the subterranean colony may experience increased oxidative stress under more aerobic conditions potentially leading to decreases in intestinal anaerobic bacteria and slowed uric acid degradation. This hypothetical mechanism could effectively upregulate antioxidant activities in termites that are exposed to aerobic conditions.

Taken together, the present data indicate that uric acid contributes to termite longevity. Specifically, whole termite castes had large quantities of uric acid. However, female nymphoid neotenics (secondary queens) and primary kings had lower uric acid contents, suggesting the presence of other mechanisms of longevity, and warranting further

analyses of antioxidant activities and enzymes and longevity in reproductive termites (Chapter II). It remains unknown how and where uric acid functions in termite bodies. In addition, high accumulation of poorly soluble uric acid may lead to crystallisation, although the present data suggest that termites can regulate the solubility of uric acid. Investigations of the associated mechanisms of uric acid solubility may lead to interventions that dissolve crystallised uric acid and improve conditions for humans with gout.

3.6 FIGURES

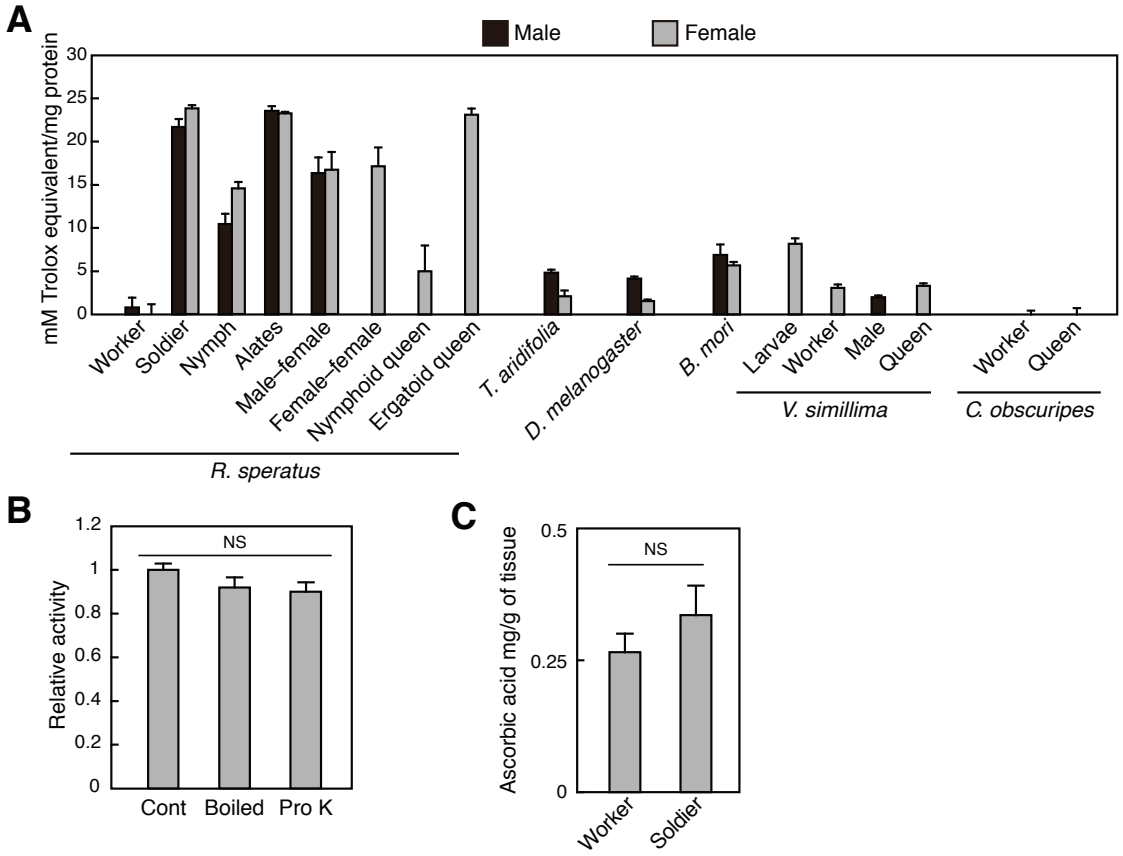

Fig 3.1 | Strong antioxidants in termites *Reticulitermes speratus*. (A) Free radical scavenging activities in various species of insects; soluble extracts from *R. speratus*, mantis (*Tenodera aridifolia*), fruit fly (*Drosophila melanogaster*), silkworm (*Bombyx mori*), hornet (*Vespa simillima*) and ant (*Pristomyrmex punctatus*) were used for DPPH radical scavenging assays. Male–female, male–female paired young primary reproductives; Female–female, female–female paired young primary reproductives. Black boxes indicate male and grey boxes indicate female (n = 3–6). (B) The antioxidant activity of termite soldiers after the control, heat (boiled), and proteinase (Pro K) treatments (n = 3–6). (C)

The ascorbic acid contents of termite workers and soldiers (n = 3). (D) Data are presented as means ± s.e.m. Statistical significance was assayed using the unpaired *t*-test followed by Holm's adjustment [no significance (ns)].

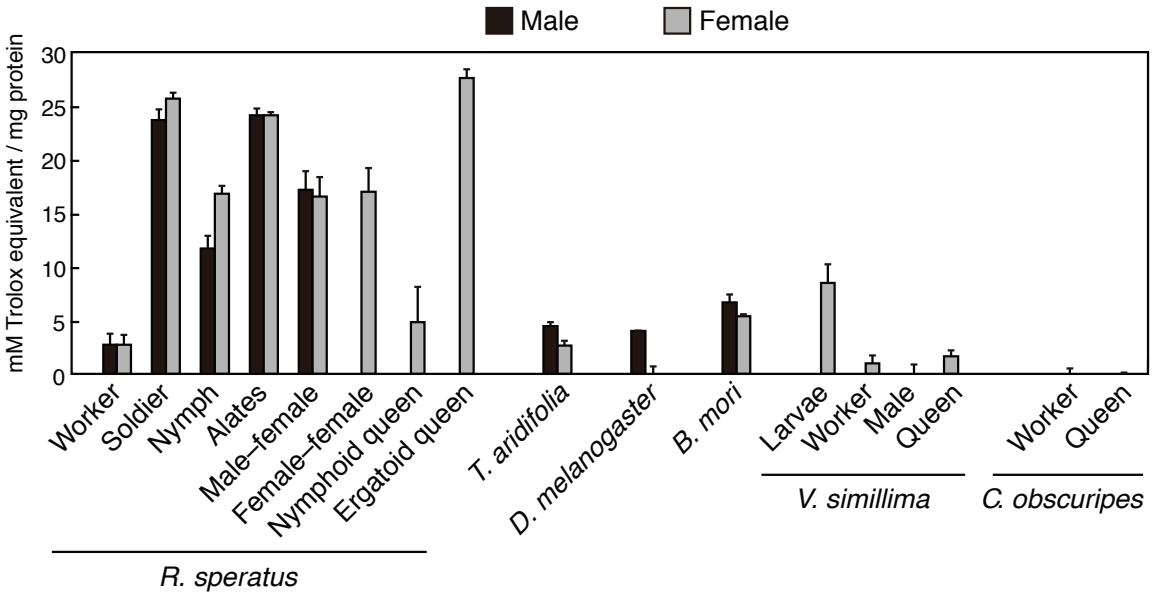

Fig 3.2 | Free radical scavenging activities of heated samples from various insect species. Soluble extracts from termite (*Reticulitermes speratus*), mantis (*Tenodera aridifolia*), fruit fly (*Drosophila melanogaster*), silkworm (*Bombyx mori*), yellow hornet (*Vespa simillima*), and ant (*Camponotus obscuripes*) were heated to boiling, and were then analysed in DPPH radical scavenging assays. Termites generally had higher antioxidant activities. Black boxes indicate male, and grey boxes indicate female (n = 3–6).

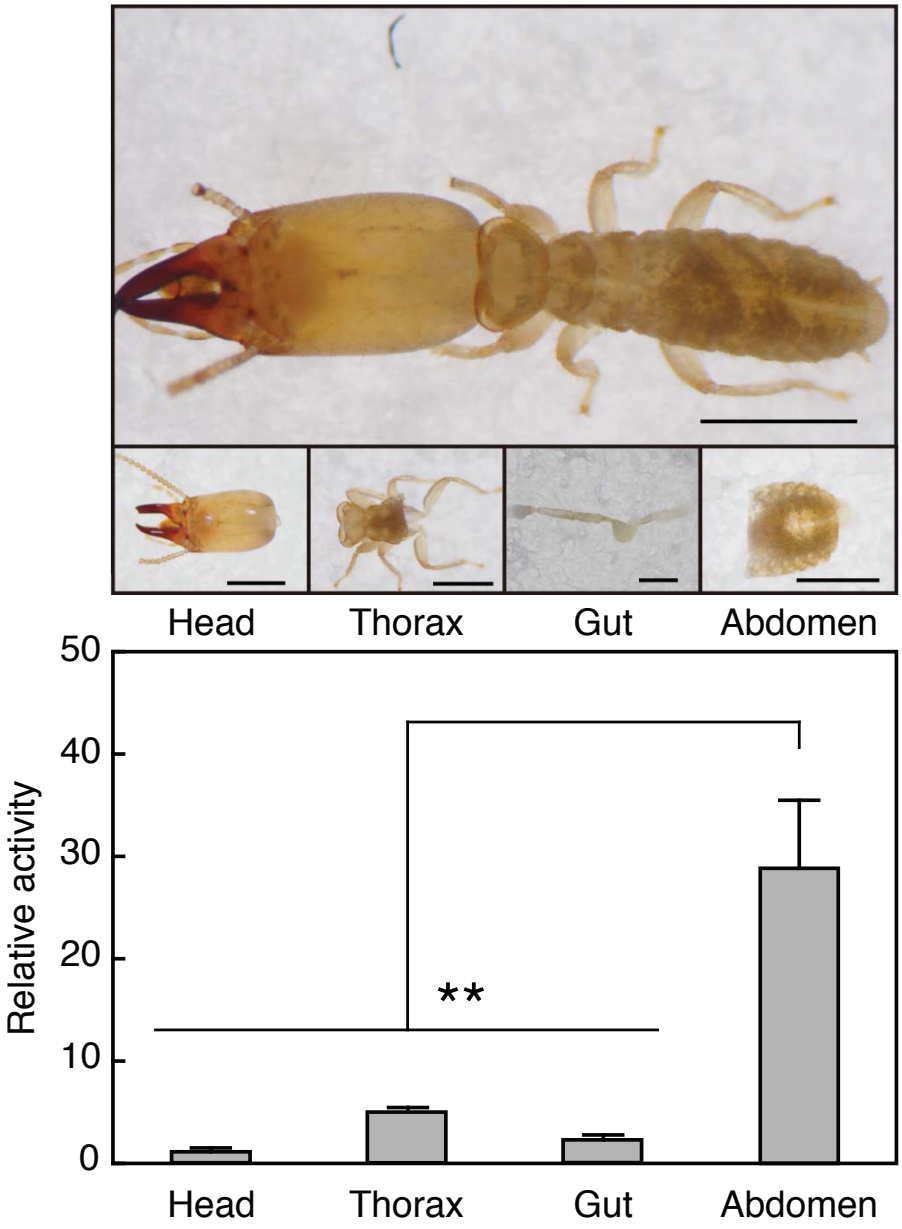

Fig 3.3 | Antioxidants are located mainly in abdominal parts except for the gut. Antioxidant activity of head, thorax, abdomen, and gut of termite soldiers (n = 3). Black scales indicate 1 mm. Data are presented as means ± SEM. Statistical significance was assayed using the unpaired *t*-test followed by Holm's adjustment: $^{**}P < 0.01$.

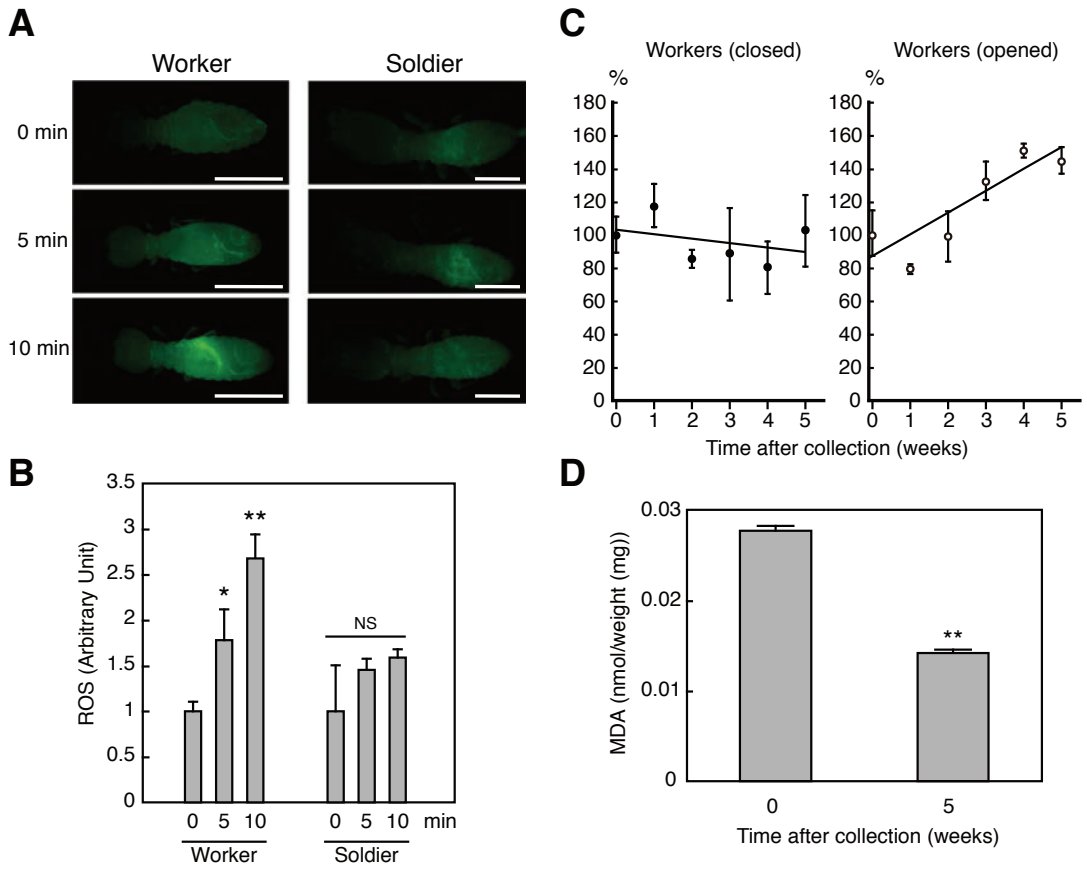

Fig 3.4 | Function of termite antioxidant in the body. (A) Resistance properties of termites against ultraviolet (UV) irradiation; Fluorescence intensities were increased following UV irradiation of termite workers which had lower antioxidant content than termite soldiers; White scales indicate 1 mm. (B) The panel shows fluorescence quantification (n = 6–9). (C) Termite antioxidant activities during captivity in the laboratory; termite workers were maintained in the open (loosely fitted; white) or closed (sealed with tape; black) dish (n = 3). (D) Protective effects of termite antioxidants against lipid peroxidation; lipid peroxidation products were lower in termite workers that had been maintained for 5 weeks than in those that were collected immediately after UV irradiation

(n = 3). Data are presented as means ± s.e.m. Statistical significance was assayed using the unpaired *t*-test followed by Holm's adjustment: **P* < 0.05; ***P* < 0.01.

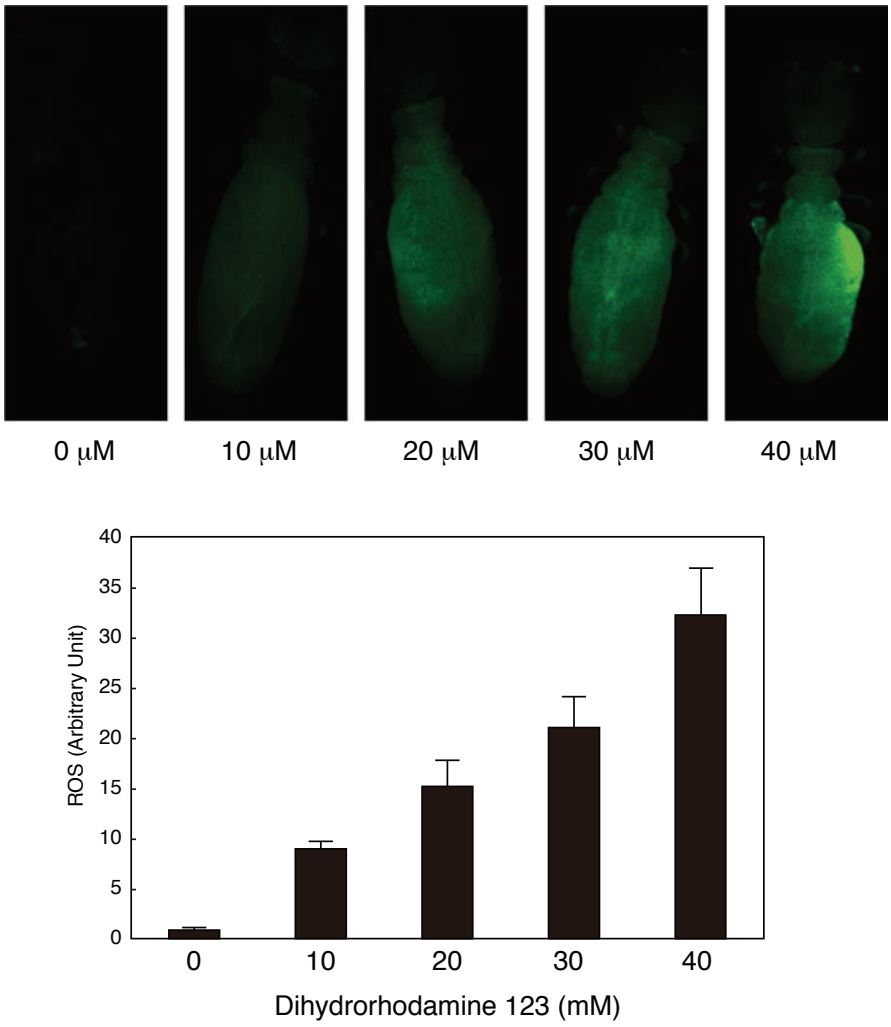

Fig 3.5 | *In vivo* ROS detection by DHR123. Fluorescence images of termite workers injected with serial concentrations of dihydrorhodamine 123 and subjected to UV irradiation. The lower panel shows image quantifications (n = 6–9).

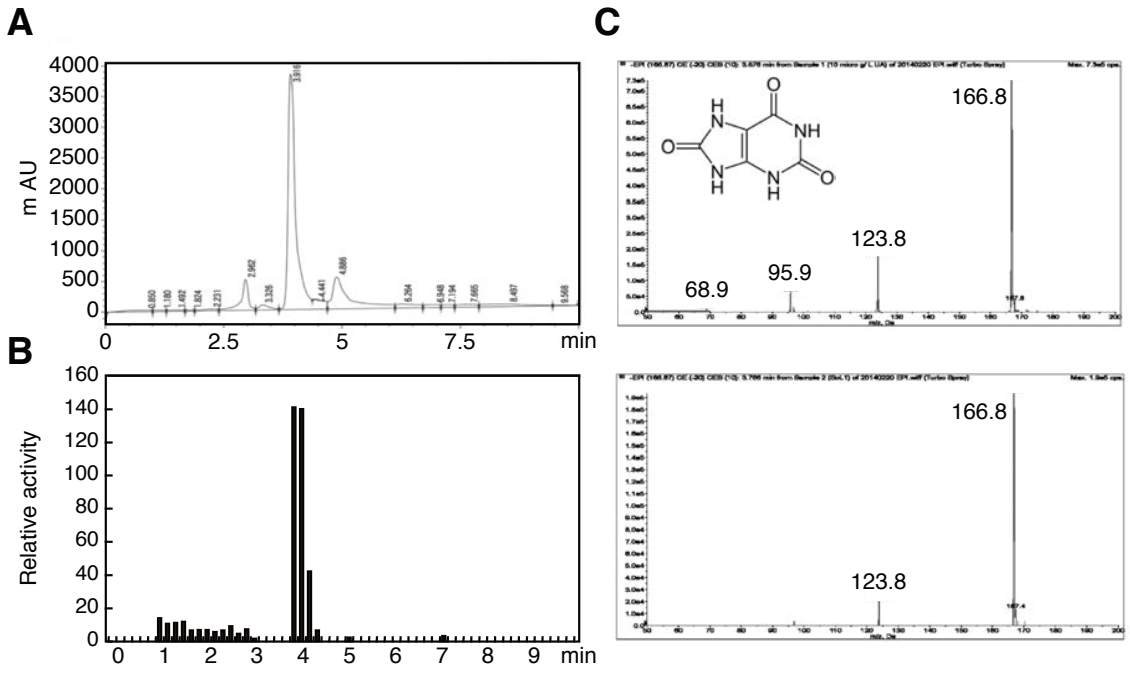

Fig 3.6 | Detection and characterisation of the termite antioxidant. (A) Chromatogram from HPLC analyses and (B) free radical scavenging activities of collected samples fractionated by HPLC; the evident peak of activity was meshed with the highest peak of the HPLC chromatogram. (C) MS-spectra from LC-MS/MS analyses; fragment ion peaks of standard uric acid (upper panel) were completely matched with those of samples from termite soldiers (lower panel).

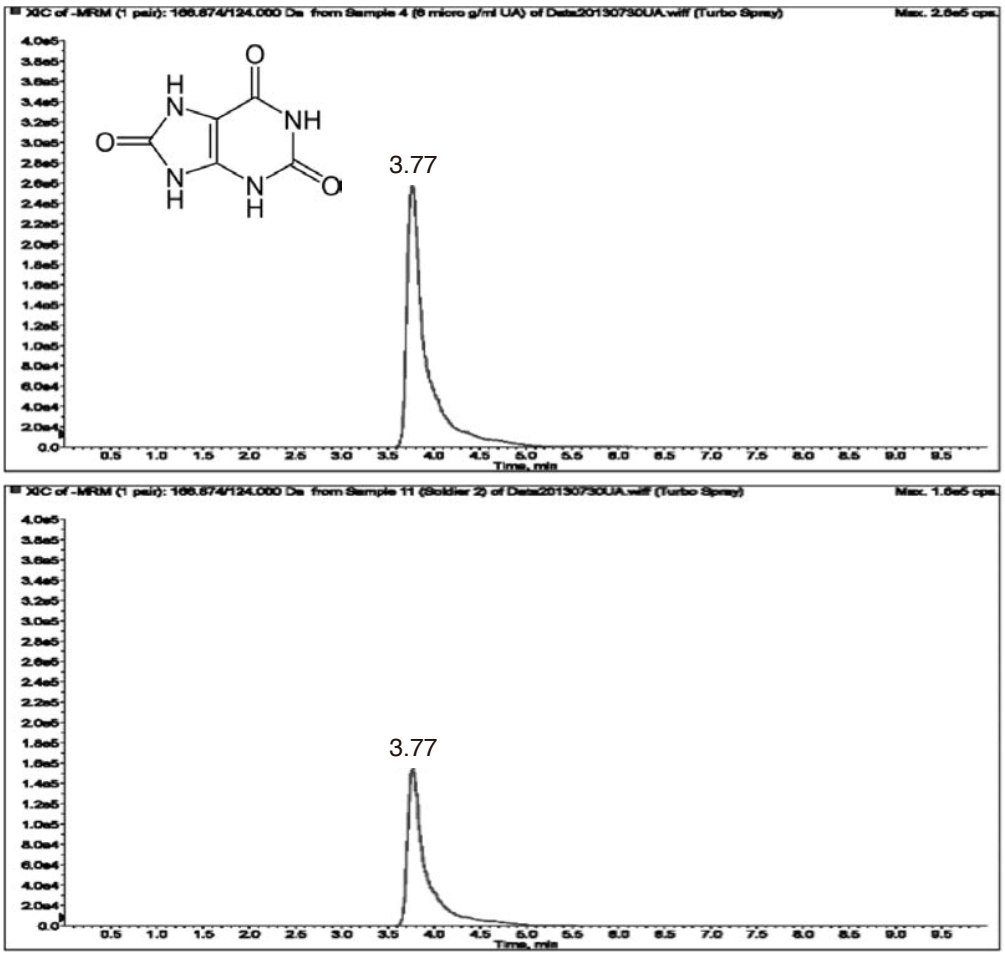

Fig 3.7 | MRM analysis between uric acid and termite soldier. MRM analysis of the uric acid standard (upper panel) and soluble extracts of termite soldiers (lower panel). The retardation time of MRM peak was matched with that of the uric acid standard.

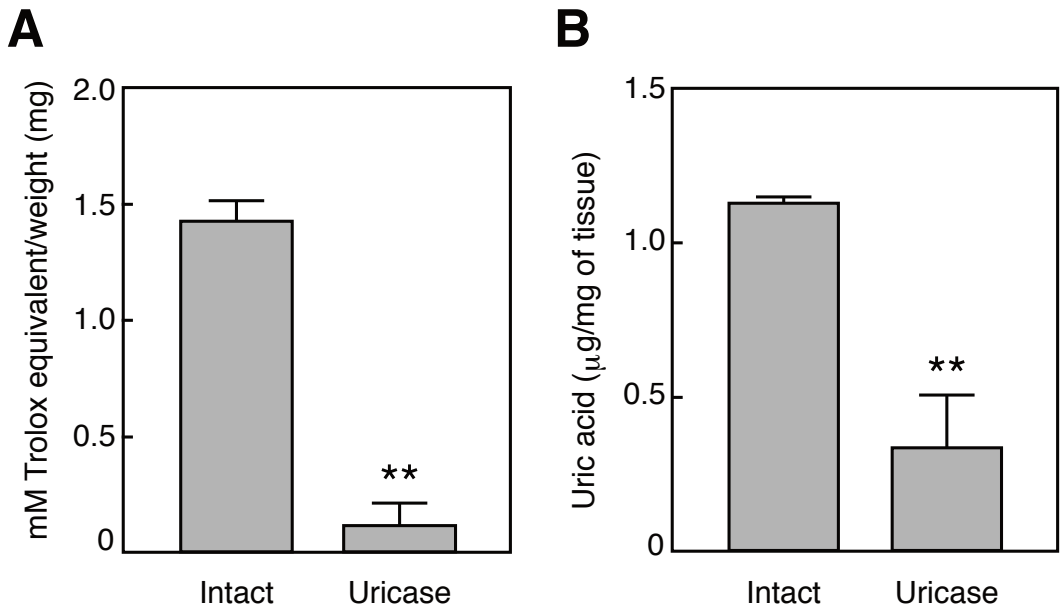

Fig 3.8 | Free radical scavenging activities depends on uric acid contents in termites. (A) Uric acid contents in soluble extracts from termite soldiers; free radical scavenging activities of soldier extracts after treatment with uricase (n = 3). (B) Uric acid contents were significantly decreased in uricase-treated samples (n = 3). Data are presented as means ± SEM. Statistical significance was assayed using the unpaired *t*-test: $^{**}P < 0.01$.

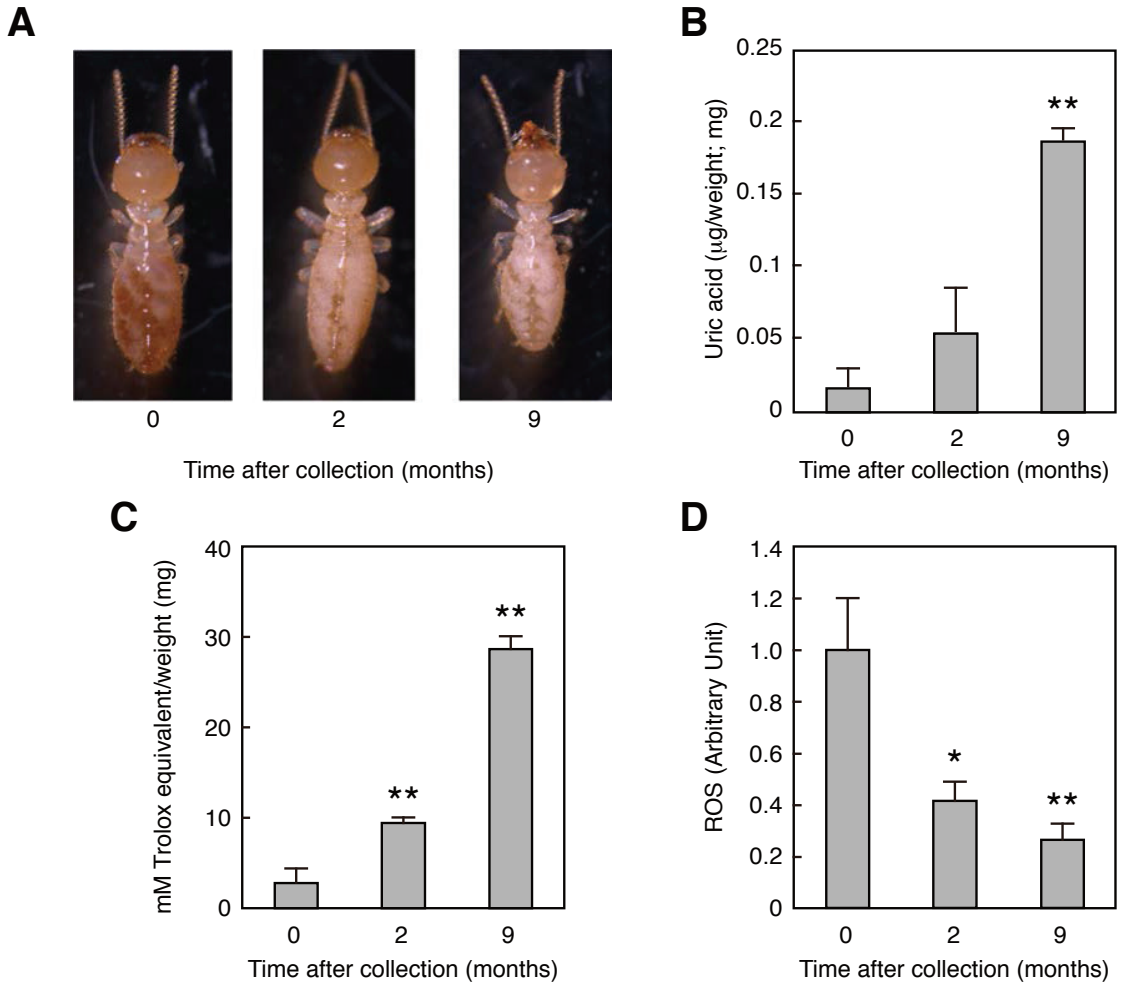

Fig 3.9 | Function of uric acid in termite bodies. (A) Body colours of termite workers changed to white during captivity in the laboratory. (B) Laboratory-maintained termites accumulated uric acid in their bodies during captivity. (C) Increase in antioxidant activities in laboratory-maintained termites. (D) ROS generated by UV irradiation were suppressed in the bodies of uric acid-accumulated termites. Data are represented as means ± SEM. Statistical significance was assayed using the unpaired *t*-test followed by Holm's adjustment: $*P < 0.05$, $**P < 0.01$.

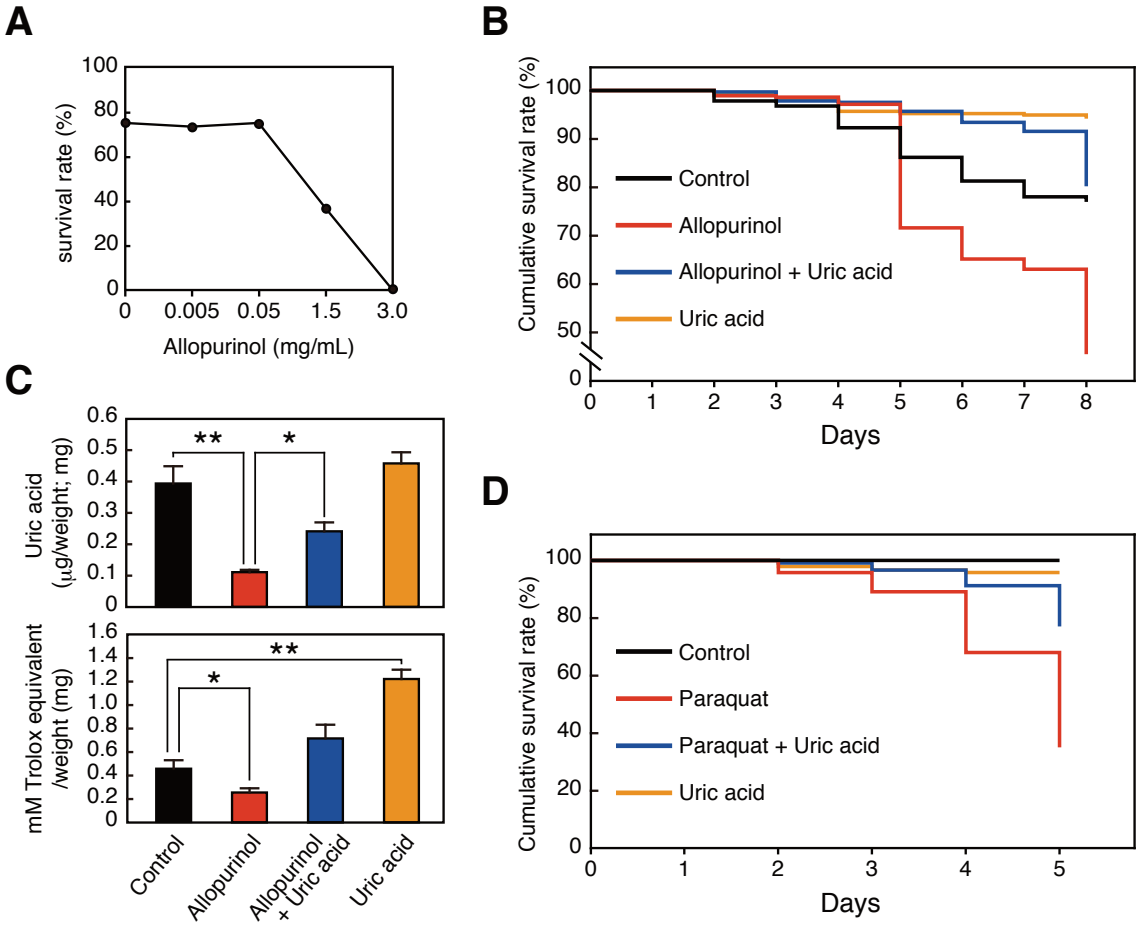

Fig 3.10 | Uric acid contributes to the survival of termite worker under laboratory conditions. (A) Survival rates of termite workers following allopurinol administration for 10 days. (B) Effects of allopurinol and/or uric acid administration on termite survival rates; Feeding of termite workers with the uric acid synthesis inhibitor allopurinol resulted in decreased survival rates (red line). Treatment with allopurinol and uric acid dramatically arrested allopurinol-mediated decreases in survival rates (blue line; n = 270). All treatment groups differed significantly $P < 0.001$, except that no differences were identified between control (black line) and allopurinol + uric acid groups. (C) Uric acid contents (upper panel)

and antioxidant activities (lower panel) of treatment groups at 8 days (n = 3). All error bars represent means ± SEM. Statistical significance was assayed using the unpaired t-test followed by Holm's adjustment: *$P < 0.05$, **$P < 0.01$. (D) Feeding of termite workers with paraquat resulted in decreased survival rates (red line); however, co-treatment with uric acid dramatically rescued paraquat-induced reductions in survival rates (blue line; n = 90). All comparisons revealed significant differences ($P < 0.001$), except for that between the control group and the uric acid group. *P* values were obtained using log-rank tests (Peto–Peto test and Cochran–Mantel–Haenszel test) and Peto–Prentice–Wilcoxon tests.

CHAPTER IV: Extrinsic factor: Hypoxia Influences the Fecundity and Survival of Termite Through Metabolic Shift.

4.1 ABSTRACT

Termites are representative eusocial insects, which exhibit caste-specific differences in their fertility and longevity derived from the same genome. This phenotypic plasticity is associated with differential gene expression via the epigenetic regulation of genomes triggered by extrinsic factors. However, the extrinsic factors have been studied little, and understanding their regulatory mechanisms is an important challenge for future aging research. In this study, we showed that hypoxia, which is possibly an important environmental factor in termite nests, can alter the caste phenotypes in a eusocial termite, *Reticulitermes speratus*. We found that hypoxia triggered the development of fertility as well as long-lived phenotypes in primary reproductives by observing the number of eggs laid and their survival, where metabolomic analysis using gas-chromatography-mass spectrometry and quantitative real-time PCR assays showed that it induced a metabolic shift from aerobic to anaerobic metabolism to facilitate hypoxia tolerance in workers. We also found that queens specifically exhibited accelerated glycolysis, similar to the Warburg effect observed in solid tumors, by default rather than due to hypoxia. Thus, we demonstrated a new role for hypoxia as an extrinsic factor that can regulate reproductive and longevity phenotypes in termites. Our study uncovers a novel finding of long-lived eusocial model.

4.2 INTRODUCTION

Anti-aging and longevity have fascinated scientists for centuries. Eusocial termite reproductives (queens and kings) are among the most promising subjects for aging research due to their extreme longevity and sustained fecundity [12]. The longevity of termite reproductives that avoid risky outer field tasks, such as guarding the nest or foraging activities, have been explained by the evolutionary theory of aging based on natural selection, which predicts that the intrinsic lifespan is directly related to the level of extrinsic mortality [10]. Consistent with this theory, queens and kings of the lower termite *Zootermopsis nevadensis* live for seven years after foundation [85]. On the other hand, a trade-off between reproduction and longevity occurs widely in most animals [32]. However, termite reproductives can live for long periods [10] and produce many offspring per day, e.g., 40,000 eggs are produced per day by the termite *Macrotermes subhyalinus* [86], thereby suggesting the presence of an extraordinary anti-aging mechanism in eusocial termites.

The reproductives and workers possess the same genome and the major differences in phenotype are thought to due to changes in the behavior of gene networks caused by epigenetic regulation. Recent studies suggest that epigenetic processes, including DNA methylation [87] and histone modifications [88], are used to regulate phenotypic plasticity in eusocial insects. However, few studies have examined the factors or triggers that initiate epigenetic regulation. A previous study hypothesized that the differentiation between termite reproductives and workers is determined entirely by extrinsic factors, primarily pheromones [89], and a pheromone was identified in the termite *Reticulitermes speratus* [90]. Understanding how different longevity phenotypes arise from the same genome is one of the most challenging tasks in aging mechanism research using eusocial termites, but this

remains unknown.

In general, low oxygen (hypoxia) levels affect many physiological processes in organisms, such as growth, development, metabolism, pH homeostasis, and angiogenesis [91,92]. It is also hypothesized that an enclosed termite nest containing a high population density of individuals typically has a low oxygen (O_2) concentration and a high carbon dioxide (CO_2) concentration because of poor gas exchange, which is supported by previous study of ant nest [93]. In termites, the primary queens and kings start to build a new nest and produce offspring after swarming in a nuptial flight, thereby indicating that the alates, i.e., the winged reproductive castes comprising the primary reproductives, migrate from enclosed hypoxic conditions to completely open air conditions, followed by reentry into their incipient nests that are separated from external air conditions. Interestingly, the eusocial subterranean rodent naked mole rat (*Heterocephalus glaber*) exhibits great longevity with a maximum lifespan exceeding 30 years [94], and it is also thought to live in hypoxic environment, where it can change the expression levels of many gene associated with energy metabolism and redox control in hypoxic conditions [95]. Moreover, several immortalized cancer cells are known to be adapted to hypoxic conditions, and they switch their metabolism in hypoxic conditions, where the altered metabolites induce epigenetic changes [96]. These previous reports support our hypothesis that termites can effectively utilize hypoxia as an extrinsic factor to regulate phenotypic plasticity.

In the present study, we attempted to understand whether hypoxic conditions influence fecundity and survival after foundation in subterranean termite *R. speratus* reproductives and change metabolism in the termite workers and queens. Importantly, there are a few studies that measure gas concentrations in natural termite nests [97]; however, the actual O_2 in natural nests of *R. speratus* is not known because of methodological difficulty. Therefore, as the first attempt to provide a model case, we designed the most common

hypoxic conditions (1%–5% O_2) for all experiments in this study; that is, 1% and 5% O_2 were selected for short- and long-term experiments, respectively. Our results demonstrate that the reproductive phenotypes of termite during/after colony foundation, such as egg production and long survival, are partly hypoxia-triggered processes and that the metabolic strategies of queens and workers exhibit fundamental differences as a response to hypoxia. In summary, the findings of this study can be applied to understanding the molecular basis of the physiology and behavior of eusocial termites, which underlie aging and longevity.

4.3 MATERIALS AND METHODS

Samples

Animal ethics committee approval was not required for this study using two insect species. To obtain *R. speratus* alates, during the swarming season from April to May, we collected 10 colonies (colony codes: YY140421A, YY140421B, YY140421C, YY140421D, YY140428A, YY140428B, YY140507A, YY140507B, YY160420A, and YY160420B, designated as colonies A–J, respectively) from the experimental forest of Yamaguchi University (approval was received from Yamaguchi University), which is part of Mt Himeyama in Yamaguchi, western Japan. Males and females were selected randomly from each colony and placed in 35-mm Petri dishes containing wet cellulose paper after they shed their wings (Dealate). Finally, we prepared 94 mating pairs, which comprised one male and one female selected randomly from different colonies. Briefly, dealated termites were assigned to one of the following foundation units: female–male mating pairs (FM). FM units were constructed using the following combinations: one female from colony A and one male from colony B (F_A M_B), F_B M_A, F_C M_D, F_D M_C, F_E M_F, F_F M_E, F_G M_H, F_H M_G, F_I M_J, and F_J M_I. The Petri dishes were kept under 21% or 5% O_2 at 27°C in a multi-gas incubator (9000EX, Waken B Tech Co. Ltd). We counted the number of live individuals and eggs laid under a stereoscopic microscope every week and added water occasionally to keep the paper wet. *R speratus* workers and mature secondary queens (queens) were collected from different colonies, i.e., YY140710A and YY131015A, respectively, in the experimental forest of Yamaguchi University, which is part of Mt Himeyama in Yamaguchi, western Japan. *D. melanogaster* (Oregon R) adults were provided by Prof. R Murakami. Termites or flies were placed in gas-permeable 35-mm Petri dishes containing wet cellulose paper or gas-permeable culture bottles containing paper with 10% glucose

(v/v), respectively, under control (21% O_2 and < 0.05% CO_2), low O_2 (1% or 4% O_2), or high CO_2 (10% CO_2) conditions in a multi-gas incubator (9000EX, Waken B Tech Co. Ltd) at 25°C for 24 h. The insect samples were frozen in liquid nitrogen and preserved at –80°C until use.

qRT-PCR

The whole transcriptome of *R. speratus* was examined using next-generation RNA-sequencing, as described in a previous study [46]. We also referred to the mRNA sequence of the vitellogenin 2 gene *Vg2* described in a previous study [46]. We obtained the mRNA sequences of metabolic genes from transcriptome data by BLAST searches using the amino acid sequences of translated metabolic genes in the termite *Zootermopsis nevadensis* and other model insects with an E-value cutoff of 1e−100, and we designed primer pairs for each gene (Table 2.1). Using ISOGEN reagent (Nippon gene), total RNA was extracted from the whole bodies of individual termite workers or queens, which were frozen in liquid nitrogen and stored at –80°C until extraction. cDNA was synthesized immediately from the RNA using a PrimeScript™ RT reagent kit (Takara) and preserved at –20°C. qRT-PCR was performed using a LightCycler (Roche) with QuantiTect® SYBR® Green PCR (Qiagen). All of the procedures were performed according to the manufacturers' protocols. Glucose-6-phosphate dehydrogenase (*RsG6PD*) and beta-actin (*RsACT*) were selected as the reference genes. Relative expression levels were calculated using the standard ΔΔCt method. Three biological replicates were performed for alate males and females, workers, and queens of *R. speratus*.

Metabolite Extraction and MS

Sample preparation and derivatization were performed using a modified version of a

previously-described method [98]. In particular, the whole bodies of insects were homogenized by sonication in tubes with 600 µL chloroform/ methanol solution (1:2) at –20°C. Next, 400 µL of ice-cold ultrapure water and 0.5 mg 2-isopropylmalic acid (Sigma-Aldrich), as an internal standard, were added to each sample and vortexed. After centrifugation at 16000 ×*g* for 10 min at 4°C, 700 µL of the upper aqueous phase containing polar metabolites was transferred to a new sample tube. The samples were dried by lyophilization (EYELA, FDU-2100) before derivatization. The samples were resuspended in 40 µL of 20 mg/mL *o*-methylhydroxylamine hydrochloride (Wako) in pyridine (Wako), before incubation on a heat block at 30°C for 90 min. Next, 20 µL of *N*-methyl-*N*-trimethylsilyltrifluoroacetamide (Thermo) was added to the samples and derivatization was continued for 60 min at 37°C. After incubation, the samples were allowed to stabilize for 120 min at room temperature. GC-MS analyses were performed using a modified version of a previously described method (Nishiumi et al., 2010). All of the GC-MS analyses were performed using a GCMS-QP2010 (Shimadzu) and a DB-5 column (length: 30 m, diam.: 0.25 mm, film thickness: 1 µm; Agilent Technology). The GC column temperature was programmed to rise from 100 to 320°C at a rate of 4°C per minute, and the total GC run time was 60 min. The injector temperature was held at 280°C, and helium was used as a carrier gas at a constant flow rate of 39.0 cm per second. A 1-µL sample was injected in the split mode (split rate: 1/10), and the mass conditions were as follows: ionization voltage: 70 eV; ion source temperature: 200°C; full scan mode in the m/z range 35–600 with a 0.20 s/ scan velocity. Three biological replicates were performed for workers and queens of *R. speratus* and *D. melanogaster*, where each replicate comprised 13 pooled workers, five queens, and 30 flies.

Respiratory quotient measurement

R. speratus units comprising 170 individual workers, five individual soldiers, and 30 individual queens; *T. emma* units comprising two individual adult females; and *B. mori* units comprising 10 individual larvae of unknown sex were placed in a completely enclosed chamber containing wet cellulose paper, with volumes of 251, 450, and 450 mL, respectively, and the O_2 consumption and CO_2 emission rates were measured by real-time monitoring (O_2 sensor: OXYMAN OM25MP20, Asone; CO_2 sensor: GMP221, Vaisala). Respiratory quotient value is calculated using the equation CO_2 eliminated/O_2 consumed. We confirmed the numbers of *R. speratus* unit members alive after 200 h under sealed conditions, but we observed the death of crickets and caterpillars after 60 h (approximately 10% O_2) and 40 h (approximately 5% O_2), respectively. All experiments were performed in dark and stable conditions.

Statistical analysis

The R software package (version 3.2.2) was used for most of the statistical analyses. Two-tailed unpaired *t*-tests followed by *P*-value correction using Holm's adjustment for multiple comparisons were performed with the different data sets [48]. All of the data in graphs were presented as the mean ± standard error of the mean (SEM). For survival tests using the Kaplan-Meier method, statistical analyses were performed with the Peto-Peto and Cochran-Mantel-Haenszel log rank method in Excel (Microsoft). All of the relevant *P*-values are shown in the figures, but the values were $P > 0.05$ if not shown.

4.4 RESULTS AND DISCUSSION

Hypoxia increases egg production and survival in a termite.

Termite nests contain a high population density of individuals, which are separated from the external environment (Fig 4.1), where there are generally low O_2 and high CO_2 concentrations due to poor gas exchange. In the termite *Reticulitermes speratus*, the life cycle has been characterized by several studies [99]. Briefly, each colony of *R. speratus* produces numerous alates in spring. A pair of female and male alates establishes a new colony in a new nest after swarming and start to produce offspring sexually as a queen and king [100]. This suggests that the hypoxic environment in the nest might trigger the metamorphosis of the alate females and males (winged adults) into mature queens and kings, respectively, thereby achieving both sustained high fecundity and greater longevity. To determine how hypoxic conditions might lead to sustained fecundity and extreme longevity in the termite reproductives, we assessed the number of eggs laid and survival in alate mating pairs. In contrast to individuals from other castes except for a part of workers, the alates naturally experience the external environment (about 21% O_2 conditions); therefore, we considered that the alates are useful for assessing the intrinsic effects of hypoxia on the fertility and lifespan of termites. We monitored the number of eggs laid as the level of fecundity and survival in female–male mating pairs (FM) under control conditions (21% O_2) or hypoxia (5% O_2) in a multi-gas incubator (Fig 4.2, Table 2.2). The FM units kept under hypoxia produced significantly more eggs per female than the pairs kept under control conditions (Fig 4.3A). While CO_2 is reportedly a known factor that affects the reproductive activity in eusocial honeybee [101,102], to our knowledge, this is the first study reporting the effects of O_2 on the reproductive activity in eusocial queens. Surprisingly, we found that hypoxia also promoted FM survival (Fig 4.3B). O_2 has been

shown to be a toxic molecule that must be supplied in carefully controlled concentration [103]. We believe that because control condition may be toxic to the termites, the survival rate rapidly decreased. Indeed, a previous study has indicated that high O_2 levels can reduce the survival rate of insects [104]. We observed that the survival decreased to 25% after 20 weeks despite the hypoxic conditions because the experimental environment illustrated in Fig 4.2, Supporting information comprised low nutrient conditions, i.e., only cellulose and water, and it was stressful compared with the natural nest. Based on these results, we conclude that hypoxia partially resembling the natural habitat promoted egg production and survival in the termite *R. speratus*.

Hypoxia may promote oocyte development in young termite queens.

In most insects, vitellogenin is known to be the precursor of the major yolk protein vitellin, which is taken up by the developing oocytes. To test whether hypoxic exposure affected the expression level of the vitellogenin gene *Vg2* in termites, we used alate females from FM units, and alate males as a negative control from FM units, which were all exposed to control (21% O_2) or hypoxia (5% O_2) conditions for 2 weeks or 4 weeks. The results of qRT-PCR experiments showed that that the *Vg2* gene expression levels in females from FM units increased at 2 weeks under hypoxia (Fig 4.4). We also observed significant differences between females and males at 4 weeks (Fig 4.5). A previous study has reported that vitellogenin gene expression levels are related to ovarian development in *R. speratus* [105]. These results suggest that hypoxic conditions promoted the expression of the vitellogenin gene in females, and they may be essential for colony foundation success and the development of mature queens with sustained high fecundity.

Hypoxia tolerance in *R. speratus.*

We demonstrated that hypoxia affects fecundity and survival in termites although most eukaryotic animals cannot live for long in hypoxic conditions. Thus, we hypothesized that the termite *R. speratus* may possess tolerance mechanisms that facilitate adaptation to hypoxia. To demonstrate adaptation to hypoxia in termites, we monitored the survival of the termite *R. speratus* and the fruit fly *Drosophila melanogaster* when kept for 24 h in 21% or 1% O_2 conditions. We found that the survival rate under hypoxic conditions was 92% in *R. speratus* and only 18% in *D. melanogaster*, thereby suggesting that this termite exhibits severe hypoxia tolerance (Fig 4.6). We also confirmed that most of the termite workers, soldiers, and queens could live for more than 200 h in enclosed conditions, whereas adult females of *Teleogryllus emma* (a cricket that typically lives under control condition) and *Bombyx mori* larvae could not live for longer than 60 h and 40 h, respectively, under hypoxic conditions (Fig 4.7). We reluctantly made the decision to use the cricket and the caterpillar instead of using the fly due to technical difficulty in the respiratory quotient measurement assay. These results suggest that this termite has higher hypoxia tolerance than solitary insects such as *D. melanogaster*, *T. emma*, and *B. mori*.

The termite *R. speratus* switches its metabolism under hypoxia.

We demonstrated high hypoxia tolerance in a termite (Fig 4.6), but the mechanisms responsible are unknown. Thus, to understand how the termite *R. speratus* acquires hypoxia tolerance, we focused on its metabolism. Previous studies indicate that most animals respond to hypoxic conditions via metabolic adaptations, including increased glycolysis and fermentation as well as reductions in the TCA cycle [92]. In particular, several organisms are known to switch their metabolism to the more intensive utilization of anaerobic glycolysis and fermentation rather than aerobic oxidative pathways in hypoxia [106]. Therefore, we hypothesized that the termite *R. speratus* also possesses anaerobic

metabolism as an adaptation to hypoxia. We used GC-MS to measure the metabolic end products associated with glycolysis and the TCA cycle in order to probe the metabolic differences between the termite *R. speratus* workers and secondary queens (queens) in a nest inhabited by a large quantity of queens due to asexual queen succession system [99] and *D. melanogaster* adults, as a control animal for living under aerobic conditions, which were kept for 24 h under control (21% O_2) or hypoxia (1% and 4% O_2 for termites and flies, respectively, because most flies cannot live in a 1% O_2 environment for more than 24 h) conditions. Interestingly, we found that there were many metabolic changes in the termite workers and queens compared with *D. melanogaster* (Fig 4.8A, Table 2.3). This indicates that the termite workers and queens exhibited a greater response to hypoxic conditions to allow adaptation to hypoxia compared with *D. melanogaster*, and these metabolic changes are key aspects of the hypoxia tolerance strategies of the termite *R. speratus*. Hypoxia dramatically changed the amino acid levels of workers, but queens had more stable levels than workers (Fig 4.9). Lactate is known to be an anaerobic glycolysis-related end product, and it was significantly elevated under hypoxic conditions compared with control conditions in both the workers and queens (Fig 4.8B and 4.8C). Moreover, we found that the respiratory quotient of *R. speratus* was equal to 1.00, whereas those of *T. emma* and *B. mori* were lower than that of the termites (Fig 4.7), thereby suggesting that *R. speratus* has the potential to increase anaerobic glycolysis in response to hypoxic exposure. A previous study also demonstrated that the respiratory quotients of several termite species were at or well above 1.00 [68], which is consistent with the results of our study. Moreover, we found that workers and queens exposed to hypoxia accumulated more succinate than the control (Fig 4.8B and 4.8C). Several parasites and stonefly nymphs with anaerobic energy metabolism also accumulate succinate according to previous studies, which is consistent with our results [107,108]. In both the workers and queens, hypoxic conditions induced

fairly significant accumulations of 2-hydroxyglutarate (2HG, which occurs in two distinct forms: D- and L-2HG) compared with the control conditions (Fig 4.8B and 4.8C). Recently, it has been shown that 2HG and succinate, which are α-ketoacids and typical mitochondrial metabolites play important roles in the epigenetic regulation of organisms, where they competitively target the active sites of several epigenetic proteins such as jumonji domain-containing histone demethylases, which are known to regulate lifespan in *Caenorhabditis elegans* [96,109]. Furthermore, previous studies have demonstrated that the expression of L-2HG dehydrogenase (L2HGDH), a mitochondrial protein that catalyzes the oxidation of L-2HG to 2-oxoglutarate (2OG), was suppressed, and this was followed by the accumulation of L-2HG in human cells under hypoxia [110], which is consistent with our results. In addition, we investigated whether high CO_2 affected metabolism in the same manner. In this experiment, we found very slight metabolic changes in queens and workers of *R. speratus*; on the other hand, amino acids decreased in *D. melanogaster* (Fig 4.10, Table 2.3). High CO_2 concentrations are known to be an anesthetic in insects, where we found that it affected the metabolism of *D. melanogaster* but not that of *R. speratus*, which may possess high CO_2 tolerance as well as hypoxia tolerance. Consequently, these results suggest that the anaerobic metabolic shift may play a role in hypoxia tolerance behavior, but it could also regulate epigenetic effects, thereby contributing to the extreme sustained fecundity and longevity in this termite.

R. speratus promotes the expression of gene associated with anaerobic metabolism under hypoxic conditions.

We demonstrated that the termite *R. speratus* changed its metabolism under hypoxic conditions (Fig 4.8A). Several adaptive genetic changes have been identified in *D. melanogaster* with tolerance of severe hypoxic conditions [111]; therefore, we considered

that the metabolic shift in the termite may be also based on the regulation of gene expression. Indeed, hypoxia affects metabolic genes, including glycolytic enzymes such as hexokinase (HK), glyceraldehyde phosphate dehydrogenase, and lactate dehydrogenase (LDH) [92]. To measure the expression levels of metabolic genes, we identified five glycolysis genes (*RsHK*, HK; *RsPFK*, phosphofructokinase, PFK; *RsPK1* and *2*, pyruvate kinase; *RsLDH*, LDH), eight TCA cycle genes (*RsPDH*, pyruvate dehydrogenase E1 component subunit beta; *RsCS*, citrate synthase, CS; *RsIDH1*, cytoplasmic isocitrate dehydrogenase [NADP], IDH1; *RsIDH2*, mitochondrial IDH [NADP], IDH2; *RsIDH3A*, mitochondrial IDH [NAD] alpha subunit, IDH3A; *RsIDH3B*, mitochondrial IDH [NAD] beta subunit, IDH3B; *RsOGDG*, mitochondrial 2-oxoglutarate dehydrogenase E1 component, OGDH), and six other metabolic genes (*RsPEPCK*, phosphoenolpyruvate carboxykinase, PEPCK; *RsTKT*, transketolase, TKT; *RsTAD*, transaldolase, TAD; *RsALT2*, mitochondrial alanine aminotransferase, ALT2; *RsMDH1*, cytoplasmic malate dehydrogenase, MDH1; *RsMDH2*, mitochondrial MDH, MDH2) using the method described below (Table 2.4). We tested *R. speratus* workers and queens kept under control (21% O_2) and hypoxia (1% O_2) conditions for 24 h in a multi-gas incubator. In agreement with the accumulation of lactate (Fig 4.8B), the LDH gene in termite workers was upregulated by 15 times in hypoxia compared with the control conditions (Fig 4.11A). Interestingly, we found that the termite queens had 6.5-fold and 3.7-fold higher gene expression levels for LDH and HK (Fig 4.11B), respectively, compared with the workers, although hypoxia did not affect the LDH and HK gene expression levels of the queens (Fig 4.12A). This suggests that the queens located in the central portion of the nest under hypoxia usually accelerate glycolysis via a default system. Moreover, this metabolism is similar to the Warburg effect known as anaerobic glycolysis [112]. The metabolism needs a high rate of glucose consumption, which is supported by termite queens receiving

tremendous amounts of glucose via trophallaxis (mouth-to-mouth transfer of nutrients) from workers. Several types of cancer cells upregulate the pentose phosphate pathway (PPP) to avoid any redox imbalance due to acceleration of glycolysis [113], where TKT and TAD are major enzymes that mediate non-oxidative PPP, but they did not differ in hypoxic and control conditions (Fig 4.9E, Fig 4.12B). These results indicate that modifiable and inherent glycolysis gene expression in termite workers and queens, respectively, are metabolic strategies based on the division of labor between outside-nest tasks, which include the risk of exposure to outside air, and within-nest tasks, which demand remaining in a hypoxic nest but that also require inordinate amounts of energy for reproduction. There were no differences in the expression levels of TCA cycle genes under hypoxia and control conditions (Fig 4.11C). The gene expression levels of CS, IDH2, and OGDH were 2.9-fold, 4.6-fold, and 6.3-fold lower, respectively, in queens than in workers (Fig 4.11D). We also found that the expression level of IDH3A, which is required for the catalytic activity of IDH3 [114], was 2.9-fold higher in queens than in workers (Fig 4.11D). In contrast to IDH1 and IDH2, which rely on $NADP^+$ as their electron acceptor, IDH3 relies on NAD^+ and reduces it to NADH. Therefore, we considered that IDH3 compensates for the absence of IDH2 in the mitochondria of queens, thereby contributing to anaerobic fumarate respiration using NADH as an electron donor. Fumarate respiration is found in prokaryotes and in some eukaryotes that are capable of functioning anaerobically, such as parasites, freshwater snails, mussels, oysters, lugworms, and other marine invertebrates [107,115]. During anaerobic fumarate respiration, the malate generated by the activity of cytosolic PEPCK is required as a source of fumarate. This pathway finally generates succinate from fumarate via fumarate reductase (ETC complex 2). We found that the expression level of the PEPCK gene increased 4.5-fold under hypoxic conditions in workers but not in queens (Fig 4.11E, Fig 4.12B). Interestingly, the expression level of the PEPCK gene was 2.4 times higher in

workers than in queens by default (Fig 4.11F). These results indicate that the termite workers are capable of fumarate respiration under hypoxia. ALT2 is upregulated by hypoxia inducible activating transcription factor 4 [116], and it activates the production of both alanine and 2OG, a known source of 2HG, but there were no difference in its expression levels under control and hypoxia conditions (Fig 4.11E).

After investigating, we found that high CO_2 (10% CO_2) exposure slightly affected the expression levels of these metabolic genes (Fig 4.13). This is consistent with no marked differences observed in the metabolites (Fig 4.10, Table 2.3). Thus, these patterns of metabolic gene expression and the metabolite patterns determined by GC-MS analysis suggest that *R. speratus* workers upregulate anaerobic glycolysis and fumarate respiration under hypoxic conditions to facilitate effective energy production without using oxidative phosphorylation (Fig 4.14).

Hypoxia has potential to influence reproductive traits and metabolism in termites.

Overall, our results partially support the hypothesis that hypoxia triggers phenotypic changes in termite reproductives during and after colony foundation through anaerobic metabolism and production of epigenetic regulators such as 2HG and succinate. This regulation system may also explain the difference of gene expression between reproductives and non-reproductive termites (in Chapter II). We used the whole bodies of termites kept under estimated O_2 or CO_2 conditions in the laboratory as samples for GC-MS analysis and qRT-PCR assay in this study. However, to address the limitations of the present study, it will be necessary to measure the actual O_2 and CO_2 concentrations in natural termite nests to quantify the actual conditions for future study. Moreover, the metabolism of wood-feeding lower termites such as *R. speratus* partially depends on the activity of various gut symbionts [69]. Therefore, further studies are required to determine

whether the hypoxia-induced metabolic shifts indicated in this study are associated with changes in the gut symbiont populations under hypoxia. Consequently, this study highlights a novel knowledge of the molecular basis of the physiology and behavior in long-lived eusocial model.

4.5 FIGURES AND TABLES

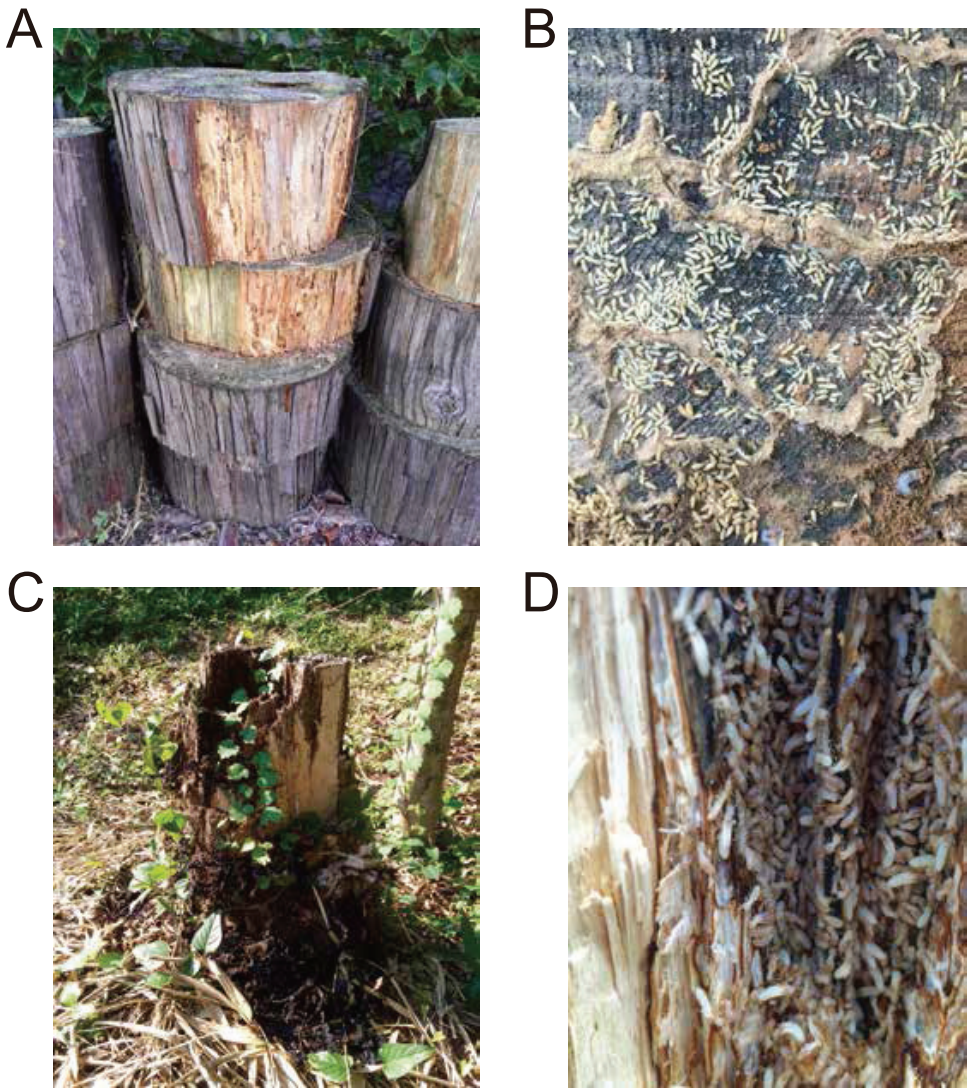

Fig 4.1 | External and internal appearance of termite nests. (A–D) External (A and C) and internal appearance (B and C, respectively) of termite nests. Images of natural *R. speratus* nests were acquired in April (A and B) and May (C and D) 2016 on Mt Himeyama in Yamaguchi, western Japan.

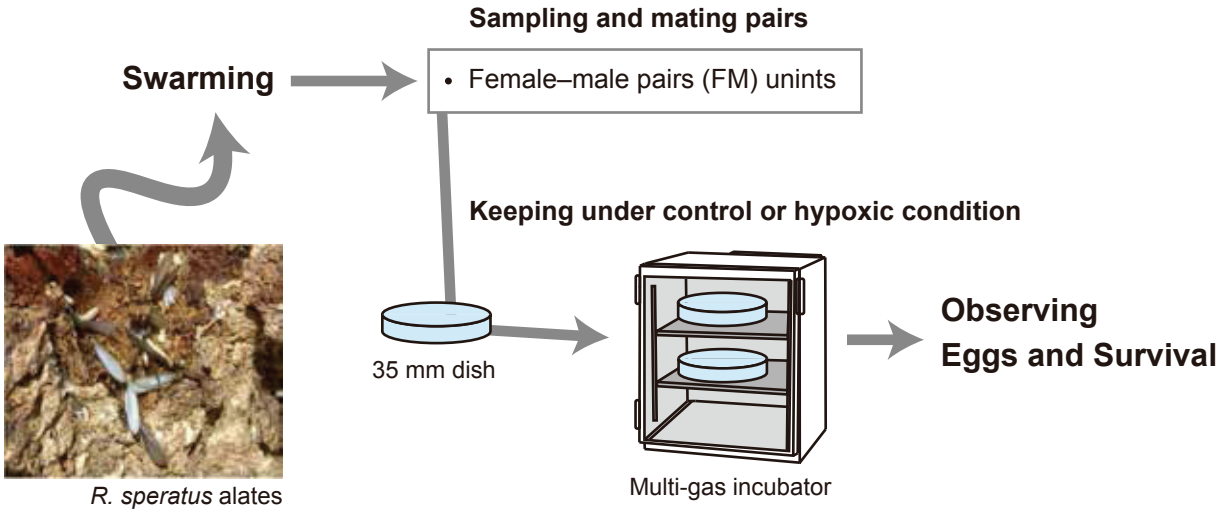

Fig 4.2 | Experimental models for the investigation of hypoxia-induced modulation of fecundity and survival by the termite *R. speratus*. We prepared 94 female–male pairs (FM) units. These colonies were kept under 21% O_2 (control) or 5% O_2 (hypoxia) in a multi-gas incubator, and we monitored the number of eggs laid and survival.

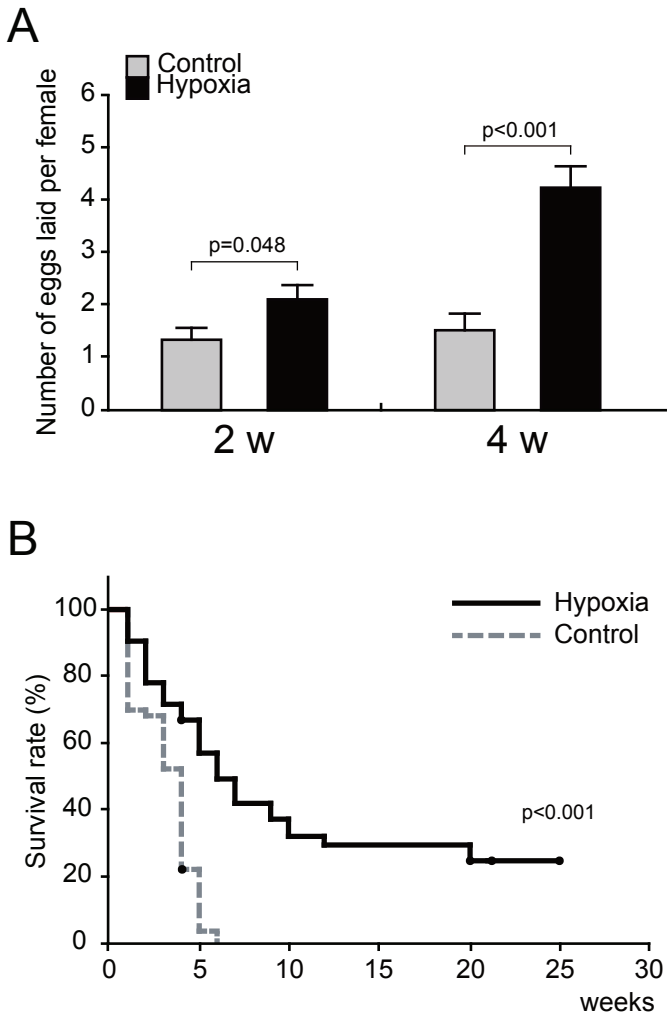

Fig 4.3 | Hypoxia increased the number of eggs laid and survival in *R. speratus* reproductives. (A) Mean number (± SEM values) of eggs laid per female per colony (n = 44 [control FM at 2 weeks (2 w)], 57 [hypoxia FM at 2 w], 33 [control FM at 4 weeks (4 w)], and 44 [hypoxia FM at 4 w]. *P*-values were obtained using unpaired *t*-tests. Error bars indicate SEM. (B) Kaplan–Meier survival curves for FM units under control (n = 63) and under hypoxia (n = 63). *P*-values were obtained using log-rank tests (Peto–Peto test and Cochran–Mantel–Haenszel test) and Peto–Prentice–Wilcoxon tests.

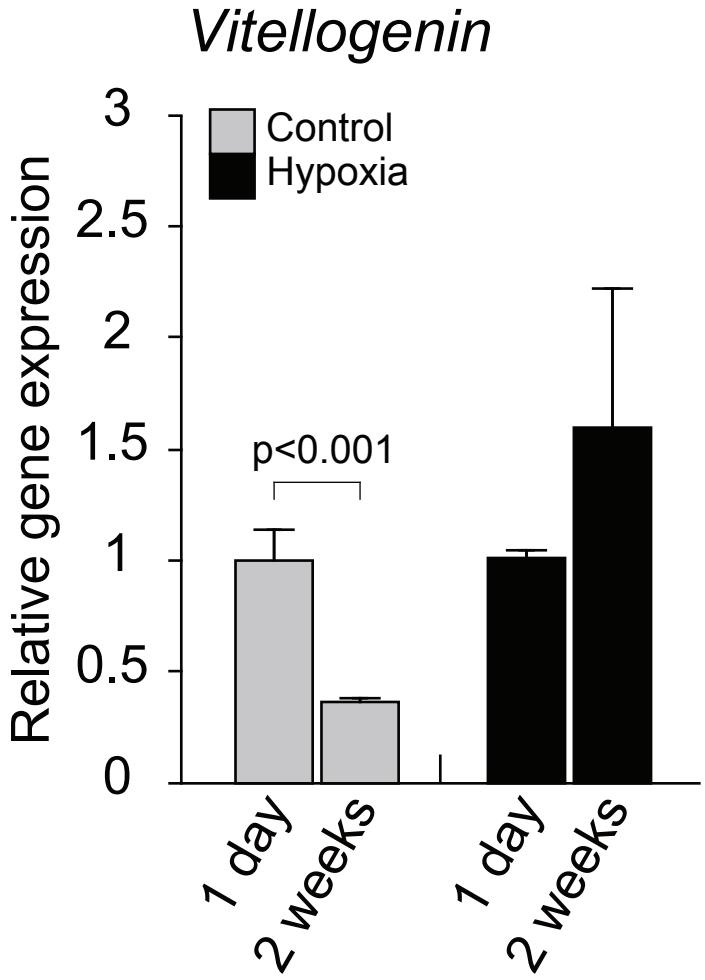

Fig 4.4 | Effects of hypoxia on the vitellogenin gene expression levels in *R. speratus* females. Vitellogenin mRNA expression. The relative mRNA levels were measured by qRT-PCR. One female from FM units: n = 3 [control (21% O_2) and hypoxic (5% O_2) conditions at 1 day] and 6 [control and hypoxic conditions at 2 weeks]. *P*-values were obtained using unpaired *t*-tests. Error bars indicate SEM.

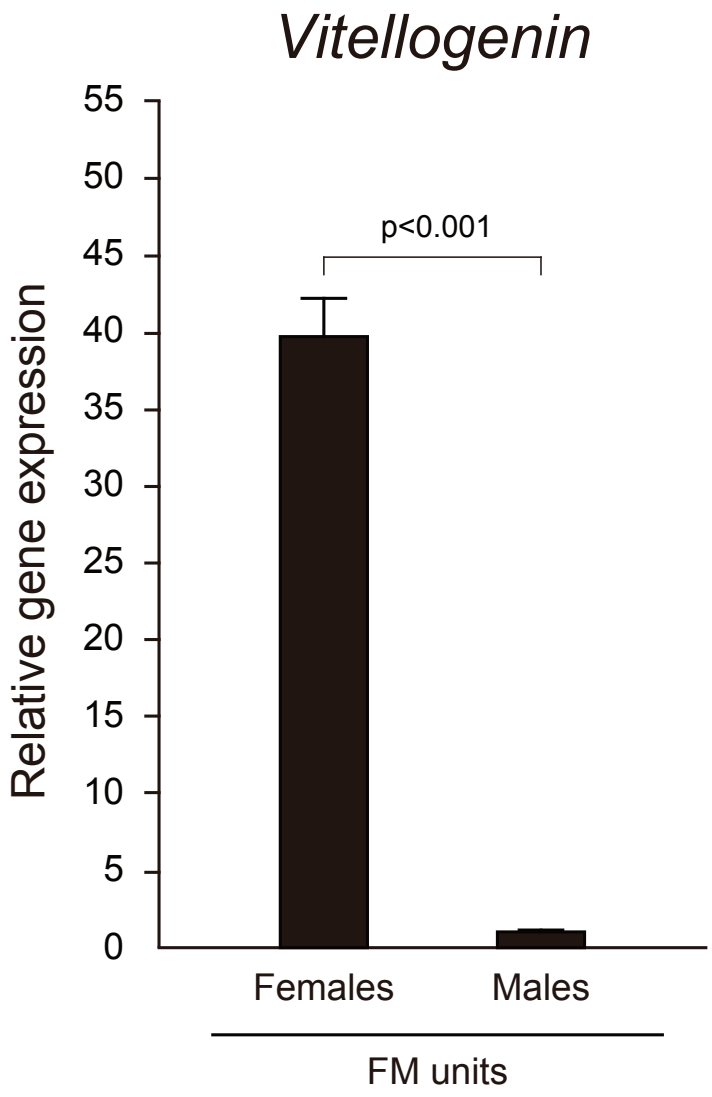

Fig 4.5 | Vitellogenin gene expression levels in termite reproductives. The mRNA expression levels were measured by qRT-PCR. Females from FM units: n = 3 [control conditions (21% O_2) at 4 weeks]. Males from FM units: n = 3 [control conditions at 4 weeks]. *P*-values were obtained using unpaired *t*-tests. Error bars indicate the SEM.

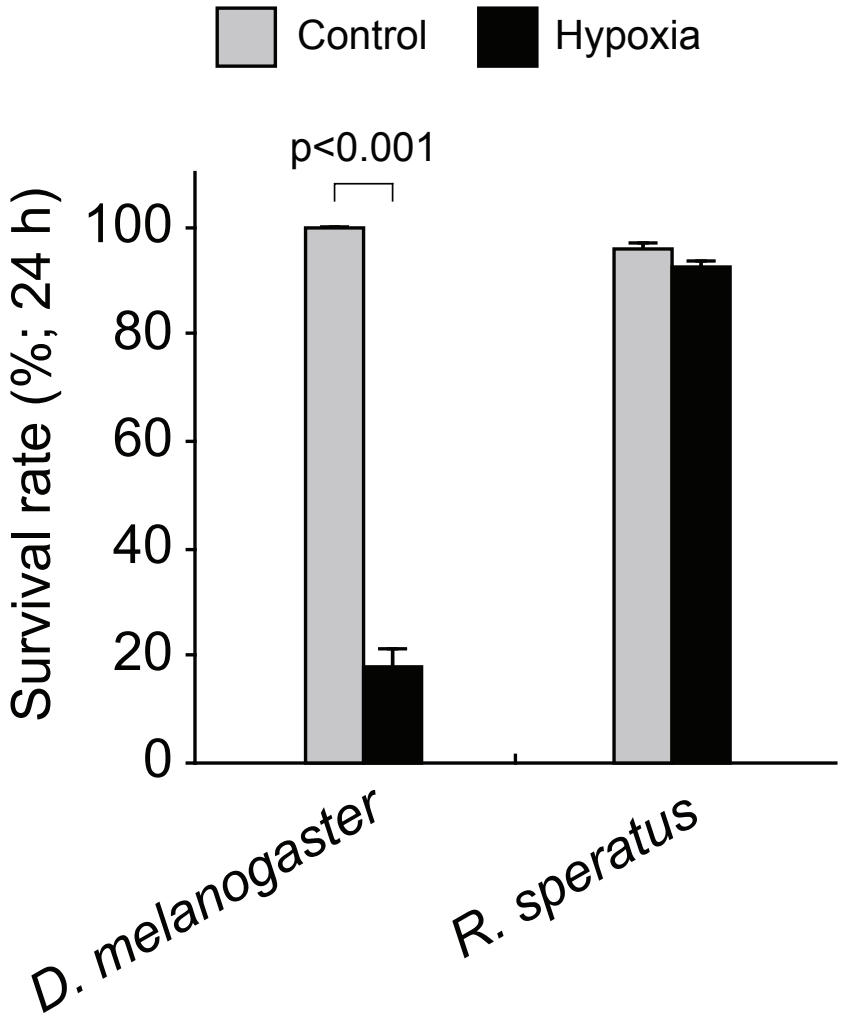

Fig 4.6 | Survival in hypoxic conditions. Average survival rate (%) of *R. speratus* and *D. melanogaster* under control (21% O_2) or hypoxic (1% O_2) conditions for 1day. One hundred individual *R. speratus* workers (n = 3) and 134–173 individual *D. melanogaster* adults (n = 3) were monitored. *P*-values were obtained using unpaired *t*-tests. Error bars indicate SEM.

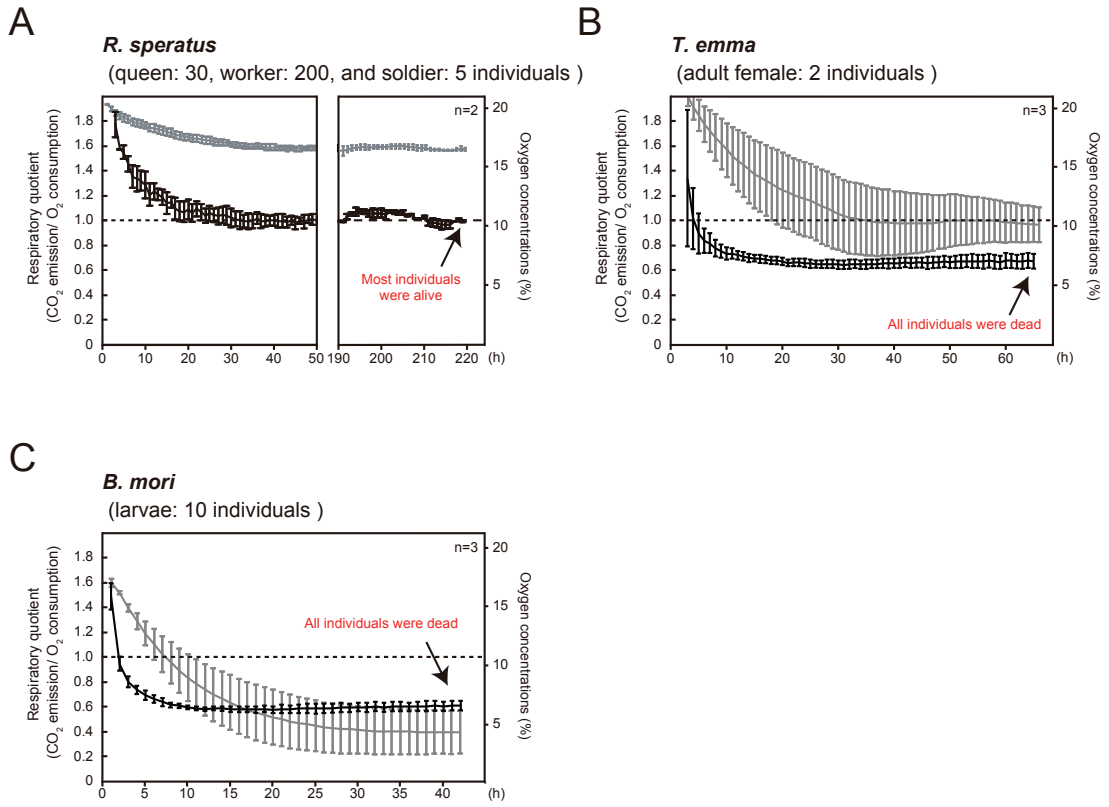

Fig 4.7 | Respiratory quotient measurement in insects. (A–C) Hourly plots of the respiratory quotient (black) and O_2 consumption (gray) in *R. speratus* units (n = 2) comprising 170 individual workers, five individual soldiers, and 30 individual queens (A), Japanese cricket *T. emma* units (n = 3) comprising two individual adult females (B), and model insect *B. mori* units (n = 3) comprising 10 individual larvae of unknown sex (C). All of the experiments were performed in dark and stable conditions.

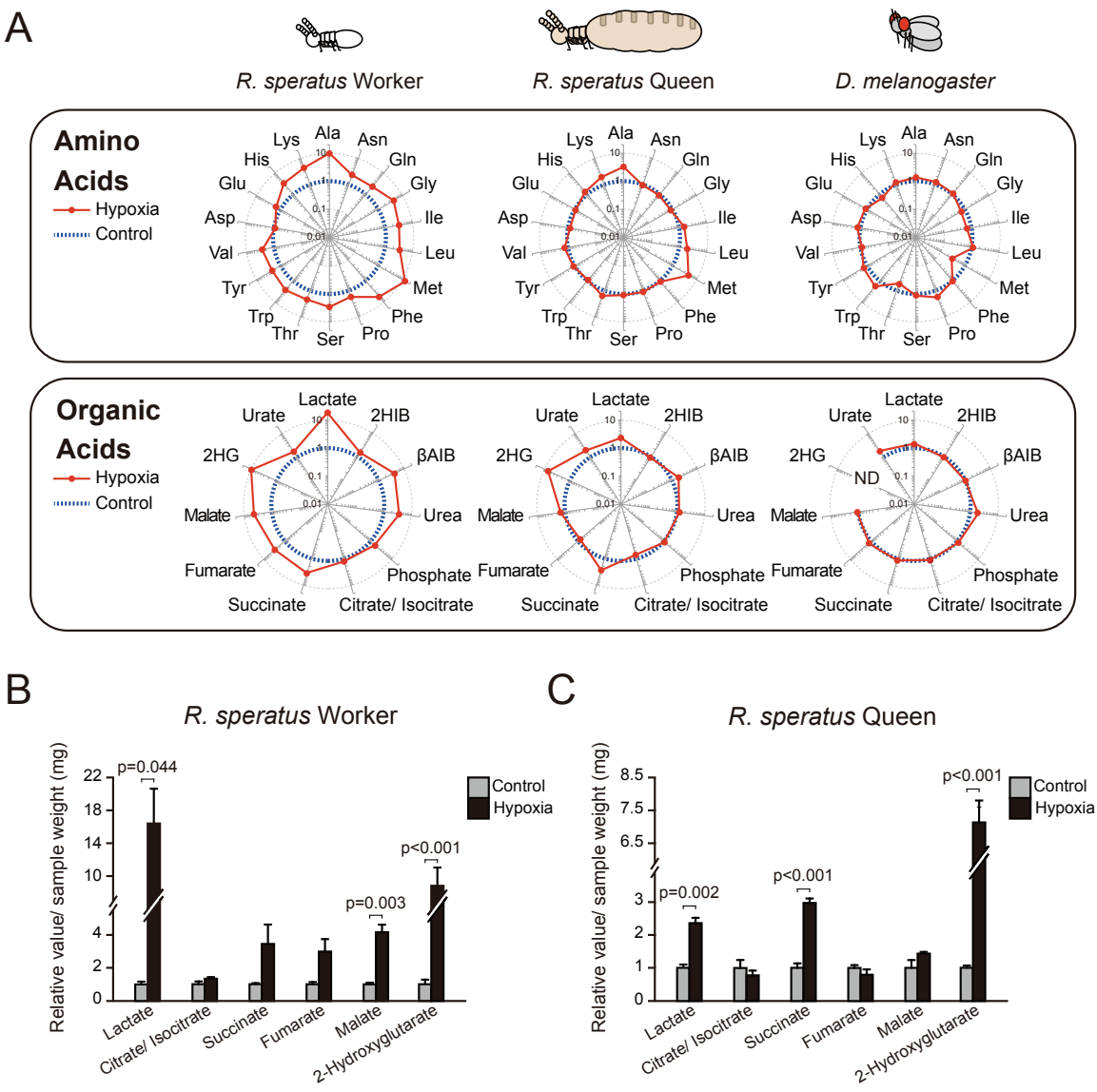

Fig 4.8 | Metabolic shift in *R. speratus* under hypoxia conditions. (A) Average levels of individual metabolites in *R. speratus* (workers and queens) and *D. melanogaster* when kept under hypoxic conditions (1% and 4% O_2, respectively) for 24 h compared with the levels under control conditions (21% O_2) for 24 h. Radar chart presentation (log2 fold change) related to Supplementary Table 2.3. *R. speratus* workers: 13 individuals, n = 3. *R. speratus*

queens: five individuals, n = 3. *D. melanogaster* adults: 30 individuals, n = 3. *Top*, amino acids. *Bottom*, organic acids. ND, not detected, 2-hydroxyglutarate (2HG), 2-Hydroxyisobutyrate (2HIB), β-aminoisobutyrate (βAIB). The red line indicates the values for hypoxia-exposed samples for each insect, and the blue dotted circle indicates the metabolite value under control conditions for each insect. (B and C) Relative average levels for representative organic acids in *R. speratus* workers (B) and queens (C) (related to Table 2.3). The levels are relative to the values obtained in control conditions. *P*-values were obtained using unpaired *t*-tests. Error bars indicate SEM.

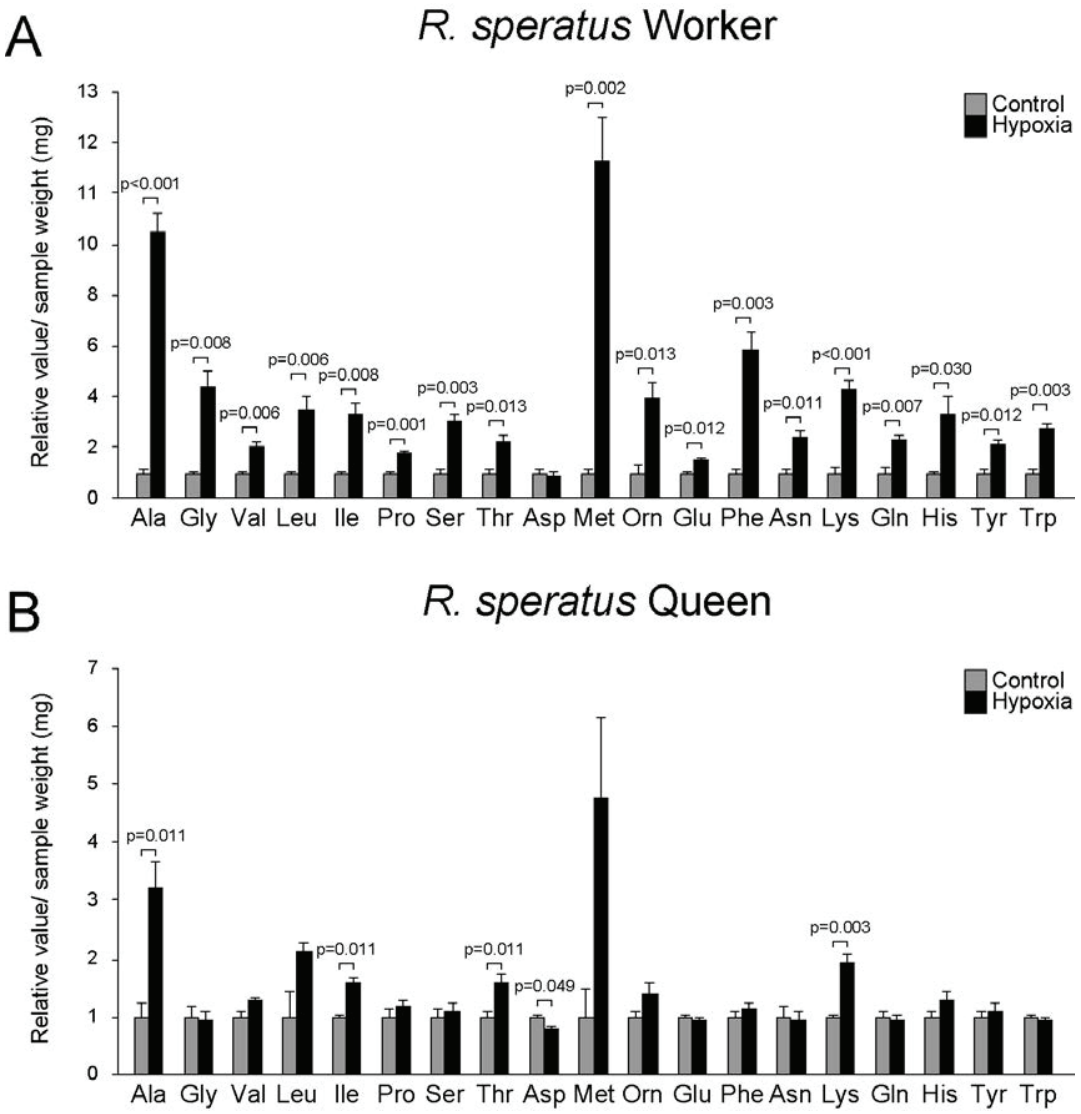

Fig 4.9 | Amino acids content of termites in hypoxic conditions. (A and B) Relative average levels of representative amino acids in hypoxia-exposed *R. speratus* workers (A) and queens (B) (related to Table 2.3). The levels are relative to the values obtained under control conditions (n = 3). *P*-values were obtained using unpaired *t*-tests. Error bars indicate the SEM.

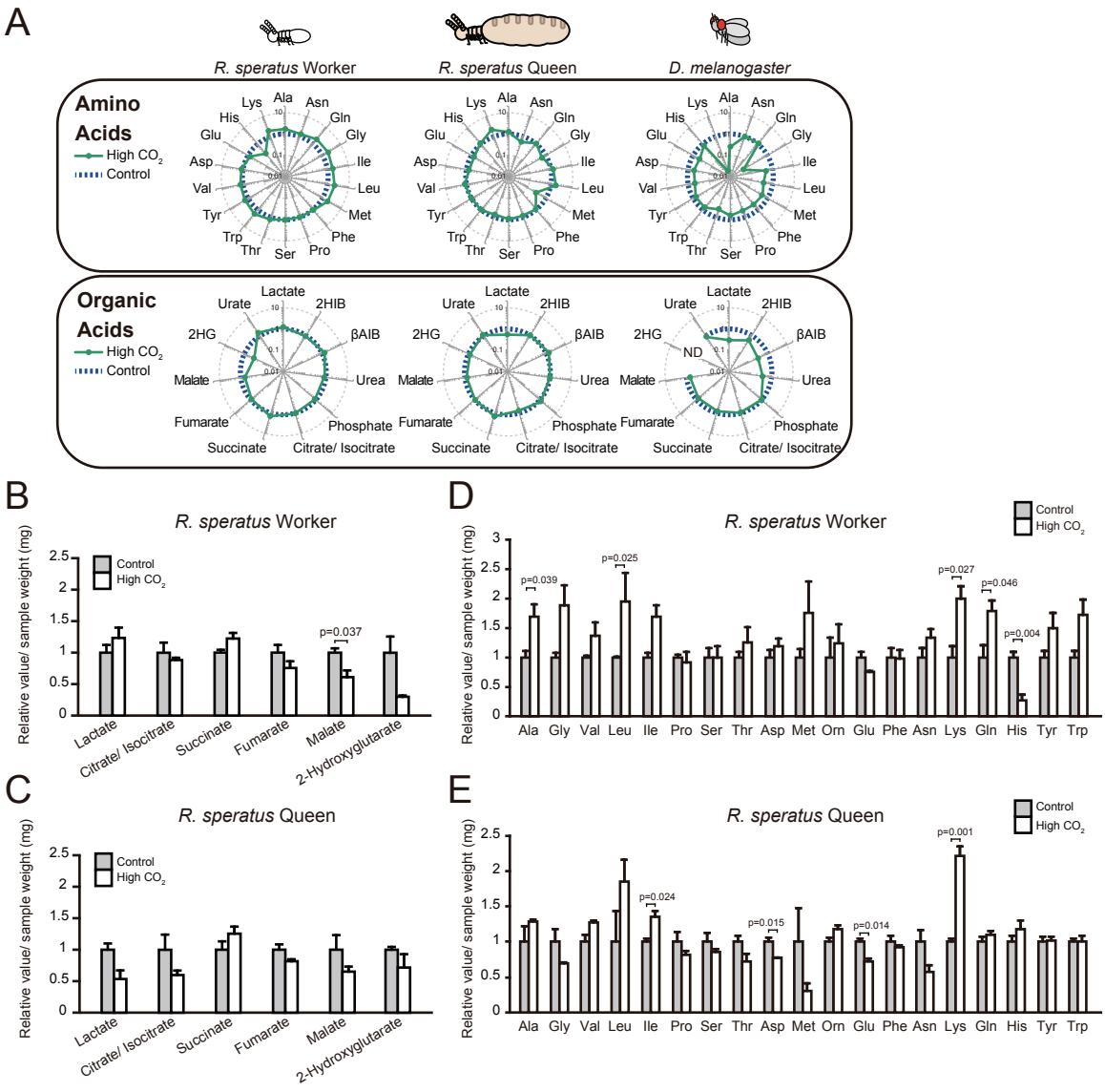

Fig 4.10 | Metabolic analysis of insects under high CO_2 conditions. (A) Average levels of individual metabolites in *R. speratus* (workers and queens) and *D. melanogaster* kept under high CO_2 conditions (10% CO_2) for 24 h relative to the levels under control conditions (< 0.05% CO_2) for 24 h. Radar chart representation (log2 fold change), related to Supplementary Table 2. *R. speratus* workers: 13 individuals, n = 3. *R. speratus* queens: five

individuals, n = 3. *D. melanogaster* adults: 30 individuals, n = 3. *Top*, amino acids. *Bottom*, organic acids. ND, not detected, 2-hydroxyglutarate (2HG), 2-Hydroxyisobutyrate (2HIB), β-aminoisobutyrate (βAIB). The green line indicates the value for high CO_2-exposed samples from each insect and the blue dotted circle indicates the value for the metabolite under control conditions for each insect. (B–E) Relative average levels of representative organic acids in *R. speratus* workers (B) and queens (C), and amino acids in workers (D) and queens (E) kept under high CO_2 condition (10% CO_2) (related to Supplementary Table 2). The levels are relative to the values obtained under the control conditions. *P*-values were obtained using unpaired *t*-tests. Error bars indicate SEM.

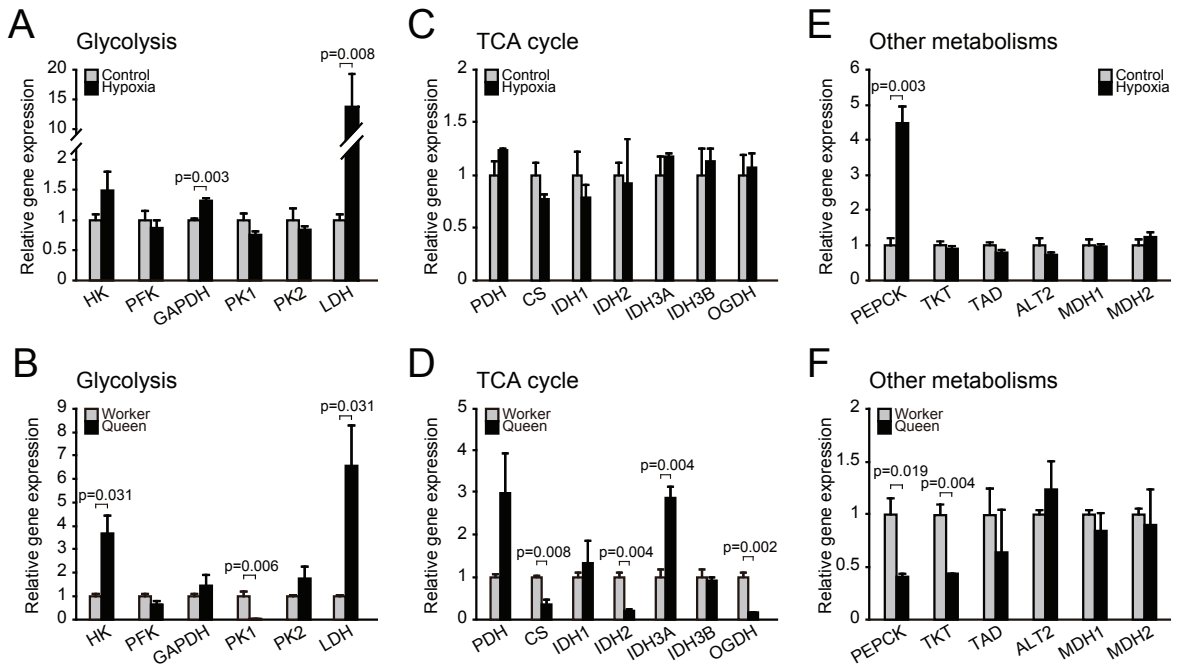

Fig 4.11 | Metabolic gene expression by *R. speratus* under hypoxic conditions. (A–F) Glycolytic genes (A and B), TCA cycle genes (C and D), and the other metabolic genes (E and F) expression. Comparisons between control (21% O_2) workers and hypoxia (1% O_2) workers (A, C, and E), and between workers and queens (B, D, and F) are shown. The mRNA levels were measured by qRT-PCR. All samples: n = 3. *P*-values were derived using unpaired *t*-tests. Error bars indicate SEM.

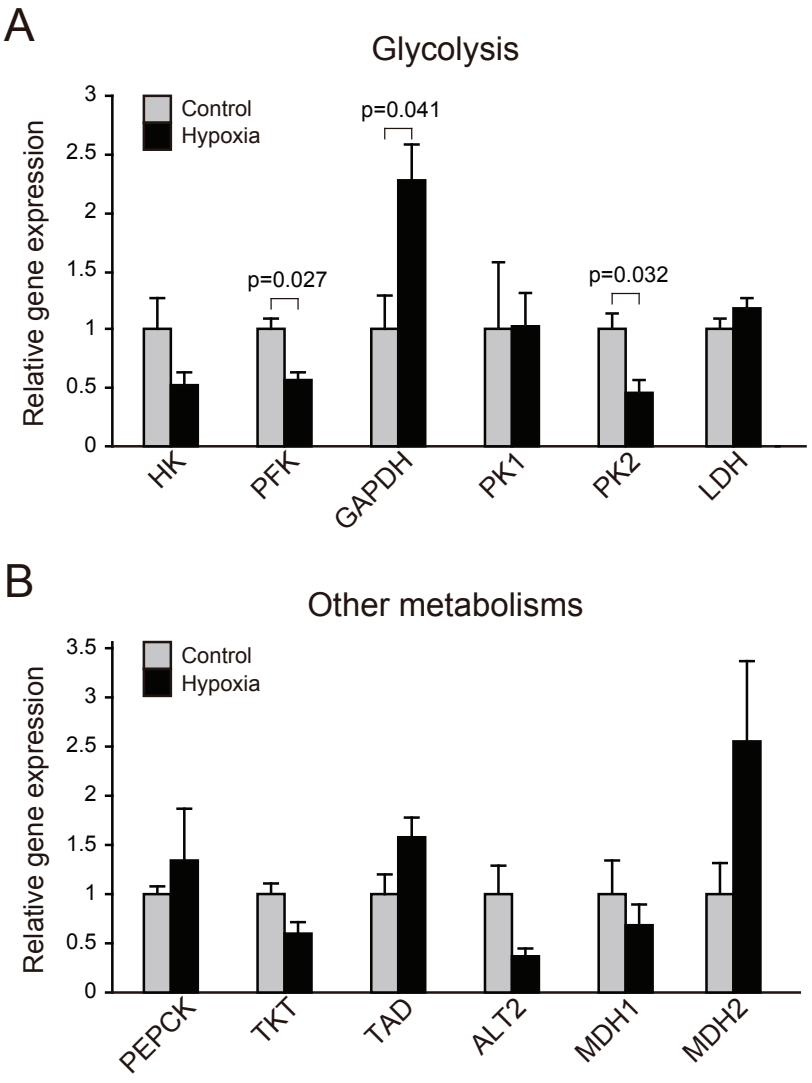

Fig 4.12 | Metabolic genes expression analysis of termite queens in hypoxic conditions. (A and B) Expression levels of glycolytic genes (A) and other metabolic genes (B) in *R. speratus* queens. Comparisons under the control (21% O_2) and hypoxia (1% O_2) conditions are shown (n = 3). The mRNA levels were measured by qRT-PCR. *P*-values were obtained using unpaired *t*-tests. Error bars indicate the SEM.

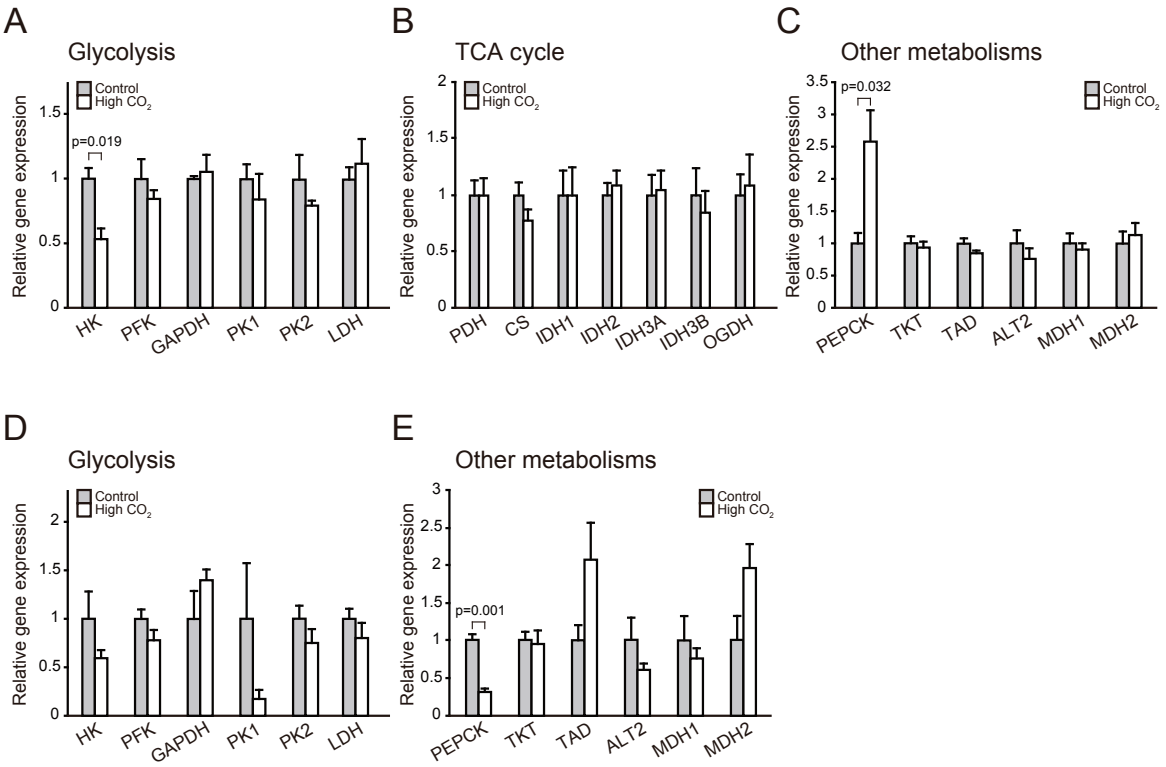

Fig 4.13 | Metabolic genes expression analysis of termites in High CO_2 conditions. (A–E) Expression levels of glycolytic genes (A and D), TCA cycle genes (B), and other metabolic genes (C and E). Comparisons of the control (<0.05% CO_2) and high CO_2 (10% CO_2) exposed workers (A–C) and queens (D and E) are shown. The mRNA levels were measured by qRT-PCR. All samples: n = 3. *P*-values were obtained using unpaired *t*-tests. Error bars indicate the SEM.

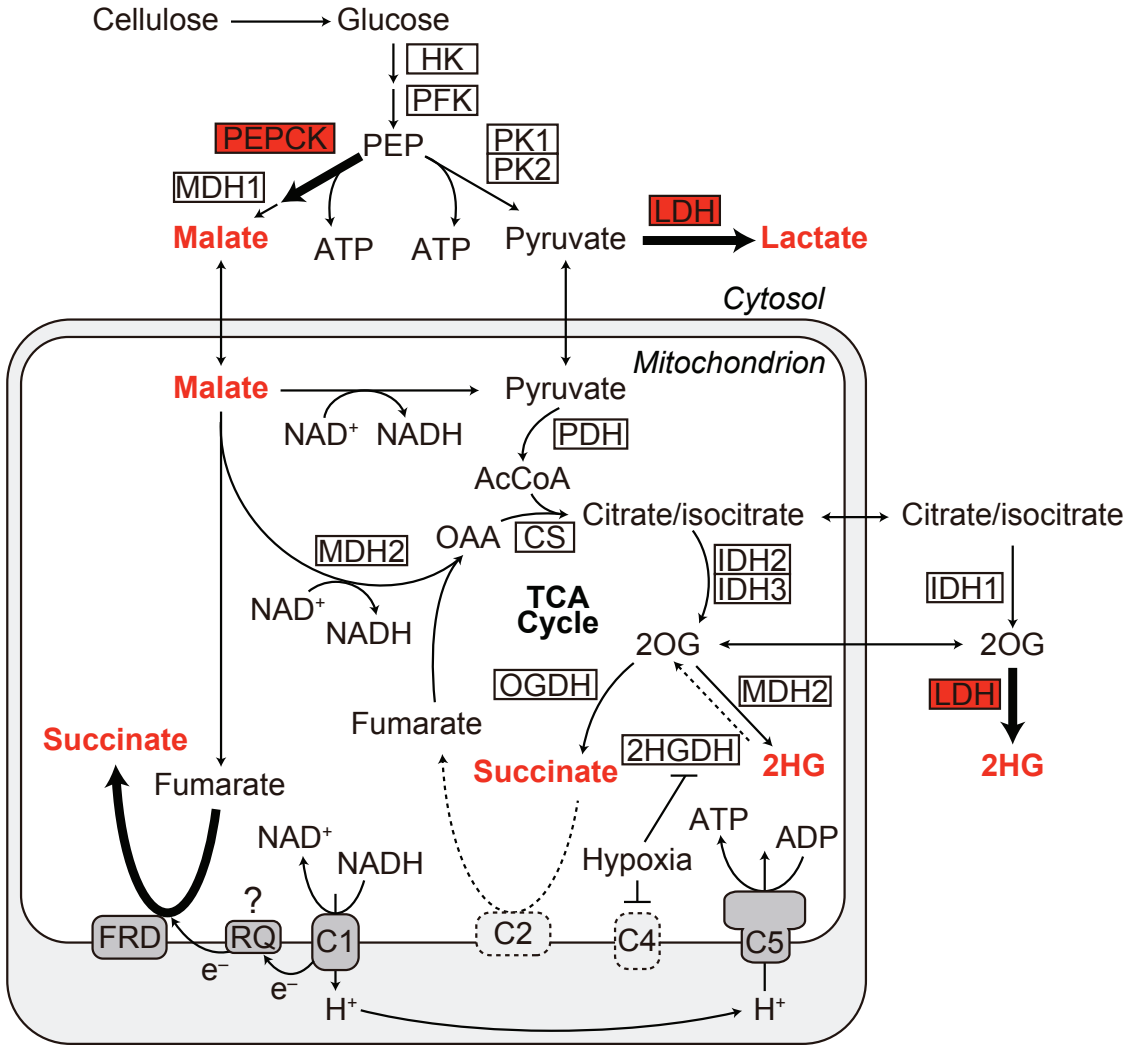

Fig 4.14 | Schematic showing the metabolic pathways affected by hypoxia. The upregulated genes and metabolites induced by hypoxia determined in this study are highlighted in red. The upregulated and suppressed pathways are shown as thick and dotted arrows, respectively. FRD, fumarate dehydrogenase; RQ, rhodoquinone; C1–5, respiratory complex1–5.

Table 2.1. Sequences of primers in this study.

Target gene	Sequence (5'–3')	Amplicon (bp)
RsHK	Forward; GAGGAAGCAGCAGGTTGAGG	125
	Reverse; GTAGAGACGATGGCTGTTGGTG	
RsPFK	Forward; CGGATTTCTCTCTTGGCTGTG	105
	Reverse; CTATGACGAACACTCTCCGCTTT	
RsPK1	Forward; GCAAGGGCATTTCAAGAACAC	150
	Reverse; GAGCGTCCATCTTATCCACATC	
RsPK2	Forward; GTGACTCGATTACGCTGACCAC	108
	Reverse; TGTTTCCCTGCTTTACCACCTT	
RsLDH	Forward; AACGTCTTAATCTGTCTCCCACAAG	85
	Reverse; ACTCCAGACCACACAGCAACA	
RsG6PD	Forward; GCACTTTGTTCGTTCTGATGAGTT	144
	Reverse; TCACTACACACTTCATCTGCCTTCT	
RsTKT	Forward; AGGCCATCCAACACCAAGA	81
	Reverse; ATTCCACAAGCAACAGAGAGACC	
RsTAD	Forward; ACAGTGAACCTCAAGCAAAGAAGA	125
	Reverse; GGTGGCATCAGTGGGTTTG	
RsPDH	Forward; GCGACGGACATTTTCAACTTC	98
	Reverse; CATCACGCTCCATTTCTTCATC	
RsCS	Forward; ATCAAGGGGCTGGTGTGTG	93
	Reverse; AAGCAGTTTCTGGCATTCAGG	
RsIDH1	Forward; GAGCAAAACTGGATGACAACAAAC	81
	Reverse; CAGCCTCAATGGTTTCCACA	
RsIDH2	Forward; CGCTTCAAGGACATCTTCCA	140
	Reverse; GCCCACACAAAACCACCAC	
RsIDH3A	Forward; ATGTGTGCTGGTCTGGTTGG	130
	Reverse; CAGTTGGGTTTGCTTTATCTTGG	
RsIDH3B	Forward; TTCACCCGTCATCCACCA	102
	Reverse; GCTCAGGTCCAACACCATCTC	
RsOGDH	Forward; GAAAATGTCTTCTCCACCACCAA	117
	Reverse; CCAAGAGCCCAATCCACAA	
RsPEPCK	Forward; GGCTACAAGGTTGAGTGTGTGG	139
	Reverse; TTGCGTTGGGATTTGTTTTG	
RsALT2	Forward; CGCCATGCTGTGTCCAA	107
	Reverse; CCTTCTTCTCGTTCACATACTGCTC	
RsMDH1	Forward; AGATAGCAGAACGCCTGAAAGTG	125
	Reverse; CACAGGACCAGACCCCAAA	
RsMDH2	Forward; AATGGACCAGAGCAGTTAAAGGA	133
	Reverse; CAAGGTCACGAACGATGGAA	

Vg2	Forward; TCGACGTGATCGCAGAAAA	127
	Reverse; GAAGAAGAGGAGGAAGAAGAAGAGG	
RsACT	Forward; AAATCGTGCGTGACATCAAA	168
	Reverse; GGAACAGAGCCTCAGGACAG	
RsGAPDH	Forward; CCATAGAAAAGGCTTCTGCACATT	89
	Reverse; AACAACAAACATTGGGGCATC	

Table 2.2. Summary of the number of eggs laid at 2, 3, and 4 weeks and the survival data.

Unit no. [1]	Combination	Condition	The number of eggs laid			Lifespan (weeks) [2]
			2 weeks	3 weeks	4 weeks	
FM_1	$F_A M_B$	Hypoxia	4	4	5	>25
FM_2	$F_A M_B$	Control	0	0	0	4
FM_3	$F_A M_B$	Hypoxia	4	5	5	12
FM_4	$F_A M_B$	Control	4	5	5	5
FM_5	$F_A M_B$	Hypoxia	4	6	7	>25
FM_6	$F_A M_B$	Control	1	3	3	4
FM_7	$F_A M_B$	Hypoxia	1	4	4	7
FM_8	$F_B M_A$	Hypoxia	2	2	4	>25
FM_9	$F_B M_A$	Control	0	0	0	5
FM_10	$F_B M_A$	Hypoxia	0	1	1	5
FM_11	$F_B M_A$	Control	-	-	-	1
FM_12	$F_C M_D$	Hypoxia	0	-	-	2
FM_13	$F_C M_D$	Hypoxia	3	4	4	6
FM_14	$F_C M_D$	Hypoxia	0	2	2	5
FM_15	$F_C M_D$	Hypoxia	0	1	1	7
FM_16	$F_C M_D$	Hypoxia	0	1	1	4
FM_17	$F_C M_D$	Hypoxia	3	3	-	5
FM_18	$F_C M_D$	Hypoxia	1	1	-	3
FM_19	$F_C M_D$	Control	4	4	-	3
FM_20	$F_C M_D$	Control	-	-	-	1
FM_21	$F_C M_D$	Control	0	0	0	4
FM_22	$F_C M_D$	Control	0	0	-	3
FM_23	$F_C M_D$	Control	4	4	4	6
FM_24	$F_C M_D$	Control	0	0	0	4

FM_25	$F_D M_C$	Hypoxia	4	4	4	7
FM_26	$F_D M_C$	Hypoxia	-	-	-	1
FM_27	$F_D M_C$	Hypoxia	0	0	-	3
FM_28	$F_D M_C$	Hypoxia	1	1	1	9
FM_29	$F_D M_C$	Control	1	1	-	3
FM_30	$F_D M_C$	Control	0	0	0	4
FM_31	$F_D M_C$	Control	0	0	0	4
FM_32	$F_D M_C$	Control	0	0	0	4
FM_33	$F_E M_F$	Hypoxia	4	6	7	10
FM_34	$F_E M_F$	Control	0	0	0	4
FM_35	$F_E M_F$	Hypoxia	2	4	4	>21
FM_36	$F_E M_F$	Control	3	3	3	4
FM_37	$F_E M_F$	Control	0	0	0	4
FM_38	$F_E M_F$	Hypoxia	-	-	-	1
FM_39	$F_E M_F$	Control	-	-	-	1
FM_40	$F_E M_F$	Hypoxia	4	5	6	>21
FM_41	$F_E M_F$	Control	-	-	-	1
FM_42	$F_F M_E$	Hypoxia	0	-	-	2
FM_43	$F_F M_E$	Control	-	-	-	1
FM_44	$F_F M_E$	Hypoxia	0	0	0	5
FM_45	$F_F M_E$	Control	-	-	-	1
FM_46	$F_F M_E$	Hypoxia	6	6	6	4
FM_47	$F_F M_E$	Control	-	-	-	1
FM_48	$F_F M_E$	Control	5	5	-	3
FM_49	$F_G M_H$	Hypoxia	4	4	7	>20
FM_50	$F_G M_H$	Hypoxia	2	2	-	3
FM_51	$F_G M_H$	Hypoxia	2	4	5	>20
FM_52	$F_G M_H$	Hypoxia	3	3	5	>20
FM_53	$F_G M_H$	Hypoxia	2	3	4	>20
FM_54	$F_G M_H$	Hypoxia	2	3	4	10

FM_55	$F_G M_H$	Hypoxia	3	5	5	20
FM_56	$F_G M_H$	Hypoxia	4	7	8	>20
FM_57	$F_G M_H$	Control	0	0	-	3
FM_58	$F_G M_H$	Control	-	-	-	1
FM_59	$F_G M_H$	Control	0	1	1	4
FM_60	$F_G M_H$	Control	-	-	-	1
FM_61	$F_G M_H$	Control	4	4	4	5
FM_62	$F_G M_H$	Control	0	0	0	4
FM_63	$F_G M_H$	Control	1	1	1	5
FM_64	$F_G M_H$	Control	-	-	-	1
FM_65	$F_G M_H$	Control	-	-	-	1
FM_66	$F_H M_G$	Hypoxia	-	-	-	1
FM_67	$F_H M_G$	Hypoxia	3	4	4	4
FM_68	$F_H M_G$	Hypoxia	1	-	-	2
FM_69	$F_H M_G$	Hypoxia	0	-	-	2
FM_70	$F_H M_G$	Hypoxia	-	-	-	1
FM_71	$F_H M_G$	Hypoxia	1	3	4	9
FM_72	$F_H M_G$	Hypoxia	5	7	8	20
FM_73	$F_H M_G$	Hypoxia	1	-	-	2
FM_74	$F_H M_G$	Hypoxia	-	-	-	1
FM_75	$F_H M_G$	Hypoxia	0	1	1	6
FM_76	$F_H M_G$	Hypoxia	0	2	2	6
FM_77	$F_H M_G$	Control	0	1	1	4
FM_78	$F_H M_G$	Control	3	3	3	4
FM_79	$F_H M_G$	Control	0	0	0	5
FM_80	$F_H M_G$	Control	0	0	0	4
FM_81	$F_H M_G$	Control	5	5	5	4
FM_82	$F_H M_G$	Control	0	1	1	4
FM_83	$F_H M_G$	Control	1	2	2	4
FM_84	$F_H M_G$	Control	-	-	-	1

FM_85	$F_H M_G$	Control	0	0	-	3
FM_86	$F_H M_G$	Control	0	-	-	2
FM_87	$F_I M_J$	Hypoxia	6	7	8	>4
FM_88	$F_I M_J$	Hypoxia	0	-	-	2
FM_89	$F_I M_J$	Hypoxia	0	-	-	2
FM_90	$F_I M_J$	Hypoxia	3	4	5	>4
FM_91	$F_I M_J$	Hypoxia	6	8	9	>4
FM_92	$F_I M_J$	Hypoxia	0	0	0	>4
FM_93	$F_I M_J$	Hypoxia	1	2	3	>4
FM_94	$F_I M_J$	Hypoxia	3	4	4	>4
FM_95	$F_I M_J$	Hypoxia	9	9	13	>4
FM_96	$F_I M_J$	Hypoxia	0	-	-	2
FM_97	$F_I M_J$	Control	0	0	-	3
FM_98	$F_I M_J$	Control	3	4	4	>4
FM_99	$F_I M_J$	Control	-	-	-	1
FM_100	$F_I M_J$	Control	1	1	-	3
FM_101	$F_I M_J$	Control	1	1	-	3
FM_102	$F_I M_J$	Control	1	3	3	>4
FM_103	$F_I M_J$	Control	1	1	-	3
FM_104	$F_I M_J$	Control	2	2	2	4
FM_105	$F_I M_J$	Control	-	-	-	1
FM_106	$F_I M_J$	Control	5	6	6	>4
FM_107	$F_J M_I$	Hypoxia	-	-	-	1
FM_108	$F_J M_I$	Hypoxia	2	3	4	>4
FM_109	$F_J M_I$	Hypoxia	0	0	0	>4
FM_110	$F_J M_I$	Hypoxia	0	0	0	>4
FM_111	$F_J M_I$	Hypoxia	1	3	5	>4
FM_112	$F_J M_I$	Hypoxia	3	5	5	>4
FM_113	$F_J M_I$	Hypoxia	2	4	4	>4
FM_114	$F_J M_I$	Hypoxia	0	0	-	3

FM_115	$F_J M_I$	Hypoxia	3	5	6	>4
FM_116	$F_J M_I$	Hypoxia	4	4	5	>4
FM_117	$F_J M_I$	Control	0	1	2	>4
FM_118	$F_J M_I$	Control	2	4	4	>4
FM_119	$F_J M_I$	Control	-	-	-	1
FM_120	$F_J M_I$	Control	-	-	-	1
FM_121	$F_J M_I$	Control	-	-	-	1
FM_122	$F_J M_I$	Control	5	5	6	>4
FM_123	$F_J M_I$	Control	0	1	2	>4
FM_124	$F_J M_I$	Control	2	2	3	>4
FM_125	$F_J M_I$	Control	-	-	-	1
FM_126	$F_J M_I$	Control	-	-	-	1

[1]FM: female–male mating pairs.

[2]Lifespan is shown as ‘colony lifespan’ (the period when one individual died in the unit).

Table 2.3. Metabolite data in GC-MS analysis[1, 2].

R. speratus **worker**

Conditions	Control 1	Control 2	Control 3	Low O_2 1	Low O_2 2	Low O_2 3	High CO_2 1	High CO_2 2	High CO_2 3
Sample weights (mg)	**25.16**	**24.90**	**25.92**	**24.35**	**23.18**	**20.26**	**22. 60**	**20.71**	**24.06**
Alanine	523562	353444	563631	4911403	5933808	4059772	612084	636513	927277
Glycine	194429	132883	173015	645485	994505	526004	190902	299481	335995
Valine	1356565	1123137	1397502	2484422	3295799	2112956	1138154	1699345	1819148
Leucine	405811	349211	374733	1043691	1600618	1244342	482298	851077	582734
Isoleucine	625182	470714	672327	1604207	2539094	1634754	876225	944341	817188
Proline	784113	601504	763741	1273911	1328552	1169971	391110	574636	769490
Serine	503613	285222	553695	1244320	1623439	1093551	258836	444876	456546
Threonine	522564	407251	629079	954408	1408888	998840	427909	694774	580161
Aspartate	324571	223423	375184	216246	268296	310710	286451	337302	337192
Methionine	72851	37800	54068	592621	902657	639430	105732	106285	38839
Ornithine	112658	30059	133387	266709	397468	364684	71184	130010	90816
Glutamate	1372117	880623	1258897	1834352	2001765	1382066	892915	650931	798683
Phenylalanine	344422	187213	361092	1464669	2173767	1463256	280649	281303	199576
Asparagine	138683	70388	126360	227150	325968	227366	127141	139394	123188
Lysine	812521	345584	686896	2629292	3136191	2008652	972760	1138509	1094444
Glutamine	3756392	1506452	2743739	5953117	7154181	5080210	3770867	4326327	4416258
Histidine	238892	277084	315275	858831	1290418	515912	48621	36165	113925
Tyrosine	3029477	2320081	3747962	5679719	6564689	6480274	4506567	4531036	2890482
Tryptophan	391846	237282	307728	775625	887720	824422	499539	530442	382064
Lactate	213642	232041	197898	3320380	6249086	2325808	360062	229022	222969
2-Hydroxyisobutyrate	60240	65892	77936	94924	127257	121641	51318	61631	71793
β-Aminoisobutyrate	40647	36297	41298	146331	212722	199201	37198	63914	53979
Urea	78761	85548	100298	247227	430857	453692	96026	61888	50871
Phosphate	1469938	718492	1824067	2941466	1960664	2583418	1618193	144880	1649882
Succinate	106469	98511	113914	251838	653137	301884	161862	104803	128410
Fumarate	38470	45883	43063	93012	196778	123939	32548	23420	44235
Malate	105288	78675	122965	403317	531489	420306	72433	35752	82406
2-Hydroxyglutarate	182110	86981	76223	913979	1590202	793861	32802	33298	35978
Citrate	3828275	1790185	3524660	4304662	4713853	4006395	2979630	2133602	2917886
Urate	2996165	1262197	2243574	3443798	3710126	3679787	2949767	2834296	2724477
IS[3]	9734986	8597025	9128505	10248072	10455680	9673664	9863892	8736368	9135889

***R. speratus* queen**

Conditions	Control 1	Control 2	Control 3	Low O_2 1	Low O_2 2	Low O_2 3	High CO_2 1	High CO_2 2	High CO_2 3
Sample weights (mg)	**32.19**	**40.69**	**38.70**	**40.40**	**40.70**	**41.75**	**39.25**	**40.09**	**39.40**
Alanine	1452778	923158	1052430	5344773	3776432	3432442	1640621	1745661	2074511
Glycine	2192913	1491663	1894307	2526329	1780896	1573684	1428166	1649083	1669082
Valine	3900390	3509732	5343818	6525543	5542420	5906901	6171648	6153402	7008413
Leucine	608066	87521	531569	1028995	807765	1138341	648894	1236401	939532
Isoleucine	700552	730507	951583	1588330	1156705	1396719	1015111	1339471	1519256
Proline	10759426	8294701	9799224	12061358	13938409	12174660	8342765	8815120	11988445
Serine	2784456	2234016	2771213	4088408	2701065	2718294	2573172	2427740	3101108
Threonine	805740	1288196	1354500	2297844	1780498	1961959	738591	901862	1373842
Aspartate	888637	910537	994527	927410	735192	842444	792103	843696	959725
Methionine	4230	34009	64129	247691	169805	82412	12787	3812	18737
Ornithine	776527	903753	1217687	1873878	1069236	1397740	1274655	1199858	1583935
Glutamate	4963770	4985132	6361245	6119616	5022843	5533493	4474678	4195828	5561560
Phenylalanine	4485860	4114984	4874542	6433250	4762123	5930139	4375007	4971306	5813398
Asparagine	140470	149804	101004	110265	142165	171686	103794	98784	71446
Lysine	2907193	3001023	3725984	7816643	5722939	6959239	8382358	7377029	9797514
Glutamine	3662672	3461640	4178740	4928464	3220875	3533570	4872044	4635698	5531713
Histidine	2788395	3954009	4923837	6528857	3958544	5620476	5639673	4257632	6299523
Tyrosine	2989861	3838023	5110889	5930061	3685807	4629226	4767400	4603860	4967354
Tryptophan	469213	502164	528156	597124	429587	496394	634099	555770	620606
Lactate	903112	867656	871745	2664017	2183954	2137474	375618	427673	957646
2-Hydroxyisobutyrate	295550	266449	316137	377846	274058	257293	282098	331228	404363
β-Aminoisobutyrate	138787	113262	123504	282308	278099	277894	155926	182661	293307
Urea	5170369	6157002	6128957	8925352	8466454	7730401	6814579	7015320	7915478
Phosphate	8065248	8375749	11152001	11876281	11026148	11945707	11840140	10422568	13655817
Succinate	380620	321591	350845	1255351	1144783	1095464	411316	525083	687278
Fumarate	84618	130901	145951	64946	117118	131555	96352	119072	132911
Malate	248874	165311	170243	329955	316656	304311	109827	153691	211621
2-Hydroxyglutarate	88453	91271	106768	845527	583700	849752	48080	63133	144663
Citrate	7777357	6414713	4392091	3425067	6320011	6676060	4107504	5490371	4070598
Urate	1230889	1126314	1568932	2959796	2415519	2746040	1642846	1073567	2034330
IS[3]	12321764	11665003	13631892	12893232	12068540	12789921	12869442	13803140	15620292

D. melanogaster

Conditions[4]	Control 1	Control 2	Control 3	Low O_2 1	Low O_2 2	Low O_2 3	High CO_2 1	High CO_2 2	High CO_2 3
Sample weights (mg)	**27.18**	**30.83**	**26.83**	**24.43**	**22.94**	**26.52**	**27.27**	**26.22**	**25.98**
Alanine	7957522	14016932	11323542	13735076	15361907	13265694	2531495	2343336	2703990
Glycine	3854579	7868129	4517497	3606545	3648411	3190422	317604	201459	218090
Valine	1050278	2120531	1498005	1346331	1141170	1195249	564200	702224	608606

Leucine	1014875	789028	1340692	1392051	1217926	844527	264461	406877	298608
Isoleucine	1035685	1993842	1706522	1234676	1012161	801882	428140	956206	464241
Proline	11732914	1782596	18108060	18182392	18898353	16213210	4132887	4303489	3903267
Serine	5999907	8749522	8078795	8444650	8212982	6968447	3818288	3990299	3974475
Threonine	1806400	4400931	4046202	1761146	1483050	1502529	820863	1156933	1009301
Aspartate	4731076	7055625	7043725	8097960	7466626	6480098	1915119	3295155	2499586
Methionine	457266	736791	641151	233941	111545	145490	246209	346791	218967
Ornithine	1764732	3894947	3644258	2726176	2435801	1656022	286254	282064	269526
Glutamate	6196877	8729286	8360478	8872570	8419680	7545045	2454156	3714244	2843351
Phenylalanine	784668	692182	599959	837598	593629	563726	233581	324478	213958
Asparagine	761003	1373832	1824211	1657492	1713898	1179198	910699	1625866	660284
Lysine	3575542	4118052	3578942	5069922	3952555	3821722	55196	81465	34031
Glutamine	12481388	15270831	14982353	15513896	15010622	14419128	12132874	15793111	12894366
Histidine	8761258	6810813	5758390	5807354	4378306	3751148	2954870	6778494	4917661
Tyrosine	2690737	3998181	2465774	4167058	4232592	2636945	1430629	2137404	1628041
Tryptophan	394546	585177	574583	784338	947167	824585	231053	289734	316786
Lactate	1793676	3327419	2986061	4010164	2644553	3010842	466173	697119	638403
2-Hydroxyisobutyrate	438055	509080	411820	393437	469133	257541	152033	335132	173562
β-Aminoisobutyrate	14437082	21718671	16878493	15867588	16070142	16558110	5734739	3439265	4069318
Urea	363457	628469	659973	1032529	717926	1038506	103887	194548	119049
Phosphate	12106806	17975258	15770638	17135439	15343393	14756283	10185763	13616850	11186949
Succinate	1871678	2955462	2669859	3075875	2673462	2124072	1437163	1928640	1129024
Fumarate	69723	214028	207015	227153	177102	137959	46338	145787	86086
Malate	2959131	4478405	4948125	4637536	3937709	3266743	1493739	2797749	1833027
2-Hydroxyglutarate	1041056	845588	861935	735301	647393	502838	121677	308390	180304
Citrate	4433348	4859155	5537443	5085283	4802276	4664285	3049466	4430624	3218624
Urate	1635988	2018524	3245164	4639112	3053194	2975834	1179006	2052342	1530958
IS[3]	18149136	22123681	22568456	22822980	22592679	19371631	16934426	21477421	18633996

[1]These list include “experimental conditions”, “using sample weights for GC-MS analysis”, and “raw data”.

[2]The value of reader charts and histograms in this paper were calculated by the average value of low O_2 samples or high CO_2 samples, which are corrected by their weight (mg) and the value of IS, compared with the average value of control samples

[3]IS is Internal standard, 2-isopropylmalate.

[4]Low O_2 in D. melanogaster is 4% oxygen condition because 1% oxygen is too low for them to survive during experiment (24 h).

Table 2.4. Target gene information in this study.

Reticulitermes speratus						
Target gene	Target gene ID	Accession no.	Query genes (Accession no.)	Query organisms	E–value	Identity
RsHK	comp782666_c3_seq1	FX983725	Hexokinase type 2 (KDR18923.1)	*Zootermopsis nevadensis*	0E+00	92%
			PREDICTED: hexokinase-1-like (XP_016767150.1)	*Apis mellifera*	0E+00	67%
			PREDICTED: putative hexokinase HKDC1 (XP_004923503.1)	*Bombyx mori*	5E−152	53%
			Hexokinase A, isoform C (NP_001259384.1)	*Drosophila melanogaster*	9E−127	47%
			PREDICTED: hexokinase type 2 isoform X1 (XP_970645.1)	*Tribolium castaneum*	2E−125	47%
			PREDICTED: hexokinase type 2-like isoform X2 (XP_001945605.1)	*Acyrthosiphon pisum*	6E−110	44%
RsPFK	comp800684_c3_seq2	FX983726	6-phosphofructokinase (KDR15026.1)	*Zootermopsis nevadensis*	0E+00	92%
			PREDICTED: ATP-dependent 6-phosphofructokinase isoform X3 (XP_003241124.1)	*Acyrthosiphon pisum*	0E+00	80%
			Phosphofructokinase, isoform B (NP_724890.1)	*Drosophila melanogaster*	0E+00	76%
			PREDICTED: ATP-dependent 6-phosphofructokinase isoform X1 (XP_012549268.1)	*Bombyx mori*	0E+00	75%
			PREDICTED: ATP-dependent 6-phosphofructokinase isoform X2 (XP_008196658.1)	*Tribolium castaneum*	0E+00	71%
			PREDICTED: LOW QUALITY PROTEIN: ATP-dependent 6-phosphofructokinase (XP_016769850.1)	*Apis mellifera*	0E+00	67%
RsGAPDH	comp666388_c0_seq2	FX983172	Glyceraldehyde-3-phosphate dehydrogenase (KDR24072.1)	*Zootermopsis nevadensis*	0E+00	92%

			PREDICTED: glyceraldehyde-3-phosphate dehydrogenase isoform X1 (XP_012545898.1)	*Bombyx mori*	0E+00	89%
			PREDICTED: glyceraldehyde-3-phosphate dehydrogenase 2 (XP_974181.1)	*Tribolium castaneum*	0E+00	88%
			Glyceraldehyde-3-phosphate dehydrogenase (NP_001280403.1)	*Acyrthosiphon pisum*	0E+00	86%
			Glyceraldehyde 3 phosphate dehydrogenase 2, isoform A (NP_542445.1)	*Drosophila melanogaster*	0E+00	83%
			PREDICTED: glyceraldehyde-3-phosphate dehydrogenase 2 (XP_393605.1)	*Apis mellifera*	0E+00	83%
	RsPK1	comp808555_c0_seq1	FX983727	Pyruvate kinase (KDR19430.1)	*Zootermopsis nevadensis*	0E+00	90%
				PREDICTED: pyruvate kinase isoform X1 (XP_966698.2)	*Tribolium castaneum*	0E+00	79%
				PREDICTED: pyruvate kinase-like isoform X1 (XP_004931176.2)	*Bombyx mori*	0E+00	75%
				PREDICTED: pyruvate kinase isoform X1 (XP_003242527.1)	*Acyrthosiphon pisum*	0E+00	75%
				Pyruvate kinase, isoform A (NP_524448.3)	*Drosophila melanogaster*	0E+00	73%
				PREDICTED: pyruvate kinase isoform X2 (XP_006565999.1)	*Apis mellifera*	0E+00	72%
	RsPK2	comp808555_c0_seq3	FX983728	Pyruvate kinase (KDR19430.1)	*Zootermopsis nevadensis*	0E+00	91%
				PREDICTED: pyruvate kinase isoform X1 (XP_966698.2)	*Tribolium castaneum*	0E+00	80%
				PREDICTED: pyruvate kinase-like isoform X1 (XP_004931176.2)	*Bombyx mori*	0E+00	78%
				PREDICTED: pyruvate kinase isoform X1 (XP_003242527.1)	*Acyrthosiphon pisum*	0E+00	75%
				PREDICTED: pyruvate kinase isoform X2 (XP_006565999.1)	*Apis mellifera*	0E+00	75%
				Pyruvate kinase, isoform A (NP_524448.3)	*Drosophila melanogaster*	0E+00	74%
	RsLDH	comp791092_c9_seq1	FX983729	L-lactate dehydrogenase (KDR10168.1)	*Zootermopsis nevadensis*	0E+00	92%

			Ecdysone-inducible gene L3, isoform A (NP_476581.1)	*Drosophila melanogaster*	9E−179	73%
			PREDICTED: L-lactate dehydrogenase-like isoform X1 (XP_394662.6)	*Apis mellifera*	2E−161	70%
			PREDICTED: L-lactate dehydrogenase isoform X1 (XP_008191446.1)	*Tribolium castaneum*	5E−163	70%
			Lactate dehydrogenase (NP_001095933.1)	*Bombyx mori*	3E−159	64%
RsG6PD	comp810099_c0_seq3	FX983730	Glucose-6-phosphate 1-dehydrogenase (KDR13948.1)	*Zootermopsis nevadensis*	0E+00	87%
			PREDICTED: glucose-6-phosphate 1-dehydrogenase isoform X2 (XP_006564786.1)	*Apis mellifera*	0E+00	75%
			PREDICTED: glucose-6-phosphate dehydrogenase isoform X1 (XP_008193170.1)	*Tribolium castaneum*	0E+00	74%
			PREDICTED: glucose-6-phosphate 1-dehydrogenase (XP_004929237.1)	*Bombyx mori*	0E+00	71%
			Zwischenferment, isoform A (NP_523411.1)	*Drosophila melanogaster*	0E+00	69%
			PREDICTED: glucose-6-phosphate 1-dehydrogenase (XP_001951527.2)	*Acyrthosiphon pisum*	0E+00	68%
RsTKT	comp796569_c11_seq2	FX983731	Transketolase (KDR18110.1)	*Zootermopsis nevadensis*	0E+00	88%
			PREDICTED: transketolase-like protein 2 isoform X2 (XP_623196.3)	*Apis mellifera*	0E+00	76%
			PREDICTED: transketolase-like protein 2 (XP_001944790.2)	*Acyrthosiphon pisum*	0E+00	75%
			PREDICTED: transketolase-like protein 2 isoform X1 (XP_967219.2)	*Tribolium castaneum*	0E+00	74%

			CG8036, isoform B (NP_649812)	*Drosophila melanogaster*	0E+00	72%
			Transketolase (NP_001040158.1)	*Bombyx mori*	0E+00	69%
RsTAD	comp815886_c9_seq1	FX983732	Transaldolase (KDR08915.1)	*Zootermopsis nevadensis*	0E+00	89%
			PREDICTED: transaldolase (XP_006563276.1)	*Apis mellifera*	0E+00	74%
			PREDICTED: probable transaldolase (XP_966585.1)	*Tribolium castaneum*	2E−176	74%
			PREDICTED: probable transaldolase isoform X1 (XP_001945887.2)	*Acyrthosiphon pisum*	5E−167	71%
			Transaldolase (NP_523835.2)	*Drosophila melanogaster*	5E−163	69%
			Transaldolase (NP_001040544.1)	*Bombyx mori*	6E−162	68%
RsPDH	comp802500_c9_seq5	FX983733	Pyruvate dehydrogenase E1 component subunit beta, mitochondrial (KDR20584.1)	*Zootermopsis nevadensis*	0E+00	93%
			Pyruvate dehydrogenase E1 component subunit beta, mitochondrial (NP_001229442.1)	*Apis mellifera*	0E+00	83%
			PREDICTED: pyruvate dehydrogenase E1 component subunit beta, mitochondrial (XP_970163.1)	*Tribolium castaneum*	0E+00	78%
			Uncharacterized protein Dmel_CG11876, isoform D (NP_651668.1)	*Drosophila melanogaster*	0E+00	76%
			PREDICTED: pyruvate dehydrogenase E1 component subunit beta, mitochondrial (XP_001948556.2)	*Acyrthosiphon pisum*	0E+00	75%
			PREDICTED: pyruvate dehydrogenase E1 component beta subunit isoform X1 (XP_012546310.1)	*Bombyx mori*	0E+00	72%
RsCS	comp805938_c0_seq1	FX983734	Putative citrate synthase 2, mitochondrial (KDR22581.1)	*Zootermopsis nevadensis*	0E+00	94%

				PREDICTED: probable citrate synthase 2, mitochondrial (XP_970124.1)	*Tribolium castaneum*	0E+00	84%
				PREDICTED: probable citrate synthase 2, mitochondrial (XP_004929851.1)	*Bombyx mori*	0E+00	80%
				Knockdown, isoform A (NP_572319.2)	*Drosophila melanogaster*	0E+00	77%
				PREDICTED: probable citrate synthase 2, mitochondrial (XP_393545.2)	*Apis mellifera*	0E+00	75%
				PREDICTED: probable citrate synthase 2, mitochondrial (XP_001950182.1)	*Acyrthosiphon pisum*	0E+00	75%
	RsIDH1	comp791136_c8_seq1	FX983735	Isocitrate dehydrogenase [NADP] cytoplasmic (KDR07905.1)	*Zootermopsis nevadensis*	0E+00	93%
				Isocitrate dehydrogenase (NP_001040134.1)	*Bombyx mori*	0E+00	85%
				PREDICTED: isocitrate dehydrogenase [NADP] cytoplasmic (XP_968850.1)	*Tribolium castaneum*	0E+00	84%
				PREDICTED: isocitrate dehydrogenase [NADP] cytoplasmic (XP_001946553.1)	*Acyrthosiphon pisum*	0E+00	83%
				Isocitrate dehydrogenase, isoform K (NP_001137910.2)	*Drosophila melanogaster*	0E+00	80%
				PREDICTED: isocitrate dehydrogenase [NADP] cytoplasmic (XP_623673.3)	*Apis mellifera*	0E+00	79%
	RsIDH2	comp816463_c14_seq2	FX983736	Isocitrate dehydrogenase [NADP], mitochondrial (KDR14081.1)	*Zootermopsis nevadensis*	0E+00	96%
				PREDICTED: isocitrate dehydrogenase [NADP], mitochondrial (XP_970446.1)	*Tribolium castaneum*	0E+00	78%
				NADPH-specific isocitrate dehydrogenase (NP_001093090.1)	*Bombyx mori*	0E+00	77%

				PREDICTED: isocitrate dehydrogenase [NADP] cytoplasmic (XP_001943698.1)	*Acyrthosiphon pisum*	0E+00	75%
				PREDICTED: isocitrate dehydrogenase [NADP] cytoplasmic (XP_623673.3)	*Apis mellifera*	0E+00	67%
				Isocitrate dehydrogenase, isoform B (NP_729366.1)	*Drosophila melanogaster*	0E+00	63%
	RsIDH3A	comp808574_c0_seq4	FX983737	Putative isocitrate dehydrogenase [NAD] subunit alpha, mitochondrial (KDR10371.1)	*Zootermopsis nevadensis*	0E+00	96%
				PREDICTED: probable isocitrate dehydrogenase [NAD] subunit alpha, mitochondrial isoform X1 (XP_015838763.1)	*Tribolium castaneum*	0E+00	89%
				PREDICTED: probable isocitrate dehydrogenase [NAD] subunit alpha, mitochondrial (XP_006564183.2)	*Apis mellifera*	0E+00	83%
				Lethal (1) G0156, isoform A (NP_573388.1)	*Drosophila melanogaster*	0E+00	82%
				PREDICTED: probable isocitrate dehydrogenase [NAD] subunit alpha, mitochondrial (XP_001951769.1)	*Acyrthosiphon pisum*	0E+00	82%
	RsIDH3B	comp751672_c0_seq2	FX983738	Putative isocitrate dehydrogenase [NAD] subunit beta, mitochondrial (KDR17889.1)	*Zootermopsis nevadensis*	0E+00	95%
				PREDICTED: isocitrate dehydrogenase [NAD] subunit beta, mitochondrial (XP_012546738.1)	*Bombyx mori*	0E+00	80%
				PREDICTED: probable isocitrate dehydrogenase [NAD] subunit beta, mitochondrial (XP_973953.2)	*Tribolium castaneum*	0E+00	78%
				PREDICTED: isocitrate dehydrogenase [NAD] subunit beta, mitochondrial (XP_624511.1)	*Apis mellifera*	0E+00	74%

			CG6439, isoform A (NP_651000.1)	*Drosophila melanogaster*	0E+00	74%
			PREDICTED: uncharacterized protein LOC100571286 isoform X1 (XP_008189402.1)	*Acyrthosiphon pisum*	1E−173	70%
RsOGDH	comp774750_c0_seq5	FX983739	2-oxoglutarate dehydrogenase E1 component, mitochondrial (KDR11185.1)	*Zootermopsis nevadensis*	0E+00	88%
			PREDICTED: 2-oxoglutarate dehydrogenase, mitochondrial isoform X3 (XP_006566127.1)	*Apis mellifera*	0E+00	78%
			PREDICTED: 2-oxoglutarate dehydrogenase, mitochondrial isoform X3 (XP_008193111.1)	*Tribolium castaneum*	0E+00	76%
			PREDICTED: 2-oxoglutarate dehydrogenase, mitochondrial isoform X3 (XP_016658315.1)	*Acyrthosiphon pisum*	0E+00	75%
			Neural conserved at 73EF, isoform F (NP_788518.1)	*Drosophila melanogaster*	0E+00	72%
			PREDICTED: 2-oxoglutarate dehydrogenase, mitochondrial (XP_004926430.2)	*Bombyx mori*	0E+00	68%
RsPEPCK	comp796148_c11_seq6	FX983740	Phosphoenolpyruvate carboxykinase [GTP] (KDR20258.1)	*Zootermopsis nevadensis*	0E+00	89%
			PREDICTED: phosphoenolpyruvate carboxykinase [GTP] isoform X1 (XP_396295.3)	*Apis mellifera*	0E+00	71%
			PREDICTED: phosphoenolpyruvate carboxykinase [GTP] isoform X1 (XP_975997.1)	*Tribolium castaneum*	0E+00	71%
			Phosphoenolpyruvate carboxykinase (NP_523784.2)	*Drosophila melanogaster*	0E+00	70%
			Mitochondrial phosphoenolpyruvate carboxykinase isoform 1 (NP_001040542.1)	*Bombyx mori*	0E+00	69%

RsALT2	comp809379_c1_seq4	FX983741	Alanine aminotransferase 2 (KDR12685.1)	*Zootermopsis nevadensis*	0E+00	91%
			PREDICTED: alanine aminotransferase 1 isoform X1 (XP_001948711.2)	*Acyrthosiphon pisum*	0E+00	70%
			PREDICTED: alanine aminotransferase 2 (XP_008191853.2)	*Tribolium castaneum*	2E−164	69%
			PREDICTED: alanine aminotransferase 1 (XP_006559494.1)	*Apis mellifera*	0E+00	66%
			CG1640, isoform B (NP_727696.2)	*Drosophila melanogaster*	0E+00	63%
			PREDICTED: alanine aminotransferase 1 (XP_012544150.1)	*Bombyx mori*	0E+00	60%
RsMDH1	comp763532_c0_seq1	FX983742	Malate dehydrogenase, cytoplasmic, partial (KDR14372.1)	*Zootermopsis nevadensis*	0E+00	93%
			PREDICTED: malate dehydrogenase, cytoplasmic (XP_975546.1)	*Tribolium castaneum*	8E−158	73%
			Malate dehydrogenase 1, isoform A (NP_609394.1)	*Drosophila melanogaster*	7E−165	72%
			PREDICTED: malate dehydrogenase, cytoplasmic (XP_394487.2)	*Apis mellifera*	1E−162	71%
			PREDICTED: malate dehydrogenase, cytoplasmic (XP_001949197.2)	*Acyrthosiphon pisum*	8E−147	71%
			PREDICTED: cytosolic malate dehydrogenase isoform X1 (XP_012548546.1)	*Bombyx mori*	9E−156	69%
RsMDH2	comp478846_c0_seq1	FX983743	Hypothetical protein L798_03098, partial (KDR07317.1)	*Zootermopsis nevadensis*	0E+00	85%
			PREDICTED: malate dehydrogenase, mitochondrial (XP_973533.1)	*Tribolium castaneum*	0E+00	80%
			PREDICTED: malate dehydrogenase, mitochondrial (XP_392478.2)	*Apis mellifera*	2E−174	71%

			PREDICTED: malate dehydrogenase, mitochondrial (XP_004928974.1)	*Bombyx mori*	1E−163	66%
			Malate dehydrogenase 2 (NP_650696.1)	*Drosophila melanogaster*	5E−159	66%
			Mitochondrial malate dehydrogenase (NP_001119675.1)	*Acyrthosiphon pisum*	3E−149	62%
RsACT	comp479365_c0_seq1	FX983744	Actin, muscle (KDR09838.1)	*Zootermopsis nevadensis*	0E+00	100%
			Actin related protein 1 (NP_001136108.1)	*Acyrthosiphon pisum*	0E+00	100%
			Actin, muscle-type A1 (NP_001119724.1)	*Bombyx mori*	0E+00	99%
			PREDICTED: actin, clone 205-like (XP_003251464.1)	*Apis mellifera*	0E+00	99%
			PREDICTED: actin, muscle (XP_966495.1)	*Tribolium castaneum*	0E+00	99%
			actin 87E, isoform A (NP_477091.1)	*Drosophila melanogaster*	0E+00	98%

REFERENCES

1. Harman D. Aging: a theory based on free radical and radiation chemistry. *J Gerontol.* 1956;11: 298–300.
2. Guarente L, Kenyon C. Genetic pathways that regulate ageing in model organisms. *Nature.* 2000;408: 255–262.
3. Cutler RG. Human longevity and aging: possible role of reactive oxygen species. *Ann N Y Acad Sci.* 1991;621: 1–28.
4. Dröge W. Free radicals in the physiological control of cell function. *Physiol Rev.* 2002;82: 47–95.
5. Finkel T, Holbrook NJ. Oxidants, oxidative stress and the biology of ageing. *Nature.* 2000;408: 239–247.
6. Wood ZA, Schroder E, Robin Harris J, Poole LB. Structure, mechanism and regulation of peroxiredoxins. *Trends Biochem Sci.* 2003;28: 32–40.
7. Rhee SG. H_2O_2, a necessary evil for cell signaling. *Science.* 2006;312: 1882–1883.
8. Woo HA, Yim SH, Shin DH, Kang D, Yu DY, Rhee SG. Inactivation of Peroxiredoxin I by Phosphorylation Allows Localized H_2O_2 Accumulation for Cell Signaling. *Cell.* 2010;140: 517–528.
9. Veal EA, Day AM, Morgan BA. Hydrogen Peroxide Sensing and Signaling. *Mol Cell.* 2007;26: 1–14.
10. Keller L, Genoud M. Extraordinary lifespans in ants: a test of evolutionary theories of ageing. *Nature.* 1997;389: 958–960.
11. Syntichaki P, Tavernarakis N. Genetic Models of Mechanotransduction: The Nematode *Caenorhabditis elegans*. *Physiol Rev.* 2004;84: 1097–1153.
12. Keller L, Jemielity S. Social insects as a model to study the molecular basis of

ageing. *Exp Gerontol.* 2006;41: 553–556.

13. Fujii J, Ikeda Y. Advances in our understanding of peroxiredoxin, a multifunctional, mammalian redox protein. *Redox Rep.* 2002;7: 123–130.
14. Fujii J, Ikeda Y, Kurahashi T, Homma T. Physiological and pathological views of peroxiredoxin 4. *Free Radic Biol Med.* 2015;83: 373–379.
15. Tavender TJ, Sheppard AM, Bulleid NJ. Peroxiredoxin IV is an endoplasmic reticulum-localized enzyme forming oligomeric complexes in human cells. *Biochem J.* 2008;411: 191–199.
16. Tavender TJ, Springate JJ, Bulleid NJ. Recycling of peroxiredoxin IV provides a novel pathway for disulphide formation in the endoplasmic reticulum. *EMBO J.* 2010;29: 4185–4197.
17. Iuchi Y, Okada F, Tsunoda S, Kibe N, Shirasawa N, Ikawa M, et al. Peroxiredoxin 4 knockout results in elevated spermatogenic cell death via oxidative stress. *Biochem J.* 2009;419: 149–158.
18. McCloy RA, Rogers S, Caldon CE, Lorca T, Castro A, Burgess A. Partial inhibition of Cdk1 in G2 phase overrides the SAC and decouples mitotic events. *Cell Cycle.* 2014;13: 1400–1412.
19. Potapova TA, Sivakumar S, Flynn JN, Li R, Gorbsky GJ. Mitotic progression becomes irreversible in prometaphase and collapses when Wee1 and Cdc25 are inhibited. *Mol Biol Cell.* 2011;22: 1191–1206.
20. Yim SH, Kim YJ, Oh SY, Fujii J, Zhang Y, Gladyshev VN, et al. Identification and characterization of alternatively transcribed form of peroxiredoxin IV gene that is specifically expressed in spermatids of postpubertal mouse testis. *J Biol Chem.* 2011;286: 39002–39012.
21. Bai J, Rodriguez AM, Melendez JA, Cederbaum AI. Overexpression of catalase in

cytosolic or mitochondrial compartment protects HepG2 cells against oxidative injury. *J Biol Chem.* 1999;274: 26217–26224.

22. Manevich Y, Sweitzer T, Pak JH, Feinstein SI, Muzykantov V, Fisher AB. 1-Cys peroxiredoxin overexpression protects cells against phospholipid peroxidation-mediated membrane damage. *Proc Natl Acad Sci.* 2002;99: 11599–11604.
23. Wang Y, Feinstein SI, Fisher AB. Peroxiredoxin 6 as an antioxidant enzyme: Protection of lung alveolar epithelial type II cells from H_2O_2-induced oxidative stress. *J Cell Biochem.* 2008;104: 1274–1285.
24. Palande K, Roovers O, Gits J, Verwijmeren C, Iuchi Y, Fujii J, et al. Peroxiredoxin-controlled G-CSF signalling at the endoplasmic reticulum-early endosome interface. *J Cell Sci.* 2011;124: 3695–3705.
25. D'Autréaux B, Toledano MB. ROS as signalling molecules: mechanisms that generate specificity in ROS homeostasis. *Nat Rev Mol Cell Biol.* 2007;8: 813–824.
26. Barone JG, De Lara J, Cummings KB, Ward WS. DNA organization in human spermatozoa. *J Androl.* 1994;15: 139–144.
27. Balhorn R. The protamine family of sperm nuclear proteins. *Genome Biol.* 2007;8: 227.
28. Zito E, Melo EP, Yang Y, Wahlander Å, Neubert TA, Ron D. Oxidative Protein Folding by an Endoplasmic Reticulum-Localized Peroxiredoxin. *Mol Cell.* 2010;40: 787–797.
29. Winston ML. The Biology of the Honey Bee. *Harvard University Press*; 1991.
30. Page RE, Peng CY-S. Aging and development in social insects with emphasis on the honey bee, *Apis mellifera* L. *Exp Gerontol.* 2001;36: 695–711.
31. Jemielity S, Chapuisat M, Parker JD, Keller L. Long live the queen: studying aging

in social insects. *Age*. 2005;27: 241–248.

32. Partridge L, Gems D, Withers DJ. Sex and death: what is the connection? *Cell.* 2005;120: 461–472.

33. Hsin H, Kenyon C. Signals from the reproductive system regulate the lifespan of *C. elegans*. *Nature.* 1999;399: 362–366.

34. M. Sgrò C, Partridge L. A Delayed Wave of Death from Reproduction in *Drosophila*. *Science.* 1999;286: 2521–2524.

35. Jones OR, Scheuerlein A, Salguero-Gómez R, Camarda CG, Schaible R, Casper BB, et al. Diversity of ageing across the tree of life. *Nature.* 2014;505: 169–173.

36. Heinze J, Schrempf A. Terminal investment: Individual reproduction of ant queens increases with age. *PLoS One.* 2012;7: e35201.

37. Sampayo JN, Olsen A, Lithgow GJ. Oxidative stress in *Caenorhabditis elegans*: protective effects of superoxide dismutase/catalase mimetics. *Aging Cell.* 2003;2: 319–326.

38. Melov S, Ravenscroft J, Malik S, Gill MS, Walker DW, Clayton PE, et al. Extension of life-span with superoxide dismutase/catalase mimetics. *Science.* 2000;289: 1567–1569.

39. Orr WC, Sohal RS. Extension of life-span by overexpression of superoxide dismutase and catalase in *Drosophila melanogaster*. *Science.* 1994;263: 1128–1130.

40. Sun J, Tower J. FLP recombinase-mediated induction of Cu/Zn-superoxide dismutase transgene expression can extend the life span of adult *Drosophila melanogaster* flies. *Mol Cell Biol.* 1999;19: 216–228.

41. Myatt L, Cui X. Oxidative stress in the placenta. *Histochem Cell Biol.* 2004;122: 369–382.

42. Agarwal A, Saleh RA, Bedaiwy MA. Role of reactive oxygen species in the

pathophysiology of human reproduction. *Fertil Steril.* 2003;79: 829–843.

43. Parker JD, Parker KM, Sohal BH, Sohal RS, Keller L. Decreased expression of Cu-Zn superoxide dismutase 1 in ants with extreme lifespan. *Proc Natl Acad Sci U S A.* 2004;101: 3486–3489.

44. Corona M, Hughes KA, Weaver DB, Robinson GE. Gene expression patterns associated with queen honey bee longevity. *Mech Ageing Dev.* 2005;126: 1230–1238.

45. Iuchi Y, Okada F, Onuma K, Onoda T, Asao H, Kobayashi M, et al. Elevated oxidative stress in erythrocytes due to a SOD1 deficiency causes anaemia and triggers autoantibody production. *Biochem J.* 2007;402: 219–227.

46. Mitaka Y, Kobayashi K, Mikheyev A, Tin MMY, Watanabe Y, Matsuura K. Caste-Specific and Sex-Specific Expression of Chemoreceptor Genes in a Termite. *PLoS One.* 2016;11: e0146125.

47. Rozen S, Skaletsky H. Primer3 on the WWW for general users and for biologist programmers. *Methods Mol Biol.* 2000;132: 365–86.

48. Holm S. A simple sequentially rejective multiple test procedure. *Scand J Stat.* 1979;6: 65–70.

49. Cooke MS, Evans MD, Dizdaroglu M, Lunec J. Oxidative DNA damage: mechanisms, mutation, and disease. *FASEB J.* 2003;17: 1195–1214.

50. Berlett BS, Stadtman ER. Protein Oxidation in Aging, Disease, and Oxidative Stress. *J Biol Chem.* 1997;272: 20313–20316.

51. Bucala R, Makita Z, Koschinsky T, Cerami A, Vlassara H. Lipid advanced glycosylation: pathway for lipid oxidation in vivo. *Proc Natl Acad Sci.* 1993;90: 6434–6438.

52. Ichihashi M, Ueda M, Budiyanto A, Bito T, Oka M, Fukunaga M, et al. UV-induced

skin damage. *Toxicology.* 2003;189: 21–39.

53. Levine RL, Williams JA, Stadtman ER, Shacter E. Carbonyl assays for determination of oxidatively modified proteins. *Methods Enzymol.* 1994;233: 346–357.

54. Yagi K. Simple assay for the level of total lipid peroxides in serum or plasma. *Methods Mol Biol.* 1998;108: 101–106.

55. Armstrong D, Browne R. The analysis of free radicals, lipid peroxides, antioxidant enzymes and compounds related to oxidative stress as applied to the clinical chemistry laboratory. *Adv Exp Med Biol.* 1994;366: 43–58.

56. Felton GW, Summers CB. Antioxidant systems in insects. *Arch Insect Biochem Physiol.* 1995;29: 187–197.

57. DeJong RJ, Miller LM, Molina-Cruz A, Gupta L, Kumar S, Barillas-Mury C. Reactive oxygen species detoxification by catalase is a major determinant of fecundity in the mosquito Anopheles gambiae. *Proc Natl Acad Sci U S A.* 2007;104: 2121–2126.

58. Diaz-Albiter H, Mitford R, Genta FA, Sant'Anna MR V, Dillon RJ. Reactive oxygen species scavenging by catalase is important for female Lutzomyia longipalpis fecundity and mortality. *PLoS One.* 2011;6: e17486.

59. Baker N, Wolschin F, Amdam G V. Age-related learning deficits can be reversible in honeybees *Apis mellifera*. *Exp Gerontol.* 2012;47: 764–772.

60. Ahmad S, Beilstein M a, Pardini RS. Glutathione Peroxidase Activity in Insects : A Reassessment. *Arch Insect Biochem Physiol.* 1989;49: 31–49.

61. Jemielity S, Kimura M, Parker KM, Parker JD, Cao X, Aviv A, et al. Short telomeres in short-lived males: what are the molecular and evolutionary causes? *Aging Cell.* 2007;6: 225–233.

62. Kamakura M. Royalactin induces queen differentiation in honeybees. *Nature.* 2011;473: 478–483.

63. Remolina SC, Hughes KA. Evolution and mechanisms of long life and high fertility in queen honey bees. *Age.* 2008;30: 177–185.

64. Corona M, Velarde R A, Remolina S, Moran-Lauter A, Wang Y, Hughes K A, et al. Vitellogenin, juvenile hormone, insulin signaling, and queen honey bee longevity. *Proc Natl Acad Sci U S A.* 2007;104: 7128–7133.

65. Radyuk S. The peroxiredoxin gene family in *Drosophila melanogaster*. *Free Radic Biol Med.* 2001;31: 1090–1100.

66. Korb J. Genes underlying reproductive division of labor in termites, with comparisons to social Hymenoptera. *Front Ecol Evol.* Frontiers; 2016;4: 1–10.

67. Murphy MP. How mitochondria produce reactive oxygen species. *Biochem J.* 2009;417: 1–13.

68. Nunes L, Bignell DE, Lo N, Eggleton P. On the respiratory quotient (RQ) of termites (Insecta:Isoptera). *J Insect Physiol.* 1997;43: 749–758.

69. Ohkuma M. Termite symbiotic systems: efficient bio-recycling of lignocellulose. *Appl Microbiol Biotechnol.* 2003;61: 1–9.

70. Kolovou GD, Kolovou V, Mavrogeni S. We are ageing. *Biomed Res Int.* 2014;2014: 808307.

71. Finkel T, Deng C-X, Mostoslavsky R. Recent progress in the biology and physiology of sirtuins. *Nature.* 2009;460: 587–591.

72. Hekimi S, Guarente L. Genetics and the specificity of the aging process. *Science.* 2003;299: 1351–1354.

73. Azpurua J, Seluanov A. Long-lived cancer-resistant rodents as new model species for cancer research. *Front Genet.* 2013;3: eCollection 2012.

74. Schriner SE, Linford NJ, Martin GM, Treuting P, Ogburn CE, Emond M, et al. Extension of murine life span by overexpression of catalase targeted to mitochondria. *Science.* 2005;308: 1909–1911.

75. Thaipong K, Boonprakob U, Crosby K, Cisneros-Zevallos L, Hawkins Byrne D. Comparison of ABTS, DPPH, FRAP, and ORAC assays for estimating antioxidant activity from guava fruit extracts. *J Food Compos Anal.* 2006;19: 669–675.

76. Kim KM, Henderson GN, Ouyang X, Frye RF, Sautin YY, Feig DI, et al. A sensitive and specific liquid chromatography-tandem mass spectrometry method for the determination of intracellular and extracellular uric acid. *J Chromatogr B Analyt Technol Biomed Life Sci.* 2009;877: 2032–2038.

77. Potrikus CJ, Breznak JA. Uric acid in wood-eating termites. *Insect Biochem.* 1980;10: 19–27.

78. Ames BN, Cathcart R, Schwiers E, Hochstein P. Uric acid provides an antioxidant defense in humans against oxidant- and radical-caused aging and cancer: a hypothesis. *Proc Natl Acad Sci U S A.* 1981;78: 6858–6862.

79. Matsuo T, Ishikawa Y. Protective role of uric acid against photooxidative stress in the silkworm, *Bombyx mori* (Lepidoptera: Bombycidae). *Appl Entomol Zool.* 1999;34: 481–484.

80. Hilliker AJ, Duyf B, Evans D, Phillips JP. Urate-null rosy mutants of *Drosophila melanogaster* are hypersensitive to oxygen stress. *Genetics.* 1992;89: 4343–4347.

81. Sadowska-Bartosz I, Bartosz G. Effect of antioxidants supplementation on aging and longevity. *Biomed Res Int.* 2014;2014: 404680.

82. Potrikus CJ, Breznak J a. Gut bacteria recycle uric acid nitrogen in termites: A strategy for nutrient conservation. *Proc Natl Acad Sci U S A.* 1981;78: 4601–4605.

83. Kômoto N. A deleted portion of one of the two xanthine dehydrogenase genes causes

translucent larval skin in the oq mutant of the silkworm (*Bombyx mori*). *Insect Biochem Mol Biol.* 2002;32: 591–597.

84. Thong-On A, Suzuki K, Noda S, Inoue J, Kajiwara S, Ohkuma M. Isolation and Characterization of Anaerobic Bacteria for Symbiotic Recycling of Uric Acid Nitrogen in the Gut of Various Termites. *Microbes Environ.* 2012;27: 186–192.

85. Thorne BL, Breisch NL, Haverty MI. Longevity of kings and queens and first time of production of fertile progeny in dampwood termite (Isoptera; Termopsidae; *Zootermopsis*) colonies with different reproductive structures. *J Anim Ecol.* 2002;71: 1030–1041.

86. Wyss-Huber M, Lüscher M. Protein synthesis in “fat body” and ovary of the physogastric queen of Macrotermes subhyalinus. *J Insect Physiol.* 1975;21: 1697–1704.

87. Terrapon N, Li C, Robertson HM, Ji L, Meng X, Booth W, et al. Molecular traces of alternative social organization in a termite genome. *Nat Commun.* 2014;5: 3636.

88. Simola DF, Graham RJ, Brady CM, Enzmann BL, Desplan C, Ray A, et al. Epigenetic (re)programming of caste-specific behavior in the ant *Camponotus floridanus*. *Science.* 2016;351: aac6633.

89. Hayashi Y, Lo N, Miyata H, Kitade O. Sex-linked genetic influence on caste determination in a termite. *Science.* 2007;318: 985–987.

90. Matsuura K, Himuro C, Yokoi T, Yamamoto Y, Vargo EL, Keller L. Identification of a pheromone regulating caste differentiation in termites. *Proc Natl Acad Sci U S A.* 2010;107: 12963–12968.

91. Harris AL. Hypoxia - A key regulatory factor in tumour growth. *Nat Rev Cancer.* 2002;2: 38–47.

92. Cassavaugh J, Lounsbury KM. Hypoxia-mediated biological control. *J Cell Biochem.*

2011;112: 735–744.

93. Kleineidam C, Roces F. Carbon dioxide concentrations and nest ventilation in nests of the leaf-cutting ant *Atta vollenweideri*. *Insectes Soc.* 2000;47: 241–248.

94. Buffenstein R. Negligible senescence in the longest living rodent, the naked mole-rat: Insights from a successfully aging species. *J Comp Physiol B Biochem Syst Environ Physiol.* 2008;178: 439–445.

95. Kim EB, Fang X, Fushan A A., Huang Z, Lobanov A V., Han L, et al. Genome sequencing reveals insights into physiology and longevity of the naked mole rat. *Nature.* 2011;479: 223–227.

96. Kaelin WG, McKnight SL. Influence of metabolism on epigenetics and disease. Cell. 2013;153: 56–69.

97. Turner JS. On the mound of Macrotermes michaelseni as an organ of respiratory gas exchange. *Physiol Biochem Zool.* 2001;74: 798–822.

98. Nishiumi S, Shinohara M, Ikeda A, Yoshie T, Hatano N, Kakuyama S, et al. Serum metabolomics as a novel diagnostic approach for pancreatic cancer. Metabolomics. 2010;6: 518–528.

99. Matsuura K, Vargo EL, Kawatsu K, Labadie PE, Nakano H, Yashiro T, et al. Queen succession through asexual reproduction in termites. *Science.* 2009;323: 1687.

100. Matsuura K, Kuno E, Nishida T. Homosexual tandem running as selfish herd in *Reticulitermes speratus*: novel antipredatory behavior in termites. *J Theor Biol.* 2002;214: 63–70.

101. Harris JW, Woodring J, Harbo J. Effects of carbon dioxide on levels of biogenic amines in the brains of queenless worker and virgin queen honey bees (*Apis mellifera*). *J Apic Res.* 1996;35: 69–78.

102. Mackensen O. Effect of carbon dioxide on initial oviposition of artificially

inseminated and virgin queen bees. *J Econ Entomol.* 1947;40: 344–349.

103. Fridovich I. Oxygen Is Toxic! *Bioscience.* 1977;27: 462–466.

104. Fenn WO, Henning M, Philpott M. Oxygen poisoning in *Drosophila*. *J Gen Physiol.* 1967;50: 1693–1707.

105. Maekawa K, Ishitani K, Gotoh H, Cornette R, Miura T. Juvenile Hormone titre and vitellogenin gene expression related to ovarian development in primary reproductives compared with nymphs and nymphoid reproductives of the termite *Reticulitermes speratus*. *Physiol Entomol.* 2010;35: 52–58.

106. Gorr TA, Wichmann D, Hu J, Hermes-Lima M, Welker AF, Terwilliger N, et al. Hypoxia tolerance in animals: biology and application. *Physiol Biochem Zool.* 2010;83: 733–752.

107. Müller M, Mentel M, van Hellemond JJ, Henze K, Woehle C, Gould SB, et al. Biochemistry and evolution of anaerobic energy metabolism in eukaryotes. *Microbiol Mol Biol Rev.* 2012;76: 444–495.

108. Verberk WCEP, Sommer U, Davidson RL, Viant MR. Anaerobic metabolism at thermal extremes: A metabolomic test of the oxygen limitation hypothesis in an aquatic insect. *Integr Comp Biol.* 2013;53: 609–619.

109. Mishur RJ, Khan M, Munkácsy E, Sharma L, Bokov A, Beam H, et al. Mitochondrial metabolites extend lifespan. *Aging Cell.* 2016;15: 336–348.

110. Intlekofer AM, DeMatteo RG, Venneti S, Finley LWS, Lu C, Judkins AR, et al. Hypoxia Induces Production of L-2-Hydroxyglutarate. *Cell Metab.* 2015;22: 304–311.

111. Zhou D, Xue J, Lai JCK, Schork NJ, White KP, Haddad GG. Mechanisms underlying hypoxia tolerance in *Drosophila melanogaster*: Hairyas a metabolic switch. *PLoS Genet.* 2008;4: e1000221.

112. Vander Heiden MG, Cantley LC, Thompson CB. Understanding the Warburg effect: the metabolic requirements of cell proliferation. *Science.* 2009;324: 1029–1033.

113. Patra KC, Hay N. The pentose phosphate pathway and cancer. *Trends Biochem Sci.* 2014;39: 347–354.

114. Soundar S, Park JH, Huh TL, Colman RF. Evaluation by Mutagenesis of the Importance of 3 Arginines in α, β, and γ Subunits of Human NAD-dependent Isocitrate Dehydrogenase. *J Biol Chem.* 2003;278: 52146–52153.

115. Van Hellemond JJ, Klockiewicz M, Gaasenbeek CPH, Roos MH, Tielensi AGM. Rhodoquinone and complex II of the electron transport chain in anaerobically functioning eukaryotes. *J Biol Chem.* 1995;270: 31065–31070.

116. Salgado MC, Metón I, Anemaet IG, Baanante I V. Activating transcription factor 4 mediates up-regulation of alanine aminotransferase 2 gene expression under metabolic stress. *Biochim Biophys Acta.* 2014;1839: 288–296.

List of main publications related to the thesis

Eisuke Tasaki, Shotaro Matsumoto, Hisashi Tada, Toshihiro Kurahashi, Xuhong Zhang, Junichi Fujii, Toshihiko Utsumi, Yoshihito Iuchi

Protective role of testis-specific peroxiredoxin 4 against cellular oxidative stress

***Journal of Clinical Biochemistry and Nutrition*. 2017;60(3): 156–161**

(PART I, Chapter I)

Eisuke Tasaki, Kazuya Kobayashi, Kenji Matsuura, Yoshihito Iuchi

An Efficient Antioxidant System in a Long-Lived Termite Queen

***PLOS ONE*. 2017;12(1): e0167412**

(PART II, Chapter II)

Eisuke Tasaki, Hiroki Sakurai, Masaru Nitao, Kenji Matsuura, Yoshihito Iuchi

Uric acid, an important antioxidant contributing to survival in termites

***PLOS ONE*. 2017;12(6): e0179426**

(PART II, Chapter III)

Summary of the thesis

Antioxidant System Contributes to Cellular Protection and Long-Life

In this study, I investigated whether antioxidant system contributes to cellular protection and long-life in organisms. To identify the mechanisms of antioxidant system in organisms, we performed two types of investigations in the thesis.

In Part I (Chapter I), I investigated the antioxidant role of testis specific antioxidant enzyme peroxiredoxin 4 (Prx4t) in mammalian cell line. The major functions of Prx family include antioxidant activity and protein quality control activity. Although these divergent biological functions have been reported for individual Prx family, the detailed antioxidant function of Prx4t remains unknown. Our findings indicate that Prx4t actually plays a protective role against oxidative stress in mammalian cells.

In Part II (Chapter II–IV), I investigated the mechanism by which eusocial termite reproductives (queens) achieve long lifespan. Previous studies indicated that the evolution of eusociality is associated with a 100-fold increase in intrinsic lifespan of reproductives (mostly females). Because of their abnormal characteristics implying the presence of an extraordinary anti-aging mechanism, eusocial insect queens have attracted much attention, and they are promising subjects for aging research. However, the molecular mechanisms that allow eusocial insects queens to have great longevity are not yet understood. In this part, I focused eusocial subterranean termite *Reticulitermes speratus* to investigate these issue. I compared the level of oxidative stress between *R. speratus* queens and non-reproductive workers in Chapter II. In addition, I also compared two major antioxidant enzyme activities among several insect species and these gene expression levels between *R.*

speratus castes. Moreover, in Chapter III, I investigated whether uric acid, which is known as an antioxidant for organisms, contributes to the termite survival.

Although eusocial reproductives and non-reproductive workers have same genome information, they exhibit phenotypic dimorphisms such as longevity and fertility by some epigenetic regulation. Although understanding the regulatory mechanism is an important challenge for future aging research, findings of the mechanism have been studied little in termites. In Chapter IV, I approached the problem by focusing on an environmental factor hypoxia in termite nest.

In summary, the findings of this thesis not only indicate that an antioxidant enzyme actually plays a protective role against oxidative stress in mammalian cells and that antioxidant system contributes to longevity of *R. speratus* queens, but also can be applied to understanding the molecular basis of the physiology and behavior of eusocial termites, which underlie aging and longevity.

Summary of the thesis (In Japanese)

抗酸化システムは細胞保護と長寿命に貢献する

本研究は、生物において抗酸化システムが細胞保護効果や長寿命（寿命延長）に貢献するかどうか、その一部の機構について新しい視点からアプローチしたものである。また、本研究は大きく２つのタイプに分かれており、各章として示している。

第１章では、比較的近年に発見された抗酸化酵素ペルオキシレドキシン（Prx）ファミリーの中でも、その機能について不明な点が多い精巣特異的 Prx4t に注目して抗酸化能評価を行った。各々の Prx ファミリーは抗酸化活性やタンパク質の品質管理に関与するといった様々な機能が報告されている一方で、Prx4t の細胞内における抗酸化効果については未だ理解されていなかった。過去の研究に Prx4t 発現の減少は精巣のサイズ減少などといった酸化ストレスの亢進を示唆するものがある。本章（チャプター１）は、本来 Prx4t を発現しない HEK293T 細胞で Prx4t を発現させることで、コントロールと比較して酸化ストレス耐性を高める結果を得た。これは、機能が不明瞭であった Prx4t が精巣内において抗酸化酵素としても機能している可能性を示唆するものとなった。

第２章では、真社会性昆虫に代表されるシロアリの生殖虫（女王）がどのようなメカニズムで長寿命を実現したかという、世界でも類を見ないアプローチで抗酸化システムと寿命の関係を評価した。いくつかのこれまでの研究は、真社会性の進化が 100 倍もの個体寿命の延長に関係していることを示してきた。このような真社会性動物の普通とは異なった特徴から、これまでの短寿命モデル動物を用いた寿命研究で未解明だった部分を、新しい長寿命モデル動物として彼らが解き明かすのではないかと期待されてきている。しかしながら、その長寿命を可能にしている分

子メカニズムは未だ理解されていない。本章において、私は真社会性のヤマトシロアリ（*Reticulitermes speratus*）に注目し、これらの未解明な問題について研究を行った。チャプター２では、*R. speratus* の長寿命形質を示す女王と短寿命形質を示すワーカーの酸化障害量及び、抗酸化酵素活性・遺伝子発現量を比較した。その結果、女王は高い抗酸化酵素活性及び発現量を示し、これと矛盾せず、低い酸化障害量を示した。加えて、チャプター３では、抗酸化酵素以外の抗酸化活性についてシロアリや一般の昆虫の間で比較検討を行ったところ、ヤマトシロアリが高いフリーラジカル消去能を示すことを見出した。さらに、LC-MS/MS システムを用いてこのフリーラジカル消去物質が古典的な抗酸化物質である尿酸であることを発見した。また、尿酸はシロアリワーカーの生存に大きく寄与することを示し、シロアリの尿酸を利用した抗酸化システムの一部分を発見した。チャプター４では、シロアリの長寿命形質の獲得に必要な環境因子として、低酸素を見出した。エピジェネティック・トリガーとしての低酸素による表現系の変化について、特にがん細胞や腫瘍においての研究が進んでいるが、今回の発見はシロアリが個体レベルで低酸素環境を利用している可能性を示唆するものとなった。

以上をまとめると、本研究は、抗酸化酵素が細胞保護効果を示し、真社会性昆虫であるヤマトシロアリの長寿にも貢献することを示しただけでなく、新しい長寿命研究のモデルとなりうるシロアリの生理学的・生態学的な分子基盤の理解に大きく貢献するものとなった。

Acknowledgement

The author is grateful to supervisor Associate Prof. Yoshihito Iuchi from Yamaguchi University, Prof. Jun Kobayashi from Yamaguchi University, Prof. Takashi Matsuzaki from Shimane University, and Prof. Masaaki Azuma from Tottori University. Prof. Kenji Matsuura and Junior Associate Prof. Kazuya Kobayashi from Kyoto University for valuable advice, assistance, and designation during this work. The author thanks Prof. Toshihiko Utsumi, Prof. Ryutaro Murakami, Prof. Kenji Matsui, Prof. Hiroyuki Azakami, Prof. Junichi Mano, and Prof. Yoshihiko Akakabe from Yamaguchi University for providing samples and laboratory instruments, and all colleagues of Yamaguchi University and Kyoto University for delightful research life and great help.